

**Content-Aware Radio Resource Management for IMT-  
Advanced Systems**

**Muhammad Syahrir Johal**

**A thesis submitted to  
Lancaster University for the degree of  
Doctor of Philosophy**

**April 2017**

## **Abstract**

### **Content-Aware Radio Resource Management for IMT-Advanced Systems**

**Muhammad Syahrir Johal**

Submitted for the degree of Doctor of Philosophy

April 2017

Radio Resource Management (RRM) is crucial to efficiently and correctly manage the delivery of quality-of-service (QoS) in IMT-Advanced systems. Various methods on radio resource management for LTE/LTE-Advanced traffic have been studied by researchers especially regarding QoS handling of video packet transmissions. Usually, cross-layer optimisation (CLO) involving the PHY and MAC layers, has been used to provide proper resource allocation and distribution to the entire system. Further initiatives to include the APP layer as part of CLO techniques have gained considerable attention by researchers. However, some of these methods did not adequately consider the level of compatibility with legacy systems and standards. Furthermore, the methods did not wholly address User Equipment (UE) mobility or performance metrics for a specific data type or a specified period.

Consequently, in this thesis, a content-aware radio RRM model employing a cross-layer optimiser focusing on a video conferencing/streaming application for a single cell long-term evolution (LTE) system has been proposed. Based on two constructed look-up tables, the cross-layer optimiser was found to dynamically adjust the transmitted video data rates depending on the UE or eNodeB SINR performance. The proposed look-up tables were derived from the

performance study of the LTE classical (baseline) simulation model for various distances at a certain UE velocity. Two performance parameters, namely the average throughput and measured SINR were matched together to find the most suitable data rates for video delivery in both the uplink and downlink transmissions.

The developed content-aware RRM model was then tested against the LTE baseline simulation model, to benchmark its capability to be used as an alternative to existing RRM methods in the present LTE system. Based on the detailed simulations, the output performance demonstrated that for video packet delivery in both uplink and downlink transmissions, the content-aware RRM model vastly outperformed the legacy LTE baseline simulation model with regard to the packet loss ratio and average end-to-end delay for the same amount of throughput.

The baseline simulation model and the newly developed cross-layer approach were investigated and compared with practical measurement results in which PodNode technology, besides other components and supporting simulation software, were used to emulate the LTE communication system. The first emulation experiment involving the baseline model was generally in sync with the uplink throughput simulation performance. The second test which implemented the cross-layer approach employing the look-up table derived from the previous emulated results, confirmed the viability of the proposed content-aware RRM model to be used in current LTE or LTE-Advanced systems for improving the performance in the packet loss ratio and average packet delay.

## **Declaration**

I declare that the material presented in this thesis consists of original work undertaken solely by myself. Whenever work carried out by other authors is referred to in this thesis, it has been duly referenced. The material presented here has not been submitted elsewhere in entirely the same form for the award of a higher degree.

**Muhammad Syahrir Johal**

April 2017

## List of Publications / Contributions

### Papers Published:

1. Mohd Khairy Ismail, Muhammad Syahrir Johal and Azmi Awang Md Isa, "Current Developments in LTE-ADVANCED: Radio Resource Management Review", in proceedings of *IEEE Student Conference on Research and Development (SCOREd 2014)*, 16-17 Dec. 2014.
2. M. K. Ismail, A. A. M. Isa and M. S. Johal, "Review of Radio Resource Management for IMT-Advanced System", *Jurnal Teknologi*, Vol. 72, No. 4, 2015, pp. 113-119.
3. MK Ismail, A Awang Md Isa, MS Johal and MSI M Zain, "Current Development in LTE/LTE-Advanced: Adaptive-Proportional Fair Scheduling in LTE", *Journal of Telecommunication, Electronic and Computer Engineering (JTEC)*, Vol. 7, Issue 1, 2015, pp. 103-108.
4. Juwita Mohd Sultan and Muhammad Syahrir Johal, "Cross Layer Scheduling in WiMAX QoS for Disaster Management", *Journal of Telecommunication, Electronic and Computer Engineering (JTEC)*, Vol. 7, Issue 2, 2015, pp. 145-151.
5. Mohd Khairy Ismail, Azmi Awang Md Isa, Muhammad Syahrir Johal and Mohd Riduan Ahmad, "Design and Development of Modified Proportional Fair Scheduler for LTE/LTE-Advanced", *ARPN Journal of Engineering and Applied Sciences*, Vol. 11, No. 5, March 2016, pp. 3280-3285.
6. Muhammad Syahrir Johal, Garik Markarian, Azmi Awang Md Isa and Yosza Dasril, "Content-Aware Radio Resource Management for IMT-Advanced", *Journal of Telecommunication, Electronic and Computer Engineering (JTEC)*, Vol. 9, Issue 2, 2017, pp. 125-131.

## **Acknowledgements**

I would like to thank and express my sincerest gratitude, firstly, to my main supervisor Professor Garik Markarian who encouraged me to pursue this topic. I honestly and firmly believe that without his wisdom and insightful suggestions during my work, I would not have achieved my immediate goal of submitting this thesis for my PhD. This thesis has significantly benefitted from his invaluable guidance, support and constant encouragement.

I would also like to acknowledge my heartfelt thanks to my supervisors, Associate Professor Dr Azmi Awang Md Isa and Dr Yosza Dasril for their meaningful and insightful feedback and advice during the period of my PhD study in UTeM, Malaysia. I much appreciate their concerns for my intellectual and personal growth.

I am very grateful to my lab colleagues of Room B28 especially Abd Shukur, Juwita, Dr Dmitry Zvikhachevskiy and Dr Ivan Manuylov. I appreciate our fruitful technical discussions together and thank them both for being wonderful neighbours during my stay for one and a half years in Lancaster. Special thanks to Rinicom's technical staff for their invaluable help and support in the realisation of my practical testbed investigation, namely Dr Hassan Girach and Dr Sean Sonander.

I would also like to thank my sponsor who is also my employer, the Universiti Teknikal Malaysia Melaka, who allowed me to further my PhD study and provided financial support, without which this research would not have been made possible.

Finally, I would like to thank my parents for their unconditional love and ongoing support throughout my PhD study. Finally, I would like to thank my beloved wife, Suhaila Kamidi and my three lovely sons, Nuruddin, Nazhan and Nazih who have always stood by my

side, giving their love, support and encouragement through the difficult and arduous times, to which, this thesis is dedicated to them all.

## Table of Contents

Abstract .....	1
Declaration .....	3
List of Publications / Contributions .....	4
Acknowledgements .....	5
List of Figures .....	10
List of Tables .....	12
List of Abbreviations .....	13
1 INTRODUCTION .....	19
1.1 Research Motivations .....	20
1.2 Research Background .....	21
1.3 Research Objectives .....	23
1.4 Research Methodology .....	23
1.5 Research Contributions .....	24
1.6 Thesis Outline .....	24
2 RADIO RESOURCE MANAGEMENT IN LTE/LTE-ADVANCED SYSTEM .....	27
2.1 Introduction .....	27
2.2 LTE Architecture .....	28
2.3 LTE-Advanced Architecture and Protocol Stack .....	34
2.4 eNodeB Protocol Stack and RRM Functions .....	37
2.4.1 Semi-Dynamic RRM Features (QoS Parameters, Admission Control and Semi-Persistent Scheduling) .....	41
2.4.2 Fast Dynamic RRM Algorithms .....	43
2.5 Research on RRM for LTE .....	44
2.6 Cross-Layer Design for LTE .....	47
2.7 Summary .....	50
3 THE CLASSICAL (BASELINE) LTE SIMULATION MODEL .....	52
3.1 Simulation Environment .....	53
3.2 Classification of Simulation Tools .....	53
3.2.1 OMNeT++ .....	54
3.2.2 OPNET Modeler (Currently known as Riverbed Modeler [77]) .....	56
3.2.3 NS-2 .....	58
3.2.4 NS-3 .....	59

3.2.5	MATLAB.....	61
3.3	Single Cell eNodeB Simulation Topology and Parameter setup for Uplink Transmission .....	65
3.4	Analysis of the LTE Uplink Baseline Model Performance.....	70
3.5	Correlation between Output Performance Parameters and SINR.....	73
3.6	Downlink Scenario of the Baseline Model .....	74
3.7	Analysis of the LTE Downlink Baseline Model Performance.....	76
3.8	Correlation between the Output Performance Parameters and SINR for the Downlink Transmission .....	78
3.9	Summary .....	79
4	CONTENT-AWARE RADIO RESOURCE MANAGEMENT MODEL.....	81
4.1	Proposed Look-up Table for the Uplink Content-Aware RRM Model.....	82
4.2	Comparison Parameters.....	84
4.3	Results Analysis of the Uplink Transmission .....	85
4.3.1	Scenario 1 .....	86
4.3.2	Scenario 2.....	89
4.3.3	Scenario 3.....	91
4.3.4	Mobility Analysis for the LTE Uplink Video Packet Transmission.....	93
4.4	Proposed Look-up Table for the Downlink Content-Aware RRM Model.....	96
4.5	Results Analysis of the Downlink Model .....	99
4.5.1	Scenario 1.....	100
4.5.2	Scenario 2.....	103
4.5.3	Scenario 3.....	105
4.5.4	Mobility Analysis for the LTE Downlink Video Packet Transmission.....	108
4.6	Summary .....	111
5	PRACTICAL MEASUREMENTS .....	113
5.1	Introduction .....	113
5.2	System Description.....	115
5.3	System Development and Implementation .....	123
5.3.1	IP Camera Configuration .....	123
5.3.2	PodNodes Configuration .....	125
5.3.3	Overall Setup (with IP Camera) .....	129
5.3.4	Overall Setup (IP Camera replaced with the second laptop) .....	130
5.4	Experimental Results and Discussion.....	133
5.4.1	Results for the Emulated Uplink LTE Baseline Model .....	133
5.4.2	Results for the Emulated Uplink LTE Content-Aware RRM Model .....	136

5.5	Summary .....	138
6	CONCLUSION AND FUTURE WORKS.....	140
6.1	Conclusion .....	140
6.2	Future Works.....	142
6.2.1	Multi-user Content-Aware RRM.....	142
6.2.2	MIMO-OFDMA .....	142
6.2.3	Context-Aware RRM.....	143
6.2.4	Internet-of-Things .....	143
7	REFERENCES .....	145

## List of Figures

Figure 2.1: LTE Release 8 architecture [17] .....	30
Figure 2.2: Basic LTE protocol structure [20] .....	32
Figure 2.3: LTE frame structure [6] [19] .....	34
Figure 2.4: LTE-Advanced E-UTRAN architecture [23] .....	36
Figure 2.5: Protocol stack [23] .....	36
Figure 2.6: Overview of the eNodeB user plane and control plane architecture and the mapping of the primary RRM functions to the different layers [30].....	40
Figure 2.7: The downlink physical layer resource space for one TTI [30] .....	40
Figure 3.1: Single eNodeB LTE - EPC simulation topology .....	68
Figure 3.2: Throughput against SINR plot for R = 4 Mbps .....	72
Figure 3.3: Packet Loss Ratio against SINR plot for R = 4 Mbps .....	72
Figure 3.4: Average delay against SINR plot for R = 4 Mbps .....	72
Figure 3.5: Throughput against SINR plot for R = 4 Mbps .....	77
Figure 3.6: Packet Loss Ratio against SINR plot for R = 4 Mbps .....	78
Figure 3.7: Average delay against SINR plot for R = 4 Mbps .....	78
Figure 4.1: Cross-layer optimiser for Content-Aware RRM at UE side .....	84
Figure 4.2: Throughput against time for uplink video delivery .....	86
Figure 4.3: Packet loss ratio against time for uplink video delivery .....	86
Figure 4.4: Average delay against time for uplink video delivery .....	87
Figure 4.5: Throughput against time for uplink video delivery .....	89
Figure 4.6: Packet loss ratio against time for uplink video delivery .....	90
Figure 4.7: Average delay against time for uplink video delivery .....	90
Figure 4.8: Throughput against time for uplink video delivery .....	92
Figure 4.9: Packet loss ratio against time for uplink video delivery .....	92
Figure 4.10: Average delay against time for uplink video delivery .....	92
Figure 4.11: Total received data in uplink video packet transmission in three different UE velocities .	94
Figure 4.12: Area under the curve for packet loss ratio in uplink video transmission in three different UE velocities .....	94
Figure 4.13: Area under the curve for average delay in uplink video transmission in three different UE velocities .....	95
Figure 4.14: Cross-layer optimiser in the downlink transmission.....	99
Figure 4.15: Throughput against time for downlink video delivery .....	101
Figure 4.16: Packet loss ratio against time for downlink video delivery .....	101
Figure 4.17: Average delay against time for downlink video delivery .....	101
Figure 4.18: Throughput against time for downlink video delivery .....	103
Figure 4.19: Packet loss ratio against time for downlink video delivery .....	104
Figure 4.20: Average delay over time for downlink video delivery .....	104
Figure 4.21: Throughput against time for downlink video delivery .....	106
Figure 4.22: Packet loss ratio against time for downlink video delivery .....	106
Figure 4.23: Average delay against time for downlink video delivery .....	106
Figure 4.24: Total received data in downlink video packet transmission in three different UE velocities	

.....	108
Figure 4.25: Area under the curve for packet loss ratio in downlink video transmission in three different UE velocities .....	109
Figure 4.26: Area under the curve for average delay in downlink video transmission in three different UE velocities .....	109
Figure 5.1: Practical testbed for LTE uplink video delivery .....	117
Figure 5.2: PodNode-I [100] .....	120
Figure 5.3: Axis P1357 network camera [96] .....	122
Figure 5.4: Basic setup of IP (network) camera .....	125
Figure 5.5: PodNode webpage: Device login.....	126
Figure 5.6: PodNode Webpage: Main page .....	127
Figure 5.7: The overall setup where the IP camera on the right is replaced with the second laptop ...	131
Figure 5.8: Average throughput versus SINR/SNR for uplink video delivery. (a) Simulated LTE baseline model. (b) Emulated LTE baseline model .....	134

## List of Tables

Table 2.1: QCI levels in LTE QoS profile [34].....	43
Table 3.1: Comparison of system level simulation software .....	62
Table 3.2: Simulation parameters for a single eNodeB.....	68
Table 3.3: Test parameters for UEs.....	69
Table 3.4: Correlation between Throughput and transmitted SINR with recommended data rate .....	73
Table 3.5: Simulation parameters for a single eNodeB.....	76
Table 3.6: Correlation between Throughput and transmitted SINR with recommended data rate .....	79
Table 4.1: Proposed look-up table for the uplink Content-Aware RRM model .....	82
Table 4.2: Comparison of Baseline and Content-Aware RRM models at UE velocity = 72 km/h.....	88
Table 4.3: Comparison of Baseline and Content-Aware RRM models at UE velocity = 50 km/h.....	90
Table 4.4: Comparison of Baseline and Content-Aware RRM models at UE velocity = 5 km/h.....	93
Table 4.5: Proposed look-up table for downlink content-aware RRM model .....	96
Table 4.6: 4-bit CQI table [33].....	97
Table 4.7: Comparison of Baseline and Content-Aware RRM models at UE velocity = 72 km/h.....	102
Table 4.8: Comparison of Baseline and Content-Aware RRM models at UE velocity = 50 km/h.....	105
Table 4.9: Comparison of Baseline and Content-Aware RRM models at UE velocity = 5 km/h.....	107
Table 5.1: Technical specifications of three PodNode variants [92].....	119
Table 5.2: Proposed look-up table for uplink practical PodNode testbed.....	136
Table 5.3: Performance of content-aware RRM model for emulated uplink video delivery .....	137
Table 5.4: Performance of content-aware RRM model for simulated uplink video delivery .....	138

## **List of Abbreviations**

2G – Second Generation

3G – Third Generation

3GPP - 3<sup>rd</sup> Generation Partnership Project

4G – Fourth Generation

16-QAM – 16-Quadrature Amplitude Modulation

64-QAM – 64-Quadrature Amplitude Modulation

AMC – Adaptive Modulation and Coding

API – Application Programming Interface

APP – Application layer

ARP - Allocation Retention Priority

ARQ – Automatic Repeat Request

AVC – Advanced Video Coding

BE - Best Effort

BLER – Block Error Rate

BS – Base Station

CBR – Constant Bit Rate

CDMA – Code Division Multiple Access

CLO – Cross-layer Optimisation/Optimiser

COFDM – Coded Orthogonal Frequency Division Multiplexing

CQI – Channel Quality Indicator

CSI – Channel state information

CSMA – Carrier Sense Multiple Access

DFT – Discrete Fourier Transform

DFTS-OFDM – Discrete Fourier Transform Spread- OFDM

DwPTS – Downlink Pilot Time Slot

eNB/eNodeB – enhanced-NodeB

EPC – Evolved Packet Core

EPS – Evolved Packet System

ertPS – enhanced real-time Polling Service

E-UTRAN – Evolved Universal Terrestrial Access Network

FDD – Frequency Division Duplex

FDMA – Frequency Division Multiple Access

FDPS – Frequency Domain Packet Scheduler

FTP – File Transfer Protocol

GA – Genetic Algorithm

GBR – Guaranteed Bit Rate

GPLv2 – General Public License version 2

GPRS – General Packet Radio Service

GTP – GPRS Tunnelling Protocol

GUI – Graphical User Interface

HARQ – Hybrid Automatic Repeat Request

HD – High Definition

HDTV – High Definition Television

HeNB – Home eNB

HSPA – High Speed Packet Access

HTTP – Hypertext Transfer Protocol

IMS – IP Multimedia Subsystem

IMSI – International Mobile Subscriber Identity

IMT-Advanced – International Mobile Telecommunications-Advanced

IMT-2000 - International Mobile Telecommunications-2000

IP – Internet Protocol

IPv6 – Internet Protocol version 6

ISI – Inter Symbol Interference

ITU – International Telecommunication Union

JPEG – Joint Photographic Experts Group

LA – Link Adaptation

LAN – Local Area Network

LTE – Long Term Evolution

LTE-Advanced – Long Term Evolution-Advanced

MAC – Medium Access Control layer

MCS – Modulation and Coding Scheme

MIMO – Multiple Input Multiple Output

MIPv6 – Mobile Internet Protocol version 6

MME – Mobility Management Entity

MPEG-4 – Motion Picture Experts Group-4

MS – Mobile Station

MU – Mobile Unit

NMS – Network Management System

NRT – Non-Real-Time

NS – Network Simulator

OEM – Original Equipment Manufacturer

OFCOM – Office of Communications

OFDM - Orthogonal Frequency Division Multiplexing

OFDMA – Orthogonal Frequency Division Multiple Access

PCFICH – Physical Control Format Indicator Channel

PCRF – Policy and Charging Rule Function

PDCCH – Physical Downlink Control Channel

PDCP – Packet Data Convergence Protocol layer

PDN – Packet Data Network

PF – Proportional Fair

PGW – Packet Data Gateway

PHY – Physical layer

PLR – Packet Loss Ratio

PoE – Power over Ethernet

PRB – Physical Resource Block

PS – Packet Scheduler/Scheduling

PUCCH – Physical Uplink Control Channel

PUSCH – Physical Uplink Shared Channel

QCI – QoS Class Identifier

QoE – Quality of Experience

QoS – Quality of Service

QPSK – Quadrature Phase Shift Keying

RAN – Radio Access Network

RB – Resource Block

RE – Resource Element

RF – Radio Frequency

RLC – Radio Link Control layer

RNC – Radio Network Controller

RNTI – Radio Network Temporary Identifier

RR – Round Robin

RRC – Radio Resource Control

RS – Relay Station

RS – Reference Signal

RT – Real-Time

RTSP – Real-Time Streaming Protocol

rtPS – real-time Polling Service

SC-FDM – Single Carrier-Frequency Division Multiplexing

SC-FDMA – Single Carrier-Frequency Division Multiple Access

SGW – Serving Gateway

SINR – Signal to Interference plus Noise Ratio

SISO – Single Input Single Output

SNR – Signal to Noise Ratio

SRS – Sounding Reference Signal

SVC – Scalable Video Coding

TCP – Transmission Control Protocol

TDD – Time Division Duplex

TDMA – Time Division Multiple Access

TTI – Transmit time interval

UDP – User Datagram Protocol

UE – User Equipment

UGS – Unsolicited Grant Scheme

UpPTS – Uplink Pilot Time Slot

UTRAN - Universal Terrestrial Access Network

VoIP – Voice over Internet Protocol

WAN – Wide Area Network

WCDMA – Wideband Code Division Multiple Access

WFA – Water-Filling Algorithm

WiFi – Wireless Fidelity

WiMAX – Worldwide Interoperability for Microwave Access

WSN – Wireless Sensor Network

# 1 INTRODUCTION

The demand for wireless communication services in recent years has been enormous and continues to grow. The performance of cellular multiple access wireless communication systems regarding user demands, mobile devices, network infrastructure sophistication, as well as resource-consuming, multimedia services for users continues to present new and emerging challenges. Furthermore, while enabling the mobility of users; future systems must assure quality-of-service (QoS) for all customers which is an extremely important requirement for network operators and subscribers. This is because QoS defines the priorities for certain customers/services during the time of high (i.e. peak) congestion in the network.

Motivated by the increasing demand for mobile broadband services with higher data rates and QoS, a novel modulation/multiple access technique called Orthogonal Frequency Division Multiple Access (OFDMA), which is a combination of Frequency Division Multiple Access (FDMA) and Orthogonal Frequency Division Multiplexing (OFDM), has been recommended by the ITU as core Physical (PHY) layer technology for the next generation of IMT-Advanced systems [1]. In OFDMA, the base stations enable multiple users to transmit simultaneously on different subcarriers during the same symbol period. What makes OFDMA stand out is its flexibility in radio frequency allocation and inherent resistance to frequency selective multipath fading. This novel modulation/multiple access technique has been incorporated in the IEEE802.16e/m (Mobile WiMAX) and 3GPP Long Term Evolution-Advanced (LTE-Advanced) standards due to their superior properties. However, due to the time-varying nature of the wireless channel, providing QoS guarantees in the multiuser environment, will continue to be a significant challenge.

## 1.1 Research Motivations

People are becoming increasingly familiar with using wireless network mediums to transfer various forms of data such as emails, images and videos, all of which benefit from fast-growing wireless communication technologies. As more and more users gain access to wireless broadband systems and services, the network traffic in-turn is becoming increasingly congested. This situation becomes increasingly worse when users are using multiple or heterogeneous services concurrently, especially broadband video streaming applications and dynamically moving from one cell to another cell simultaneously. This leads towards the importance of needing Radio Resource Management (RRM) to manage these type of situations effectively. Radio Resource Management (RRM) is critical to achieving the desired performance requirements by managing key components of both the PHY and MAC layers [2]. Also, this component is crucial for OFDMA wireless broadband networks where scarce spectral resources are shared by multiple users in the same transmission channel. This concept is fortunately well developed, as several techniques currently exist which are implemented in the latest releases of IEEE802.16m and 3GPP LTE Release 10, also known as 4G systems.

However, the IMT-Advanced standard does not cover the aspects of RRM open issues as all IMT-Advanced developers especially researchers, device manufacturers and vendors can invent and implement their own novel algorithms to optimise network throughput and to provide QoS guarantees. One of the techniques used for RRM in IMT-Advanced is cross-layer optimisation (CLO) which usually involves the interaction between the PHY and MAC layers before appropriate resource scheduling can be planned and implemented. In the future, it will be vital to know the type and structure of information content for efficient communication beforehand so that more efficient resource scheduling decisions can be made earlier and pre-empted. This calls for the interaction between the lower layers with, the higher layers especially

the APP layer. Furthermore, the APP layer is not part of the IMT-Advanced standard [21] because it only covers the PHY and MAC layers [3 - 6], and therefore enables the opportunity for further research in this area to be performed. Notably, any new methods for RRM should be made backwards compatible with any legacy standards and systems as dictated by 3GPP. For mobile broadband users who are always travelling or ‘on the move’, it would be interesting to examine just how much their mobility could affect the performance of their services, especially for real-time applications such as video streaming/conferencing and VoIP services.

## **1.2 Research Background**

Many researchers have developed new RRM techniques to improve the performance of the IMT-Advanced system and to instil some degree of fairness or equity among the users; however, RRM research for specific applications, e.g. broadband video application, is limited in this area. Authors in [7] and [8] introduced generic end-to-end cross-layer QoS mapping architecture for video delivery over a wireless environment. However, the framework does not consider the mobility of end-users, and furthermore, it was not intended to be implemented explicitly in WiMAX or LTE-Advanced.

Another critical issue regarding video applications is within the healthcare area, and in particular for mobile healthcare. Authors in [9] introduced a novel segmented distribution framework to support object-based MPEG-4 video streams over a WiMAX network. By using a coded representation of media objects, each segmented video stream (called Elementary Stream) was treated as a part of a complex audio-visual scene, which could be perceived and processed separately. A cross-layer mapping table was also introduced to set up the matching rules between the individual segment video stream and the assigned QoS class from the APP layer down to the MAC layer for delivering packets through the protocol suite. However, the

system only considers uplink communication, and the cross-layer mapping table does not consider PHY layer information. Furthermore, most video distribution techniques aim at delivering MPEG streams with a defined recommendation for the protocol stack exploited within the communication procedures which means, that a WiMAX base station (BS) would misjudge the bandwidth requirement and could allocate excess bandwidth to the mobile terminal for the uplink video delivery.

In [10], we proposed cross-layer scheduling for a WiMAX disaster management situation. In a typical operation, real-time applications are connected to UGS, rtPS, and ertPS QoS classes while non-real-time applications are linked to nrtPS and BE. By using a cross-layer approach, we realigned or rescheduled the non-real-time applications to rtPS QoS and the real-time applications to BE QoS with the aim to investigate the possibilities of the BE service class producing improved performance more than the rtPS service class. However, there are only a certain number of user combinations and QoS, where, the BE QoS class demonstrates higher throughput than that of the rtPS class. Also, the aspect of the users' mobility has not been taken into consideration.

In a separate development, WINNER+ developed a new cross-layer optimiser (CLO) implemented in Traffic-Aware RRM [11], through the optimisation between the MAC and APP layers. However, the scheduler allocates resources based on the number of arriving packets or network traffic, (i.e., the required data rates, delay constraints of the packets and the channel qualities of the users) and does not consider the content types of the packets. Hence, this CLO concept requires further enhancement and a new technique to be investigated, namely "CONTENT AWARE RADIO RESOURCE MANAGEMENT" or CARRMa. This CLO concept will be expanded from the PHY layer up to the APP layer and will utilise specific properties of the data transmitted over the network while ensuring backward compatibility with

legacy standards and systems.

### **1.3 Research Objectives**

This thesis focuses on the development of cross-layer optimisation for both the uplink and downlink transmission of an LTE network as part of the RRM technique to leverage on system capacity.

The objectives of this thesis are:

1. To establish new sets of criteria for RRM to further optimise wireless broadband network performance and to maintain the QoS requirement for IMT-Advanced;
2. To design a new cross-layer optimiser (covering the APP & PHY layers) to produce an optimal solution for resource allocation techniques for a single user by taking into account the worst channel condition;
3. To compare the performance of the proposed CARRMa model with the baseline LTE RRM communication simulation model; and
4. To investigate and compare the baseline LTE model and the developed CARRMa model with the deployment of a real-time testbed.

### **1.4 Research Methodology**

The research will consist of two interrelated components: the theoretical and practical parts. In the theoretical part, we aim to develop optimisation criteria for the proposed CARRMa technique and optimise the said criteria under the various channel and content conditions. In the practical part, we aim to conduct extensive computer simulations which will serve to cover the concept of OFDMA, channel state information (CSI), based on the theoretical model developed earlier. This will be later supported by undertaking practical investigations at Rinicom Ltd. [87],

a UK-based wireless broadband company, and lastly, producing practical recommendations for the CARRMa setting for a different channel and data conditions.

## **1.5 Research Contributions**

The contributions made through this thesis are summarised as follows:

- i) Identifying the performance behaviour of video streaming packets for a particular UE towards measured SINR for various distances between the eNodeB and UE in a single cell for both uplink and downlink transmissions.
- ii) Based on the results from Part i), the author proposes to construct a new look-up table for each uplink and downlink video packet transmission which will update the video data rates based on the channel estimation measured at either the eNodeB or at the UE.
- iii) The proposed look-up table in Part ii) is used to design a content-aware RRM model which utilises cross-layer optimisation to maximise output performance of the LTE system.
- iv) The development of a practical testbed by using PodNode technology developed by Rinicom Ltd. to perform practical comparisons with the theoretical simulation models for both the LTE baseline model and the proposed CARRMa model.

## **1.6 Thesis Outline**

This thesis is organised into the following sections. Chapter 2 presents an overview of LTE Release 8 and 10, including the architectures and protocol stacks. Further explanations are directed to the E-UTRAN where all the RRM functions take place in the eNodeB. Several areas of interest on the RRM methods, especially the aspects of video data transmission for LTE are also presented with particular focus on the cross-layer design to achieve specific RRM

objectives along with existing primary problems highlighted.

Chapter 3 discusses the development of the classical or baseline LTE communication simulation model together with the simulation tools employed for the simulation and starts with a brief description of the study and comparison of various simulation software before selecting the software deemed most suitable for performing the LTE simulation. The software selected is NS-3 and MATLAB. The software will be used for the baseline LTE simulation model based on the described topology to be developed and simulated for various distances between the eNodeB and the UEs for both uplink and downlink transmissions. Several important output performance parameters including user throughput and SINR values, focusing only on the video streaming application, are recorded before relevant graphs are plotted. Finally, the chapter introduces a summary determining the correlation between the measured SINR and its corresponding throughput.

Chapter 4 discusses the development of the content-aware RRM model resulting from the correlation between the measured SINR and its throughput hypothesised as presented in Chapter 3. Cross-layer optimisation for LTE system using a look-up table is proposed in which the video data rates can be dynamically adjusted depending on the measured SINR on either side of the communications link. Extensive simulations are conducted for three different UE velocities for both uplink and downlink transmissions to evaluate the effectiveness of the proposed model and the baseline model.

Chapter 5 discusses in detail the practical investigation activities undertaken at Rinicom Ltd to perform the practical comparisons with the theoretical simulation models developed in Chapters 3 and 4. Since the LTE infrastructure is not available at the company due to the spectrum licensing requirement by the OFCOM, UK, the simulation scenarios are emulated using PodNode technology, together with other hardware and software components that provide

support to the overall LTE emulation activities to serve as the LTE platform. Two experiments are conducted during the emulation process in which the first experiment is to correlate the measured SINR and the corresponding throughput for the baseline model in the uplink with the one obtained in Chapter 3. The second experiment is to compare the performance of the proposed CARRMa model developed in Chapter 4, also in the uplink. The results obtained from both experiments are then presented and analysed. Lastly, Chapter 6 provides overall conclusions together with suggestions for future works.

## **2 RADIO RESOURCE MANAGEMENT IN LTE/LTE-ADVANCED SYSTEM**

Since the initial release of the LTE Release 8 standard in 2008, some improvements and amendments have been added to meet the IMT-Advanced requirements recommended by the ITU. The limitations of the first version were overcome in subsequent releases of the standard in which carrier aggregation is implemented to achieve up to 100 MHz transmission bandwidths [12 - 13]. Besides the bandwidth requirement, it is useful to note that the demanding targets of 4G systems regarding QoS and data rates can only be achieved with effective Radio Resource Management (RRM). In this chapter, an overview of the LTE Release 10 (LTE-Advanced) standards and system architecture are provided, beginning with the evolution of the standards which is next followed by the description of the LTE system in which the work in this thesis is based upon. The previous and current research interests in RRM for those systems are also highlighted in this chapter.

### **2.1 Introduction**

Currently, the ITU is working to enhance the system requirements for next-generation mobile communication systems called IMT-Advanced and beyond. The IMT-Advanced systems are mobile broadband communication systems which include new capabilities that go far beyond those of the IMT-2000 family of systems such as wideband code division multiple access (WCDMA) or WiMAX and LTE. The main reason why the ITU has introduced IMT-Advanced is to enhance the capability of prior technology and to eliminate the limitations in existing communication networks to provide a much higher level of service. The performance of IMT-Advanced will support low to high mobility of applications; 100 Mbit/s for high and 1 Gbit/s for low mobility conditions [14 - 16].

In response to the recommendations proposed by the ITU, 3GPP has proposed ‘Long Term Evolution’ which is the name provided to the new standard developed by 3GPP to meet the enormous market demands for throughput. LTE is the next evolution of 2G, and 3G systems and the performance level of the system is expected to be on par with those of current wired networks.

The LTE/EPC standardisation project commenced in December 2004 by the 3GPP RAN working groups to develop a feasibility study for an evolved UTRAN and for all IP-based EPC. The initial phase of the project was called the ‘Study Item’ phase. In December 2007, the specifications for all LTE functions were completed while the specifications for the EPC functions achieved significant milestones for interworking with 3GPP and CDMA networks. Subsequently, in 2008, the 3GPP working groups hastened to complete all protocol and performance specifications where the groups finally completed the tasks by December 2008 with Release 8 being made available [17].

LTE is a radio access technology based on Orthogonal Frequency Division Multiplexing (OFDM), with conventional OFDM on the downlink and single carrier frequency division multiplexing (SC-FDM) or more specifically, discrete Fourier transform spread OFDM (DFTS-OFDM) [18] on the uplink. The purpose of having a different type of radio interface on the uplink is because SC-FDM can reduce terminal power consumption, allowing for a more efficient power-amplifier operation. Also, equalisation in conventional OFDM can efficiently eliminate the inter-symbol-interference (ISI) problem in the received signal [19].

## **2.2 LTE Architecture**

In any cellular network, the network functions can be divided into two parts: the radio access network part and the core network part. Functions such as modulation, handover and header compression are part of the access network, while other functions such as mobility management and charging, are part of the core network. In LTE, the radio access network is called E-UTRAN, and the core network is called EPC [17] as shown in Figure 2.1.

*Radio Access Network:* E-UTRAN, the radio access network of LTE, supports all services including real-time over shared packet channels. Consequently, by using packet access, better integration among all multimedia services, wireless and fixed services can be achieved. The central philosophy behind LTE is to reduce the number of nodes, which as a result, LTE developers then decided to adopt single-node architecture. Given this decision, the previous node in the WCDMA/HSPA radio access network, namely the Radio Network Controller (RNC), is merged with its Node B, thereby leading to higher complexity for the new base station in LTE, called eNB (Enhanced Node B). Since the eNBs are fast becoming more complicated than their predecessor (UTRAN), additional tasks and functionalities can now be performed, including radio resource management functions.

*Core Network:* The new core network is the result of the radical evolution of third-generation systems which cater for the packet-switched domain only. Therefore, a new name is given, the Evolved Packet Core (EPC). Similar philosophy towards the LTE radio access network is applied again to its core network, which results in minimising the number of nodes. The EPC splits the user data flows into data and control planes. For each plane, a specific node is defined together with the generic gateway that links the LTE network to external networks such as the internet and other systems.

The EPC consists of several functional entities:

- (i) The MME (Mobility Management Entity): is responsible for processing signalling messages in the control plane and to manage the connections for subscribers.
- (ii) The Serving Gateway: acts as the router to other 3GPP technologies and serves as the packet data interface for E-UTRAN.
- (iii) The PDN Gateway (Packet Data Network): is the router to the Internet and hence, the termination point for the sessions towards the external packet data network.
- (iv) The PCRF (Policy and Charging Rules Function): supports the policy-making process and manages tariff charges for all subscribers.

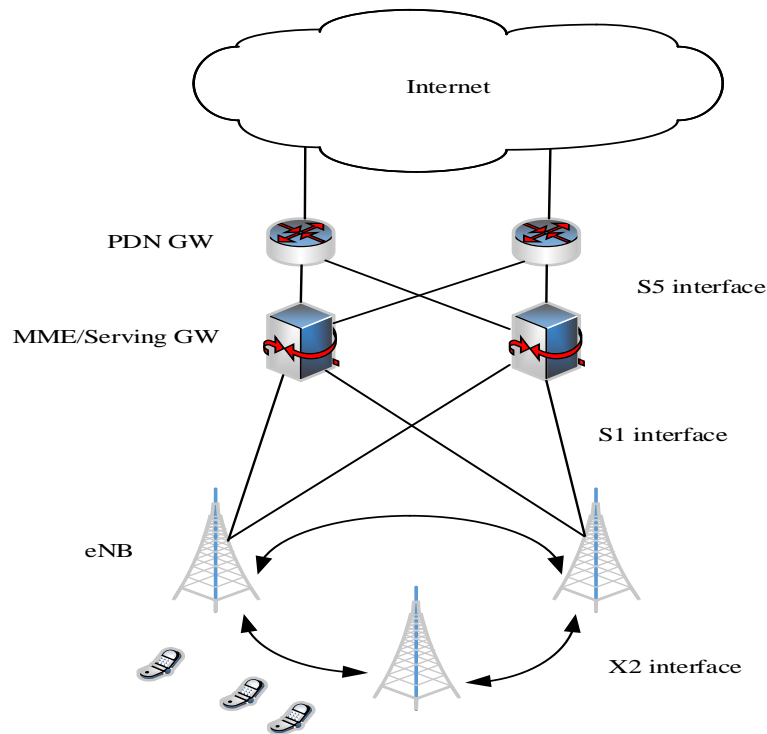


**Figure 2.1:** LTE Release 8 architecture [17]

Figure 2.2 illustrates the basic protocol structure of LTE. Some of the tasks that are performed by both the radio link control (RLC) and the medium access control (MAC) layers are related to data flow multiplexing and retransmission handling. In the physical layer, a series of processes occur before the information data is ready to be transmitted. The data is first turbo coded and then, modulated using one of the following modulation techniques: quadrature-phase shift keying (QPSK), 16-QAM, or 64-QAM, followed by OFDM modulation. The OFDM subcarrier spacing is set at 15 kHz. To prevent the problem of multi-path delay spread, two different cyclic-prefix lengths are employed in both the downlink and uplink. For most scenarios, a normal cyclic prefix length of 4.7  $\mu$ s is used whereas, for highly dispersive environments, an extended cyclic prefix length of 16.7  $\mu$ s is used, instead.

In the downlink, distinct types of multi-antenna processing are applied, preceding the OFDM modulation. Also, cell-specific reference signals are transmitted in the downlink to perform channel estimation and measurements for several reasons including coherent demodulation, mobility management and channel state information. The LTE transmitted signal is built upon multiple 1-ms duration subframes in which each subframe comprises of 12 or 14 OFDM symbols, depending on which type of cyclic prefix is used. Figure 2.3 illustrates the formation of a radio frame by cascading ten subframes together. As a result, of the 1 ms short subframe duration, small delays are unavoidable for both the user data and the control signals which include the hybrid automatic repeat-request (ARQ) feedback and channel-quality feedback from the user terminals to the eNB. One distinct feature of the downlink and uplink protocol, as shown in Figure 2.2, is the presence of DFT precoder only in the uplink transmission. This DFT precoder is used preceding the OFDM modulator to produce SC-FDM or DFTS-OFDM symbols while preserving the orthogonality among the subcarriers [20].

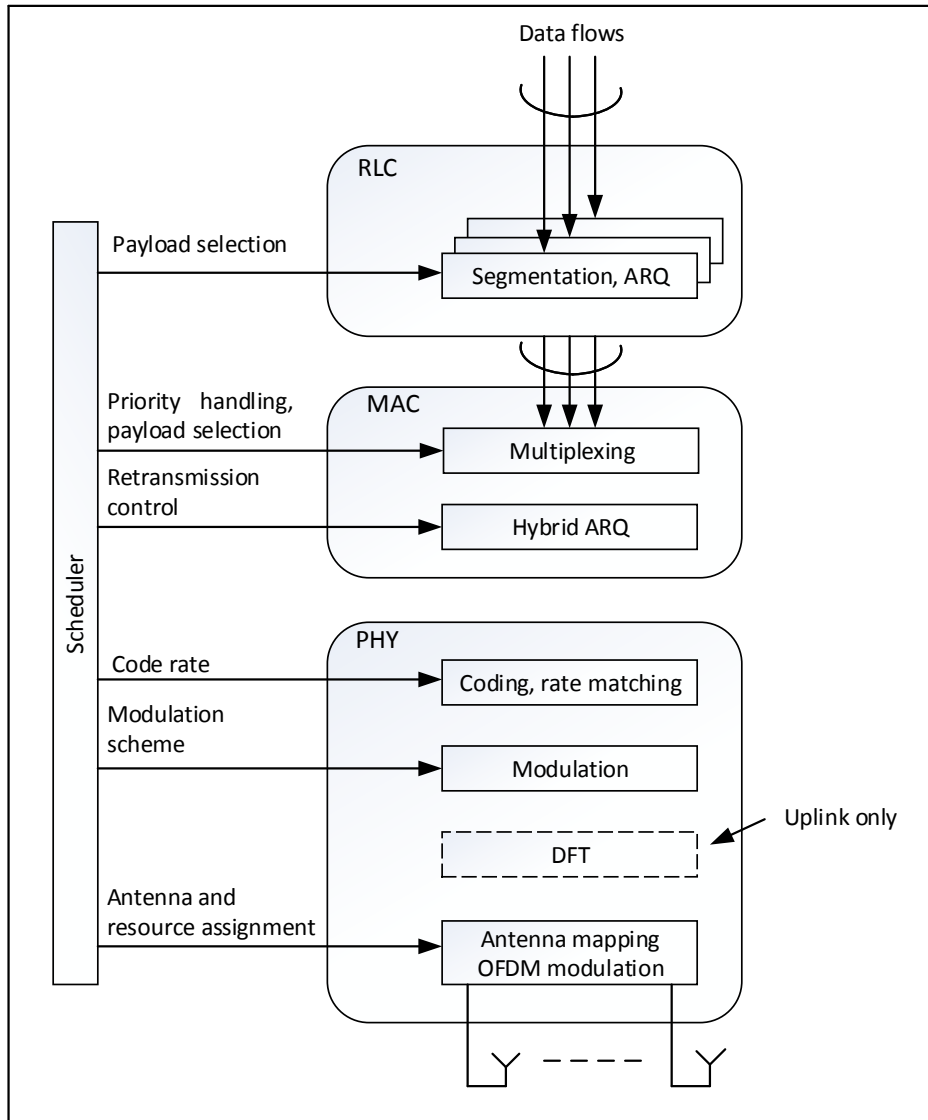


**Figure 2.2:** Basic LTE protocol structure [20]

LTE can operate in both Frequency Division Duplex (FDD) and Time Division Duplex (TDD) modes as depicted in Figure 2.3. Even though the time domain representation is mostly the same for both duplex modes, one of the most significant differences between the two, is the existence of a unique subframe in the TDD mode. The purpose of this particular subframe is to provide the necessary guard time for downlink-to-uplink switching.

In the case of FDD, two carrier frequencies are allocated for its operation, one for downlink transmission ( $f_{DL}$ ) and one for uplink transmission ( $f_{UL}$ ). In each transmission, ten subframes are cascaded together to form the radio frame in which both the uplink and the downlink transmissions can occur simultaneously within a cell.

In the case of TDD, only one single carrier frequency is present, and hence, the downlink transmissions are continuously alternating with the uplink transmissions to avoid colliding with each other in the same cell. As FDD requires a guard band between the two uplink and downlink frequency bands, the TDD however, requires a guard period for its operation. It is realised by splitting one or two of the ten subframes in each radio frame into three special fields, namely a Downlink Pilot Time Slot (DwPTS), a guard period and an Uplink Pilot Time Slot (UpPTS). The function of the downlink field, DwPTS is the same as any other downlink subframe whereby data transmission can be performed using this field. The uplink Pilot Time Slot (UpPTS), however, is usually used for channel sounding purposes and connection requests by user terminals.

Despite the significant differences between the FDD and TDD modes mentioned earlier, it is worth noting at this juncture, that all baseband processing is virtually identical for both duplex modes, making it possible to develop low-cost terminals supporting both FDD and TDD operation modes [6], [19].

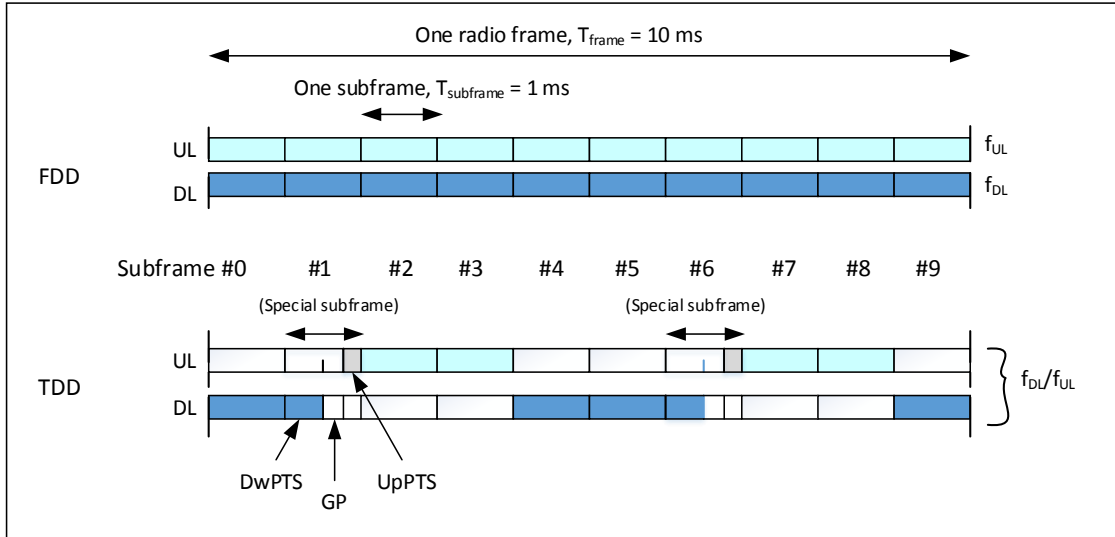


**Figure 2.3:** LTE frame structure [6] [19]

## 2.3 LTE-Advanced Architecture and Protocol Stack

LTE Release 10 was finalised towards the end of 2011 by 3GPP which conforms to the IMT-Advanced specifications. Currently, the LTE Release 11, 12, 13 and 14, that are the enhancements to the previous completed LTE Release 10 specification are being researched to provide better performance. The capability of LTE-Advanced is highly recommended by 3GPP because it can support transmission bandwidths up to 100 MHz and increases the capacity of the UE during transmission and reception processes [1], [13], [22]. This is in line with the objectives of the targets set for IMT-Advanced, which are higher data rates, improved coverage, better QoS performance and equality for all users. Also, it is further capable of providing support for positioning services, broadcast/multicast services and enhanced emergency-call functionality [5], [16]. Figure 2.4 shows the E-UTRAN architecture for LTE-Advanced, which complies with the IMT-Advanced specifications. The most important and the only available node in E-UTRAN architecture is the enhanced Node B (eNB or eNodeB). eNB, which is also

the base station in LTE, that provides the air interface for the UE by establishing communication links through the user plane and control plane termination protocols. Each eNB can control one or more E-UTRAN cells and can also interconnect with its adjacent eNBs through the X2 interface. Also, lower-cost Home eNBs (HeNBs also known as femtocells), that are introduced primarily to improve indoor coverage can be linked up with the EPC directly or via a gateway where more HeNBs can be further supported [23]. Furthermore, 3GPP is also proposing further strategies to enhance network performance by applying relay nodes.

As mentioned earlier, eNBs provide the E-UTRAN with the necessary user and control plane termination protocols. Figure 2.5 displays a graphical representation of both protocol stacks. In the user plane, the related protocols consist of the Packet Data Convergence Protocol (PDCP), the Radio Link Control (RLC), Medium Access Control (MAC), and the Physical Layer (PHY) protocols. The control plane stack, however, has an additional protocol, namely, the Radio Resource Control (RRC) protocol.

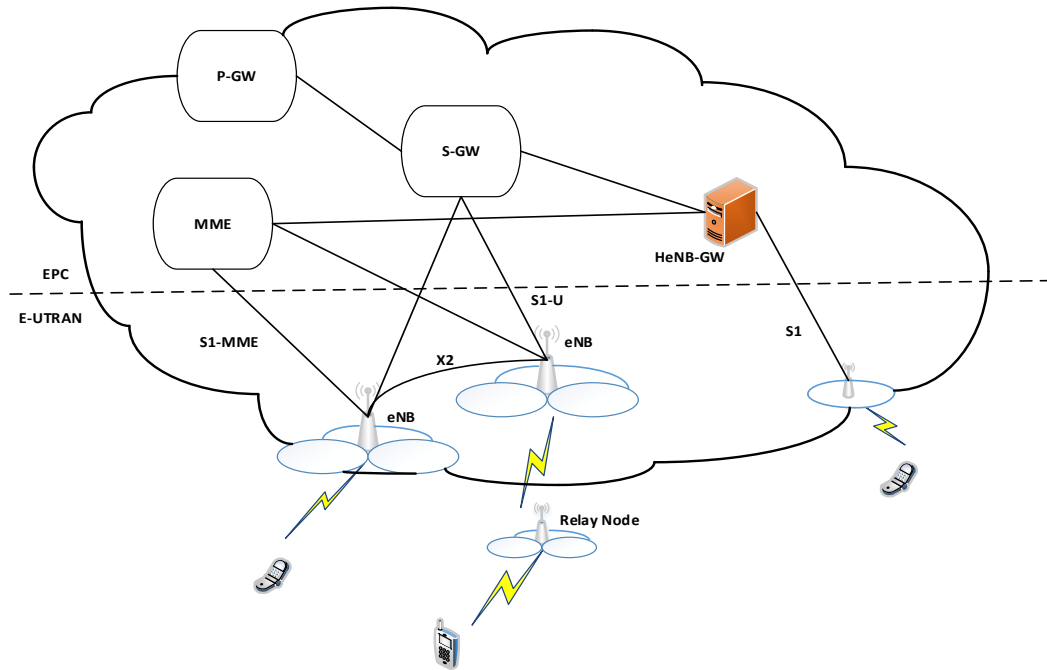


**Figure 2.4:** LTE-Advanced E-UTRAN architecture [23]

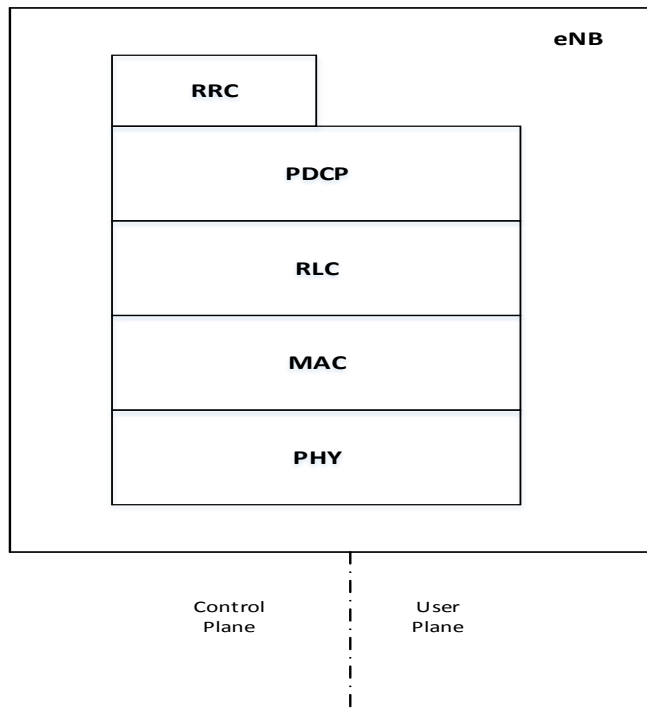


**Figure 2.5:** Protocol stack [23]

## 2.4 eNodeB Protocol Stack and RRM Functions

Radio Resource Management (RRM) is one of the key components of the OFDMA modulation technique in a wireless system. RRM is the system level control of co-channel interference and other radio transmission characteristics in wireless communication systems, for example, in cellular networks such as LTE, wireless networks and broadcasting systems [16]. It can also be defined as a control mechanism for the entire system used to manage radio resources in the air interface within a cellular network [16], [28]. Both LTE and LTE-Advanced technologies implement resource management to ensure that the process of data transmission and reception are carried out efficiently. Basically, RRM analyses several factors such as traffic load, interference, noise and coverage to produce efficient data transmission and high capacity. RRM functions should further consider the constraints imposed by the radio interface to make decisions regarding the configuration of different elements and parameters influencing air interface behaviour [16]. As in the case of the LTE/LTE-Advanced system, all RRM functions occur in the eNodeB such as transmission power management, mobility management and radio resource scheduling [29].

Figure 2.6 illustrates the user plane and control plane protocol stack at the eNodeB with the mapping of the primary RRM functions to the corresponding layers [30 - 31]. The user plane protocol at the eNodeB incorporates the packet data convergence protocol (PDCP) at layer 3, followed by the radio link control (RLC) and the medium access control (MAC) protocols at layer 2. One of the RLC functions is to provide an outer ARQ mechanism, whereas the MAC function involves asynchronous hybrid ARQ. It is possible for the outer ARQ and hybrid ARQ functions to closely interact with each other for additional performance optimisation since both, RLC and MAC are in the same layer. The PDCP function manages each data flow, also called 'bearer', coming from the access gateway. In contrast, the control plane protocol stack is

terminated at the eNodeB, with the radio resource control (RRC) serving as the main function at layer 3.

There are various RRM functions at the eNodeB which can be exploited from layer 1 to layer 3 as shown in Figure 2.6. At layer 3, the related RRM algorithms such as admission control, QoS management and semi-persistent scheduling, are defined as semi-dynamic mechanisms. Usually, they are implemented during the setup of new data flows or during non-frequent reconfigurations. A different situation for layers 1 and 2 exists, however, because the RRM functions are more dynamic as new decisions need to be made at every transmission time interval (TTI) of 1 ms.

The physical layer (PHY) of the eNodeB is based on OFDMA, applying the shared channel concept for unicast data transmission which is like IEEE 802.16 (WiMAX). Figure 2.7 illustrates the PHY time-frequency resource space representation for one TTI or duration of 1 ms. Each TTI possesses 14 OFDM symbols if the default configuration with a short cyclic prefix is assumed [32]. In each downlink TTI, data transmission and control information are multiplexed at the same time, where the first 1 to 3 OFDM symbols in a TTI are reserved for downlink control channels such as the physical control format indicator channel (PCFICH) and the physical downlink control channel (PDCCH). The PCFICH determines the time duration of the control channel space (1 – 3 OFDM symbols), while the PDCCH transports the dynamic scheduling grants for both downlink and uplink. The remaining OFDM symbols within the TTI can be used for transmitting common or dedicated reference signals and more importantly, user data. The PDCCH also carries information on the used modulation and coding scheme and the user's frequency domain allocation indicator, etc. The combination of the allocated resources and the modulation and coding scheme can additionally be used to define the used transport

block size. With this information, the user can demodulate and decode the transport blocks transmitted by the eNodeB.

In the frequency domain of the TTI, the resources are separated into equally-sized physical resource blocks (PRBs). Each PRBs contains 12 subcarriers, which is equivalent to a 180-kHz bandwidth, with a subcarrier spacing of 15 kHz [32]. The number of PRBs can be varied depending on various system bandwidth configurations (e.g. 25, 50 and 100 PRBs for system bandwidths of 5, 10 and 20 MHz, respectively). There are several reference symbols (also called pilots) allocated on the subcarrier symbols to provide reliable channel estimation at the mobile terminal, even though these are not shown in Figure 2.7. The data transmission in the downlink path is dependent on fast link adaptation by varying the modulation technique from quadrature phase shift keying (QPSK) to 64-quadrature amplitude modulation (64-QAM), assuming the transmit power of the PRBs for a user are equal and constant. This is in contrast to the PDCCH transmission where a fixed modulation (QPSK) is used, together with variable coding and dynamic power control to achieve sufficient reliability.

In Figure 2.6, the sole responsibility of the channel quality indicator (CQI) manager is to process received CQI reports from active users in the cell, which are later used for scheduling decisions and link adaptation purposes. The CQI feedback configurations can be carried out as follows:

- Measuring a wideband channel quality;
- Separate reporting for some subbands; and
- Reporting of the average channel quality of the best  $M$  subbands [33]. A sub-band, in this case, comprises  $k$  contiguous PRBs, in which the  $k$  and  $M$  values are determined by the specifications depending on the system bandwidth.

The first two configurations are used for selective frequency measurements, which are useful for the frequency domain packet scheduler (FDPS). CQI feedback may be configured periodically and requested by the eNodeB explicitly when scheduling a specific user in the uplink.

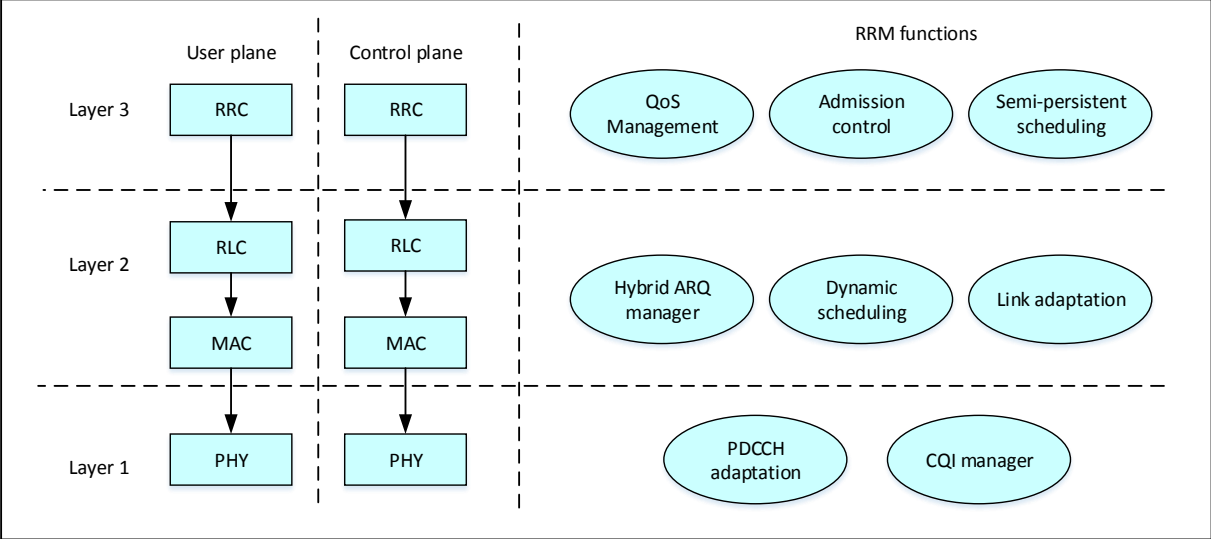


**Figure 2.6:** Overview of the eNodeB user plane and control plane architecture and the mapping of the primary RRM functions to the different layers [30]

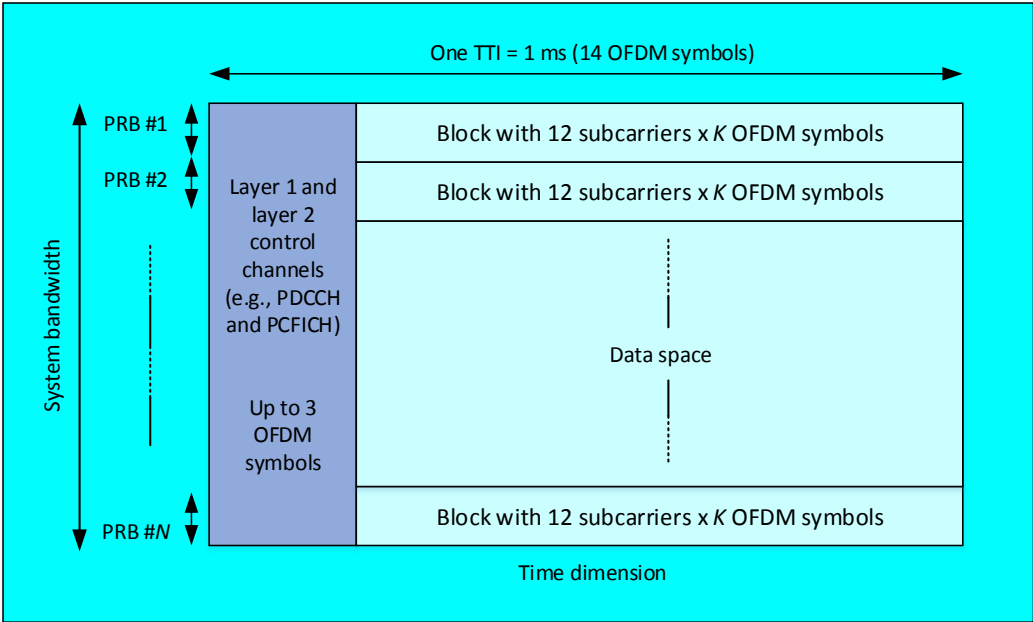


**Figure 2.7:** The downlink physical layer resource space for one TTI [30]

#### **2.4.1 Semi-Dynamic RRM Features (QoS Parameters, Admission Control and Semi-Persistent Scheduling)**

All semi-dynamic RRM functionalities such as QoS management, admission control and semi-persistent scheduling) are operated in layer 3 of the eNodeB's control plane as depicted in Figure 2.6. In the case of QoS management, each data flow (or bearer) is associated with a QoS profile containing the following downlink related parameters [34]:

- Guaranteed bit rate (GBR).
- Allocation retention priority (ARP).
- QoS class identifier (QCI).

The GBR parameter is specified only for GBR bearers while the parameter for non-GBR bearers is defined by an aggregate maximum bit rate. The ARP parameter is mainly related to priority settings when handling admission control decisions. The parameter is specified as an integer between 1 and 16. The QCI parameter acts as an indicator of a more detailed set of QoS attributes listed in Table 2.1. Such QCI parameters are the layer 2 packet loss rate and the packet delay budget. The information contained in both parameters can be used by the eNodeB to adjust the outer ARQ mechanism in the RLC layer, and the layer 2 packet delay budget can also be used by the packet scheduler in the eNodeB when prioritising specific queues to achieve the head-of-line packet delay targets.

Based on the QoS profile, the admission control function may decide whether to grant or reject radio or network access requested by new bearers in the cell. Some considerations might be considered by the admission control algorithm before decisions are made such as the current resource condition in the cell, the new bearers' QoS requirements, the related priority level and the present QoS level attained by active users in the cell. The situation where a new request may be granted is when the QoS estimated for the new bearer does not compromise the

QoS level of the currently active users in the cell having the same or higher priority as discussed in [35].

The fundamental semi-persistent scheduling principle in layer 3 is to allocate certain transmission resources periodically for a specific user or bearer. This is undertaken by the RRC protocol whereby a specific timing pattern is initially configured for the semi-persistent scheduled resources. The semi-persistent scheduling method represents regular scheduling of a fixed data amount, which is the reason why it is mainly intended for deterministic data flows such as voice over Internet Protocol (VoIP) service.

**Table 2.1:** QCI levels in LTE QoS profile [34]

QCI Number	Resource Type	Service Priority	Layer 2 Packet Delay (ms)	Layer 2 Packet Loss Rate	Applications
1	Guaranteed Bit Rate (GBR)	2	100	$10^{-2}$	Conversational voice
2		4	150	$10^{-3}$	Conversational video (live streaming)
3		3	50	$10^{-3}$	Real-time gaming
4		5	300	$10^{-6}$	Non-conversational video (buffered streaming)
5	Non-Guaranteed Bit Rate (Non-GBR)	1	100	$10^{-6}$	IMS (IP multimedia subsystem) signalling
6		6	300	$10^{-6}$	Video (Buffered Streaming), TCP, Web, e-mail, chat, file sharing, etc.)
7		7	100	$10^{-3}$	Voice, Video (Live Streaming), Interactive Gaming
8		8	300	$10^{-6}$	Video (Buffered Streaming), TCP, Web, e-mail, chat, file sharing, etc.)
9		9	300	$10^{-6}$	

#### 2.4.2 Fast Dynamic RRM Algorithms

The most important RRM entity at layer 2 is the dynamic packet scheduler (PS), which decides on resource scheduling by allocating PRBs every TTI to the users. It also performs link adaptation whereby a suitable modulation and coding scheme is assigned to the users, accordingly. The allotted PRBs and selected modulation and coding scheme are then transmitted to the targeted users using the PDCCH. The final objective of the scheduling mechanism is to maximise cell capacity, and concurrently, maintaining the minimum QoS requirements for the bearers while ensuring adequate resources are available for best-effort bearers which do not require strict QoS requirements [36]. It is important to note at this point, that scheduling decisions are decided on a per-user basis although a user may have one or more data flows. In a normal situation, an active user with a bearer may have at least two layer 2 data flows; the RRC

protocol governs one data flow in the control plane, and one or more data flows that are to be used in the user plane. The MAC protocol determines the amount of data to be transmitted from each data flow, depending on the transport block size scheduled for a certain user. The packet scheduler and the hybrid ARQ manager need to interact closely with each other as the former is also responsible for scheduling retransmissions. This is because in one TTI, the packet scheduler is not allowed to schedule both a new transmission and a pending hybrid ARQ transmission to a scheduled user at the same time, and therefore, must decide between the two transmissions making sure that the minimum QoS requirements are preserved. The link adaptation unit further assists the packet scheduler by relaying information on the supported modulation and coding scheme for a user based on the selected set of PRBs. The information provided by the link adaptation is decided based mainly upon the CQI feedback received from the users in the cell and the QoS requirements.

## **2.5 Research on RRM for LTE**

In recent years, RRM techniques have undergone extensive research to cater for the large targets in IMT-Advanced with the objectives of optimising network performance (network-centric), maintaining QoS requirements (user-centric) and providing fairness (equity) for all users. Depending on the ultimate objective established by network operators, Radio Resource Allocation (RRA) algorithms, which are part of the RRM, can also be designed to be fairness-oriented or by providing a trade-off between fairness and throughput [37]. For example, the Resource Allocation (RA) algorithm introduced in [38] provides a balance between efficiency and fairness which optimises system performance while producing improved performance, to guarantee the user's QoS requirement in a heterogeneous traffic condition. Several common RRM techniques implemented in many cellular systems are for power control, handover, load

and admission control and the most important, for scheduling [29], [39].

In wireless communication, scheduling plays a significant role in determining system performance such as the throughput, delay, jitter, fairness and loss rate [40 - 41]. Being different from wired cases, scheduling in LTE networks needs to consider unique characteristics such as the location-dependent channel status. It is well acknowledged that packet scheduling (PS), which is one of the core functionalities for radio resource management, is an essential element to enhance the performance of an LTE system. In efficiently utilising scarce radio resources, different PS algorithms, as a result, have been proposed and deployed.

In [42], a new packet scheduling (PS) framework called the adaptive time domain scheduler, with built-in congestion control has been added to existing conventional QoS aware PS algorithms for the LTE-Advanced downlink transmission. This framework optimises multi-user diversity in both time and frequency domains by jointly considering the channel condition, queue status and QoS feedback. Eventually, this technique improves QoS of real-time (RT) traffic and a fair share of radio resources to non-real time (NRT) traffic.

The authors, in [39], have proposed a new modified-proportional fair scheduler to further improve the throughput and spectral efficiency of an LTE system. Conceptually, the new scheduler divides a single subframe into multiple time slots and allocates the RBs to the targeted UE in all time slots for each subframe based on the instantaneous CQI feedback from the UEs. In that sense, no UEs will be left out of the scheduling process in all time slots. For the overall performance, the Modified-PF scheduler outperforms Round Robin (RR) and PF schedulers by almost 92 % of the RR throughput and significantly boosts the PF throughput by 10 %.

It is normal for each user to expect high throughput to enjoy various multimedia and data services regardless of their location and mobility. However, in cellular architecture, if a mobile station (MS) is located at the edge of a cell then it will experience severe path loss and

poor spectral efficiency as compared to the MSs that are near to the base station (BS). By virtue of Adaptive Modulation & Coding (AMC) which is one of the resource allocation techniques for the OFDMA system, it will select the lowest-order modulation scheme and high coding rate to maintain the link quality without increasing the signal power. Channel gain is obtained through multiuser diversity in which the BS will focus its communication with the nearby MSs having good channel condition. As a result, to satisfy the 'victimised' user's QoS requirement, an effortless way to solve the problem is by deploying relay stations (RSs) which can assist in data delivery. Many researchers have studied the advantages of deploying fixed relay stations in cellular architecture [43 - 44]. The relay stations can overcome the need for high transmission power and concurrently, can transmit at high forwarding data rates inside the BS remote areas while network infrastructure is minimally maintained. Due to this reason, the relaying system was chosen to maximise the uplink and downlink system throughput and its ability to relay information from the BS to the user to, thereby, improve system performance [13], [45]. However, as mentioned in [46], RS has a drawback whereby it consumes additional resources as compared to using the direct path. As a result, the signalling overhead for the relay communication will increase, which will naturally reduce the throughput gain. To some extent, delay-sensitive services such as video streaming and video gaming will be adversely affected due to the longer paths the signals need to travel [13]. Consequently, improved RRM techniques need to be developed to manage these issues.

Another RRA technique which focuses on network throughput is implemented in [47]. The strategy, known as the interference-aware RRM scheme, re-examines the system interference dynamics for a given sub-channel assignment to improve system throughput. It adopts 2-level optimisation as performed in [38] where subchannel allocation is followed by power distribution among the subchannels pre-assigned to a user. From a micro level

perspective, the new proposed scheme appends the basic Water Filling Algorithm (WFA) which results in the enhancement over the basic WFA and at the same time, power allocation calculations are also modified to achieve better throughput.

## **2.6 Cross-Layer Design for LTE**

Cross-layer design for achieving the desired performance in wireless networks is not a new area of research and started when wireless communication became more and more attractive to implement especially in remote areas where fixed-line communication was expensive to deploy. Although it may appear that the concept itself is violating the philosophy around the layering concept in networking, the complex issues related to wireless environments such as time-varying channels and propagation loss, suggests the need for cross-layer design to be considered.

Most of the cross-layer designs for radio resource management as in [48 - 49] involve the interactions between the MAC layer and the PHY layer, wherein the MAC layer, proper scheduling techniques are carried out based on specific QoS requirements for each user or data bearer depending on the channel state information feedback from the PHY layer. One interesting technique is shown in [50] where the cross-layer optimisation technique does not require CQI information to be fed back from the user's side. The real-time video packet transmission is undertaken by adapting the sent bit rate automatically, according to the estimated packet loss due to the expiration of the packet delay deadline based on queuing analysis by considering both the packets queuing delay and transmission delay. Ironically, this technique has somewhat deviated from the 3GPP standards which require the eNodeB to monitor the channel condition of each user continually.

In recent years, researchers and network engineers have felt the need to further increase

the performance of their system due to the ever-growing demand for data services, especially for video-related applications by users which have led to a higher volume of traffic at the eNodeB. Consequently, some of the initiatives that have been adopted include the APP layer as part of CLO techniques for radio resource decision making in LTE networks. With this type of cross-layer design architecture, the LTE/LTE-Advanced can achieve multitude objectives towards improving spectrum efficiency, multi-layer diversity gain, adapting to wireless channels and satisfying users within different traffic classes [13]. Most of the APP and MAC/PHY cross-layer architectures are targeted towards data-hungry services such as video streaming applications where high-quality video frames are adjusted and scheduled efficiently to a particular user or users while considering the channel state information for each user as demonstrated by [51 - 54]. In their methods, the video frames or the video encoding parameters are dynamically adjusted to suit the channel conditions for all users by employing the appropriate scheduling methods. However, the study on the performance parameters, such as system throughput, packet loss ratio and delay in a particular time for high delay non-tolerant services, such as video streaming applications, is not stated in those papers. This study is, therefore, considered to be important for network providers if those strict QoS requirements can be achieved for each real-time user.

In some research, the design of the cross-layer optimiser has grown even more complicated when more than two layers (i.e., PHY, MAC and APP layers) need to communicate with the cross-layer optimiser before decisive action can be taken. This means that more information is required to be relayed to the CLO including the channel status from the PHY layer, the queue status from the MAC layer and video content information from the APP layer. For example, the authors in [24] developed a 3-step approach in their video packets multi-user transmission involving all three layers. In the initial step, the video packets from the required

video streams are arranged based on their importance to the reconstructed quality and assigned with different priorities during transmission. Next, all available subchannels are allocated to each user equitably, according to the size of their chosen packet on the condition that the transmit power is equally distributed across all subchannels. Depending on the subchannel allocation outcome, a modified water-filling power distribution algorithm is applied to distribute the transmit power across the subchannels assigned to each MU. In [25], a different approach is adopted even though the cross-layer architecture still involves the APP, MAC and PHY layers. Besides adapting the source rate based on channel statistics in the APP layer, the authors have introduced a QoS-to-QoE mapping technique to adaptively estimate the visible loss of each video layer over time using ACK history. Alongside the channel state information, the QoS-to-QoE mapping technique has been used to select the suitable MCS in its link adaptation operation. Naturally, a slight violation of the 3GPP standard [21] is observed as the link adaptation is implemented primarily due to the channel condition in each user. In some instances, although the specifications established by 3GPP are met, the issues of MAC complexity and its practical implementation are considered as concerns, as proposed by [26]. This is when the genetic algorithm (GA)-based scheduler implemented together with the cross-layer optimiser, is applied to solve complex optimisation problems.

In previous papers, most cross-layer designs are focused on downlink transmissions. Recently, cross-layer optimisation for m-Health has been proposed by [27] to provide real-time emergency support for mobile patients using SVC multi-video transmission over LTE TDD-SC-FDMA uplink in a single cell. The cross-layer design strategy is to dynamically adjust the overall transmitted multi-video throughput to meet the available bandwidth without compromising the high-quality provision of diagnostic video sequences as compared to less critical ambient videos. Even so, it is the MAC scheduler in the eNodeB that determines the

suitable rates for the users in the cell to transmit which means; the UEs have no ability to make their own decisions.

Finally, cross-layer optimiser performance resulting from user mobility in the high-speed vehicular environment, such as in a high-speed train and the live transmission of flight recorder data, has been carried out by [75]. The study is carried out by implementing TCP and UDP based throughput measurements on an LTE base station emulator and a mobile radio channel emulator which includes SNR variations as well as user velocity emulation. Even though the study shows that LTE, with the cross-layer implementation, can provide reliable communication links in both high-speed scenarios, further study on normal vehicular and pedestrian scenarios is desirable to study the impact of cross-layer design on their performances.

## **2.7 Summary**

In this chapter, we presented an overview of LTE Release 8 and 10, together with their architectures and protocol stacks in which only the later release is in complete compliance with the IMT-Advanced requirements. We have also explained the importance of implementing the RRM functions at the eNodeB where critical decisions are made to accurately allocate and manage the limited radio resources to respectable users with the objectives of maximising network capacity and preserving QoS requirements. Also, research on RRM methods including those that involve cross-layer designs is described which provide options to network operators or vendors to cater for their own pre-set targets before actual deployment. However, we have identified several deficiencies on the current RRM methods needing to be addressed, especially those which employ cross-layer designs. Some of the issues raised by the author are related to limited consideration for backward and forward compatibility with legacy systems, the lack of a mobility study, the high complexity of the CLO design and the lack of a performance study

for certain users and a certain period. Due to the complexity of the wireless environment, a new RRM technique which involves cross-layer optimisation should be designed to overcome those issues mentioned previously and also, to improve the performance of the LTE system further while remaining forward and backward compatible with the LTE-Advanced standard itself and with legacy systems.

### **3 THE CLASSICAL (BASELINE) LTE SIMULATION MODEL**

The enormous demand for wireless broadband services globally has prompted the ITU to specify and release the latest mobile communication technology standard known as IMT-Advanced, which is the evolution from IMT-2000. In addition to supporting mobility, the candidates should be able to transmit high data rate applications of up to 1 GHz in low mobility and 100 MHz in high mobility. The most significant challenge faced by the two competitors, 3GPP LTE Release 10 and IEEE 802.16m for Mobile WiMAX, is not due to the specifications set out by the ITU, but instead on how both can realise reliable transmission links in a multiuser environment and in the event of extreme adverse channel conditions. This is where RRM has a vital role in achieving the targets set out in the standard.

This chapter presents the description of a classical LTE simulation model in LTE in which only basic RRM is applied to the system. This baseline model is important as a standard performing platform as it conforms to the LTE Release 8 standard mentioned in Chapter 2. Furthermore, this model will be used later to compare against the proposed content-aware RRM model in the following chapter. Besides, we need to study the impact of normal RRM towards the performance of the current LTE system while experiencing adverse channel conditions and to identify relevant criteria or parameters that could affect its overall performance. Before any simulations can be performed, a study on potential simulation software is needed. The following section will describe the simulation environment of the LTE network and compare various simulation software applications for consideration. This is then followed by the simulation and performance study of a classical or baseline LTE simulation model.

### **3.1 Simulation Environment**

It is acknowledged that simulation is a cost-effective way to evaluate the performance of a system. By conducting a simulation, an algorithm or a protocol for a system can also be included or added into the testing or applied to fine tune, before implementation or deployment to the real (live) system environment. Simulations may further reduce the time in obtaining the desired results which may take longer to achieve in a real system. By employing assumptions based on the original system, the simulation exercise is more straightforward without sacrificing or jeopardising the correctness of the final results.

From describing the details of the LTE system in the previous chapter, a simulation tool is required to evaluate the performance of the system. In this chapter, the simulation of the LTE network using a simulation tool is presented. Various tools available to simulate an LTE system are described followed by a description of the NS-3 and MATLAB software used for the simulation performed in this thesis.

### **3.2 Classification of Simulation Tools**

Simulation tools are classified based on the nature of their development [55]:

- Open-source or closed-source software: open-source software publicly and openly reveals its source code. Consequently, users or programmers can identify errors and report these errors them back to the maintainer(s) or developers. Furthermore, they can also modify or enhance the source code by adding new features and, later, publicise the updated (revised) software. The disadvantage of open-source software is related to the lack of accountability. Volunteers manage most open-source software projects. Since anyone can modify the software, there are no guarantees that the functionality or behaviour of the software will meet the users'

expectations. A different situation occurs for closed-source software, where software modifications can only be made by software developers who are responsible and accountable for the integrity and functionality of the software.

- Commercial or free software: usually, commercial software is well documented and further supported by the technical support group. It is possible for freely available software to lack adequate support and accountability despite being free of charge.
- Publicly available or in-house developed software: publicly available software is not linked to the two classifications noted above, which means, it may be open-source or closed-source software and commercially available or free of charge. A significant amount of time and effort can be saved instead of developing the same simulated software. Furthermore, publicly available software is frequently reviewed and scrutinised (rated) by the public which in some cases may characterise the software as being trustworthy. In contrast, internally developed in-house software, has more flexibility even though the developers have to spend considerable time and effort to develop the software. It can help others save substantial effort required to develop simulation software. Only the developers know what, where, when, why and how to make the necessary changes to the software.

### **3.2.1 OMNeT++**

OMNeT++ is a discrete event simulator, built primarily for modelling communication networks. OMNeT++ is publicly available and is licensed under an Academic Public License enabling the software to be freely available only for educational and research purposes.

OMNeT++ adopts a framework approach where necessary procedures and tools are provided to write (code) the simulations, instead of providing simulation components directly for communication networks or other domains. For example, various simulation models and frameworks are included in the INET framework, developed for the OMNET++ simulation environment [56]. The INET package includes a wide range of Internet stack models. Furthermore, other packages such as the Mobility Framework and Castalia [57] enhance the capability of the software to examine the mobility aspects of wireless networks and to simulate networks with low-power embedded devices such as mobile ad hoc networks, wireless sensor networks or body area networks.

OMNET++ simulations consist of so-called simple modules that implement the behaviour of a model, e.g. a certain protocol, where simple modules can be interconnected, forming a compound module. For example, a host node can be represented by a compound module if several simple modules providing the protocol models are joined together or combined. Even the network simulation implemented in OMNET++ is a compound module which is integrated with another compound module, like the host node as mentioned earlier.

The simple modules that are implemented in OMNET++ are based on the C++ programming language. Although, when these simple modules are assembled to form compound modules, leading towards the creation of the network simulation, a different scripting language needs to be used; namely NED, the network description language of OMNET++. NED is converted into C++ code when the entire simulation is compiled [58].

One exciting feature of OMNET++ is that it completely supports the graphical-user-interface (GUI) for simulation purposes [76], thereby making it simpler to observe the overall network topology and to modify the specific simulation parameters or models.

The development of the LTE module for OMNeT++ was carried out under a project called “SimuLTE” by the Computer Networking Group at the University of Pisa, Italy [59]. Most of the models developed conform to the standard, for example, the user plane aspects of the radio link and basic Serving Gateway (SGW) and Packet Gateway (PGW) functionality. However, some aspects of the technology were omitted, (e.g. the handover process and control plane implementation).

### **3.2.2 OPNET Modeler (Currently known as Riverbed Modeler [77])**

Considered to be one of the most widely used network simulation software by researchers and engineers, the OPNET Modeler or Riverbed Modeler provides a comprehensive communication network modelling solution among the OPNET product family. Like OMNeT++, the OPNET Modeler is a discrete event simulator and is easy to use due to its user-friendly GUI-based simulation environment. Furthermore, a complete set of tools for the model design, simulation, data collection and analysis are provided. The suitability of the OPNET Modeler application used as a platform for developing system models, incorporates various application standards for a standard-based local area network (LAN) and for wide area network (WAN) performance modelling, hierarchical internetwork planning, R & D of protocols and communication network architecture, mobile network, sensor network and satellite network [60].

OPNET is built using C and C++ source code blocks, and high-level user interfaces, supported by a vast library of OPNET specific functions. The hierarchical structure of OPNET modelling can be categorised into three primary domains:

- (i) Network domain – where the position and interconnection of communicating nodes need to be defined. Each network is represented by a block-structured data

flow diagram, consisting of networks and sub-networks, network topologies, geographical coordinates and mobility.

- (ii) Node domain – describes the interrelationships of the processes, protocols, and subsystems. In a node model, the functionality of every programmable block is defined by a given process model. The node model defines the objects in a network domain and the single network nodes (e.g., routers, workstations, mobile devices etc.).
- (iii) Process domain – synergises the graphical power of a state-transition diagram with the flexibility of a standard programming language and a broad library of pre-defined modelling functions. The process model specifies the object(s) in the node domain and the single modules and source code inside the network nodes (e.g. data traffic source model).

OPNET is highly regarded and is expensive commercial software. However, free licenses are awarded to qualifying universities globally for academic purposes such as for teaching and research. Its expensive nature is due to its vast selection of current ready-made protocols including IPv6, MIPv6, WiMAX and Mobile WiMAX, LTE/LTE-Advanced, QoS, Ethernet and many others.

The distinct difference between OPNET and other open source software is that the OPNET models are always of fixed topology, whereas OMNET++ and NS-3 allow for variable topologies. As mentioned previously, the network topology defined in OPNET is preferably undertaken using a graphical editor. The editor stores simulation models in a proprietary binary file format, which means that the OPNET models are usually challenging to generate by the programme. Moreover, this is because it requires writing a C programme that uses an OPNET

API, whereas, NS-3 models utilise plain text files which can be written in C++. Furthermore, OPNET does not provide the source code to the simulation kernel. Most non-commercial tools, however, are available to the public allowing easier source level debugging.

OPNET's main advantage compared to other simulation software mentioned previously, is undoubtedly due to its vast protocol model library, while its closed nature (proprietary binary file formats and lack of source code) makes development and problem solving much harder [56].

### **3.2.3 NS-2**

NS-2 is a discrete event network simulator and is popular within the networking research community. Like OMNET++, NS-2 is developed based on C++ code. However, a different scripting language, namely OTcl, is used to control the network simulation and to specify further aspects such as network topology [58].

NS-2's library of protocols and network objects can be divided into two class hierarchies: the compiled C++ hierarchy, and the interpreted OTcl one as the front-end. Both hierarchies are directly related to each other, with one to one correspondence between them. The advantages of having the compiled C++ hierarchy include faster execution times and higher simulation efficiency, particularly, when detailed behaviour definition and operation of protocols are of concern. This will lead to a reduction in both packet and event processing times. The user can control simulation development by writing an OTcl script which may cover specific protocols and applications, including any network topology. For example, a user may wish to simulate the type of presentation output obtained from the simulator. Further, since the OTcl and the C++ hierarchy have one to one correspondence, each OTcl object created in the OTcl script will be matched to the object compiled in C++ through an OTcl linkage.

Some of the established NS-2 models may be classed as general Internet protocols which include newer protocols, such as reliable multicast and TCP selective acknowledgement [61]. A unique feature called Nam [62] is a network animator which can be used to display specific protocol graphs and packet-level animation. Furthermore, the fact that NS-2 is open-source software, different configuration levels are possible including modifying the simulation parameters at all layers as well as generating custom applications and protocols [63].

Since NS-2 is a discrete event simulator, the time progression depends on the timing of events that are maintained by a scheduler. An event, which is one of the objects in the C++ hierarchy, is allocated with a unique ID together with the scheduled time and a pointer to manage the event. The scheduler maintains an ordered data structure with the events to be executed and executes them sequentially, thus invoking the handler of the event [64].

Regarding 3GPP specifications, unfortunately, there is no built-in LTE module in NS-2, but only an external patch which can be found in [78]. This, therefore, means that there is no inherent support for LTE which will result in inaccurate simulation outcomes/results. Furthermore, NS-2 has since matured and is no longer maintained by the public because a new successor to NS-2 is currently being replaced by another NS project, called NS-3.

### **3.2.4 NS-3**

The Network Simulator 3 (NS-3) is an actively developed discrete-event network simulator mainly used for educational and research purposes. NS-3 is a further type of free open-source software which is licensed under the GNU GPLv2 license [65]. It is the successor of NS-2 which is the most used network simulator in academia and the industrial community. However, NS-3 is not backward compatible with NS-2 as it was designed to eventually replace the ageing NS-2 simulator which suffers from specific design issues.

NS-3 is written in the C++ language and is developed based on the object-oriented structure. Coupled with the Python bindings feature and user-friendly nature, NS-3 provides a modular environment in which future new models can be integrated with the current software package while current models can be reused for simulation analysis. Besides simulation, NS-3 also supports emulation which helps to reduce implementation time [58], [66]. For instance, once researchers have implemented their simulation work, the same source code can be used to evaluate their emulation work.

Some of the more prominent features of NS-3 have been completely re-written in the core source code with fully documented API. This makes it much easier for software integration, support for simulating virtual networks and testbeds, configuring simulator parameters, high emphasis on conformance to real networks, automatic memory management and a configurable tracing system [67]. The first version of NS-3, (NS-3.1), was released in June 2008 with the introduction of several modules such as TCP, UDP, IPv4, CSMA, Point-to-Point and 802.11 WiFi. NS-3 allows third-party contributors to design new models and incorporate them into the main NS-3 code, resulting in dynamically increasing its scope. What makes NS-3 well suited for wireless network simulations is the availability of various components such as mobility models, routing protocols and WiFi, WiMAX and LTE standard implementation methods.

Specifically, the first LTE module was developed in the summer of 2010 under the Google Summer of Code 2010 project. This module implements basic LTE devices, including propagation models and PHY and MAC layers. The developed module also allows for the simulation of several important aspects of LTE systems, such as downlink RRM and MAC scheduling. Therefore, it can function as an excellent platform for future extensions. In summary, the most vital features provided by the developed module are:

- (i) A basic implementation of both the UE and the enhanced NodeB (eNB) devices;

- (ii) Radio Resource Control (RRC) entities for both the UE and the eNB;
- (iii) State-of-the-art Adaptive Modulation and Coding (AMC) scheme for the downlink [68];
- (iv) Management of the data radio bearers (with their QoS parameters), the MAC queues and the RLC instances;
- (v) Channel Quality Indicator (CQI) management;
- (vi) Support for both uplink and downlink packet scheduling;
- (vii) A PHY layer model with Resource Block level granularity; and
- (viii) A channel model with the outdoor E-UTRAN propagation loss model [69].

Following up regarding the status of the Google Summer of Code projects that were undertaken in subsequent years, presently, the LTE module has been implemented using various models which have not been implemented in OMNeT++ such as a building propagation model, handovers, fractional frequency reuse, and uplink power control, etc.

### **3.2.5 MATLAB**

MATLAB is one of a number of commercially available, sophisticated mathematical computation software tools in addition to Maple, Mathematica and MathCad. MATLAB was originally written in Fortran, and later rewritten in C. MATLAB excels in performing numerical calculations especially matrices and graphics [70], and can be further used for network simulations and complex numerical evaluations. The software is easy to use and is versatile due to the user-friendly and interactive features of the software. Furthermore, with a built-in programming language as opposed to a general-purpose language like C++ or Java, the length of programming scripts can be minimised. Table 3.1 displays a list of comparisons between four-simulation software applications.

**Table 3.1:** Comparison of system level simulation software

	OMNeT++	OPNET	NS-2	NS-3
Programming languages	<ul style="list-style-type: none"> <li>Implemented using a combination of NED (for scripts describing the network topology) and C++ (the core of the simulator)</li> </ul>	<ul style="list-style-type: none"> <li>Implemented using C++</li> </ul>	<ul style="list-style-type: none"> <li>Implemented using a combination of OTcl (for scripts describing the network topology) and C++ (the core of the simulator)</li> </ul>	<ul style="list-style-type: none"> <li>Implemented using C++</li> </ul>
Cost	Free	Commercial. Free only to qualified institutions.	Free	Free
Detailisation [71]	Medium	High. <ul style="list-style-type: none"> <li>The most detailed system structure</li> </ul>	Low <ul style="list-style-type: none"> <li>The least detailed system structure</li> </ul>	Medium

	OMNeT++	OPNET	NS-2	NS-3
Availability of LTE module	<p>Some limitations.</p> <ul style="list-style-type: none"> <li>• Only model user plane (Control plane is not modelled).</li> <li>• radio bearers not implemented, not even statically configured radio bearers (dynamically allocating bearers would need the RRC protocol, which is Control Plane</li> </ul>	<p>Most complete.</p> <ul style="list-style-type: none"> <li>• Both user plane and control plane is implemented</li> <li>• For the EPC Model, the S-GW and P-GW are implemented as individual nodes linked together and thus, preserve the S5 or S8 interfaces specified by 3GPP.</li> </ul>	<p>Incomplete.</p> <ul style="list-style-type: none"> <li>• Initially, available as a patch but now it is no longer available.</li> </ul>	<p>Almost complete.</p> <ul style="list-style-type: none"> <li>• All the limitations mentioned in OMNeT++ are implemented in NS-3</li> <li>• For the EPC Model, both the S-GW and P-GW functionalities are included in S-GW/P-GW single node which removes the need for S5 or S8 interfaces</li> </ul>

	OMNeT++	OPNET	NS-2	NS-3
	<p>so not implemented)</p> <ul style="list-style-type: none"> <li>handovers not implemented (no X2-based handover, that is; S1-based handover would require an S-GW model)</li> </ul>			specified by 3GPP.

Based on the software descriptions and comparisons listed in Table 3.1, we decided to use NS-3 for the LTE network simulation, because it was free, has an acceptable level of accuracy, without the need to program with more than one programming language and its LTE technology is already integrated within the simulator by the LENA module [79]. Furthermore, the primary reason was also due to the complexity of its LTE module, as it is almost at par with the commercial simulator, OPNET. LTE networks also appear to be progressively becoming more dominant longer term, and as an additional feature, NS-3 can also perform as a network emulator for real network traffic [80]. MATLAB, however, complements NS-3 for plotting graphs and calculating the comparison parameters described in Chapter 4.

### **3.3 Single Cell eNodeB Simulation Topology and Parameter setup for Uplink Transmission**

Specific parameters have been set up and created to analyse the performance of the baseline model and the proposed content-aware RRM model to substantiate the objectives highlighted in Section 1.3 of Chapter 1. Each scenario simulates the same parameter setup with regard to the operating bandwidth and frequency, the number of UEs and transmission power, but with different transmission rates depending on the application types for each UE, while moving at the same velocities from the edge of a cell towards the eNB in a random waypoint direction.

For all simulation scenarios, the LTE topology is designed to have a Remote Host connected to an SGW/PGW Gateway which is then linked (together) with an eNodeB before finally acquiring a wireless interface with four UEs. At the beginning of all simulations, all four UEs are placed in a square position at the edge of a cell which is at the farthest distance from each other, while the eNodeB is located at the centre of the cell. Figure 3.1 displays the single cell eNodeB topology for the entire LTE communication link where the SGW and PGW are cascaded together in the same node while the MME has only a logical connection with the SGW/PGW and eNodeB.

We next consider an LTE macro-cell with a bandwidth of 5 MHz (i.e., equivalent to 25 resource blocks) and a coverage radius of up to 21213.2 m for the uplink transmission up to 197.99 km for the downlink transmission. The transmission power of the eNodeB is set to 43 dBm and the eNodeB noise figure set to 5 dB and uses the Friis propagation loss model for the channel model. For the UEs, the transmission power is set to 21 dBm and the noise figures set to 9 dB. The main simulation parameters were based on 3GPP specifications [99], and each of

the UEs configured to cater for different types of application services; namely, Web browsing (HTTP protocol), file transfer (FTP protocol), VoIP and Video streaming. Table 3.2 summarises the implementation of the necessary simulation settings and parameters used for 4 UEs in a single cell with one eNodeB. Table 3.3 displays the UE applications for the test parameters.

The simulation of VoIP traffic in NS-3 is based on G.711 codec and is characterised by two periods; ON and OFF. ON is the time, the user spends talking where constant packets are transmitted at regular intervals, and hence constant bit rate traffic is generated. The OFF time is the time when the user stops talking, and packets are not transmitted [81]. The ON and OFF times are given as 0.352 and 0.650 seconds respectively [15], [81]. OnOffHelper is used to generate the VoIP traffic which is also derived from the OnOffApplication class provided by the NS-3 framework.

The video traffic simulation is assumed to be coded based on H.264 or MPEG-4 Part 10 Advanced Video Coding (AVC) codec, and its behaviour is according to real-time services such as video conferencing or video streaming. Since the simulator does not provide for appropriate video service implementations, the corresponding traffic has been modelled as Constant Bit Rate (CBR) traffic, with the video source generating video packets at a rate of 4 Mbit/s, and with the packet size set to 1024 Bytes [82]. Both, the VoIP and video traffic are implemented using UDP transport protocol which is the most used transport protocol, especially for real-time applications.

For the best effort traffic represented by the web browsing and the file transfer applications, a TCPSocketFactory abstract class is utilised, because there is no NS-3 module available that provides an HTTP or FTP application layer protocol. Regarding the Hypertext Transfer Protocol (HTTP) or File Transfer Protocol (FTP), this would only add a slight protocol overhead at the beginning of the transmission and at the start of each segment through the

presence of some headers. Typically, for long-running experiments, the influence of this can be ignored [80].

Notably, both the video and the best effort traffic in this setup are performed by the MyApp class, derived from the Application class provided by the NS-3 framework. Therefore, the simulation can be used to imitate any UDP or TCP transport approach or content type. The client and server could be adjusted accordingly, depending on the desired outcome, e.g., to either resemble a video conference session, web browsing or file transfer. All in all, there are three attributes defined in the application module that are, the constant data rates, packet size and the number of packets.

Each user is expected to report its channel condition to the eNodeB via the Channel Quality Indicator (CQI) as recommended in [33] at an interval of 1 ms, which is equivalent to 1 transmit-time-interval (TTI). The reported CQI is used for transmission and scheduling purposes at the eNodeB.

At the MAC layer of the eNodeB, the packet scheduler functions with the Link Adaptation (LA) module and Hybrid Automatic Repeat Request (HARQ) to schedule users on resources at every TTI. The basic time-frequency resource allocated is the Physical Resource Block (PRB), and the smallest unit of the PRB is the Resource Element (RE). An RE can be 2, 4 or 6 bits depending on the modulation applied and the modulation type that will be used depends on the reported CQI value from the UE to eNodeB [83]. The PF scheduler was chosen because it is widely accepted as an attractive solution for scheduling, and provides an excellent compromise between the maximum throughput and user fairness by exploiting multi-user diversity and the game-theoretic equilibrium in the wireless environment [41], [72]. Besides, the scheduler itself has low implementation complexity and provides excellent performance [41], [73 - 74].

As previously highlighted in the research objectives, the primary focus of our simulation relates to the performance of the video streaming uplink transmission in one of the UEs which represents single-user performance for the entire system.

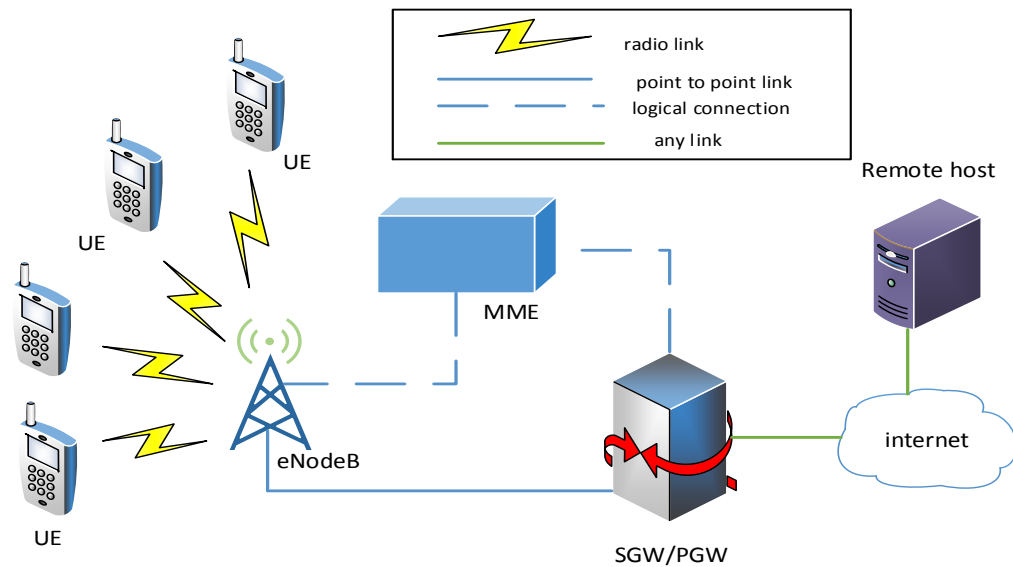


**Figure 3.1:** Single eNodeB LTE - EPC simulation topology

**Table 3.2:** Simulation parameters for a single eNodeB

Parameter	Value
Bandwidth	5 MHz
Operating Frequency	1.93 GHz
Duplex Mode	FDD
Transmission Scheme	SISO
Channel Model	Friis Propagation Loss Model
Scheduler	Proportional Fair (PF)
UE velocity	20 m/s = 72 km/h

<b>Parameter</b>	<b>Value</b>
eNodeB – UE Distance	7071.1 – 21213.2 m
Number of UEs	4
eNodeB Transmission Power	43 dBm
UE Transmission Power	21 dBm
Simulation Time	600 seconds

**Table 3.3:** Test parameters for UEs

<b>UE</b>	<b>Application Type</b>	<b>Data Rate, R (kbps)</b>	<b>Packet Size (bytes)</b>	<b>Number of Packets</b>
1	Web Browsing (HTTP)	32	1024	100000
2	File Transfer (FTP)	32	1024	100000
3	VoIP	64	1024	100000
4	Video Streaming	4000 [83]	1024 [85]	1000000

The simulation initiates at 0 seconds with the Web Browsing, and File Transfer application services initialised at the Remote Host. Whereas, VoIP and Video Streaming applications are initialised in their respective UEs located at 7071.1 m away from the eNodeB. During transmission, the existing LTE framework establishes the lower layer protocols, which include the radio stack and the GPRS Tunnelling Protocol (GTP) core network bearer, accordingly [80]. Only after 2 seconds, are the UEs allowed to move, following a random waypoint mobility model with a constant velocity of 20 m/s or 72 km/h closing towards the eNodeB. After 600 seconds, the simulation stops, and the output performance parameters are

measured. The output performance parameters of interest such as the throughput, packet loss ratio, end-to-end delay and the UE SINR values for the video streaming application are then recorded in a text file format. For clarification purposes, the throughput, packet loss ratio and end-to-end delay calculations are measured in the Remote Host which acts as the receiver and only the UE SINR is measured in the eNodeB. The same simulation setup is next repeated while incrementing the eNodeB – UE distance by 707.1 m for each simulation time until the UEs reach the distance of 21213.2 m from the eNodeB.

Again, all output performance parameters for each simulation time, as mentioned previously, are recorded only for the video streaming service which will be later evaluated for throughput, packet loss ratio and average end-to-end delay, and the key metrics to assess the performance of real-time video streaming applications.

### **3.4 Analysis of the LTE Uplink Baseline Model Performance**

In Section 3.3, we obtained 51 simulation results where the only variable in the results was for the distance between the eNodeB and the respective UEs. Each simulation result was recorded specifically for UE 4 which contained the video streaming service comprising of four types of data:

- i) Throughput against time;
- ii) Packet Loss Ratio against time;
- iii) Average Delay against time; and
- iv) UE SINR against time.

The first three output data represent the vital performance metrics which are described as follows:

**Throughput:** A measure of how much data is transferred from the source to the

destination in a certain period (in bits/sec.).

**Packet Loss Ratio:** A ratio determined as the difference between the transmitted packets and the received packets to the sent packets.

**Average Delay:** The total time taken for all transmitted packets to arrive at the destination node divided by the number of received packets.

Based on the four types of data, we then plot three graphs accurately using MATLAB; namely, the Throughput against SINR, the Packet Loss Ratio against SINR and the Delay against SINR graphs for UE 4 travelling at 72 km/h to a certain waypoint, determined by the random waypoint mobility model, which is also closing towards the eNodeB, while generating a 4 Mbps data rate. As shown in Figures 3.2, 3.3 and 3.4, all three graphs display a staircase-like pattern with PLR and Delay graphs showing a downward pattern for higher SINRs, and only the Throughput graph displays an upward trend for higher SINRs. This is an incredibly exciting observation since, for example, the UE throughput which was measured at the Remote Host does not increase linearly with the SINR as expected. This is similar to both the PLR and Delay graphs which do not decrease linearly with the higher SINR. This observation indicates that for a certain range of SINR, the three output parameters will remain constant or stable regardless of how high the transmission data rate is increased. For instance, for an SINR between 2.29 and 4.63 dB, the highest achievable throughput is 1.650 Mbit/s. This means that if anything is sent less than 1.650 Mbit/s, the achievable throughput will then follow precisely at its transmitted data rate. However, if sending the data higher than 1.650 Mbit/s, the same amount of throughput would still be received which is 1.650 Mbit/s in this instance. This will naturally result in higher data or packet loss and at the same time, increasing the end-to-end delay for packet transmission.

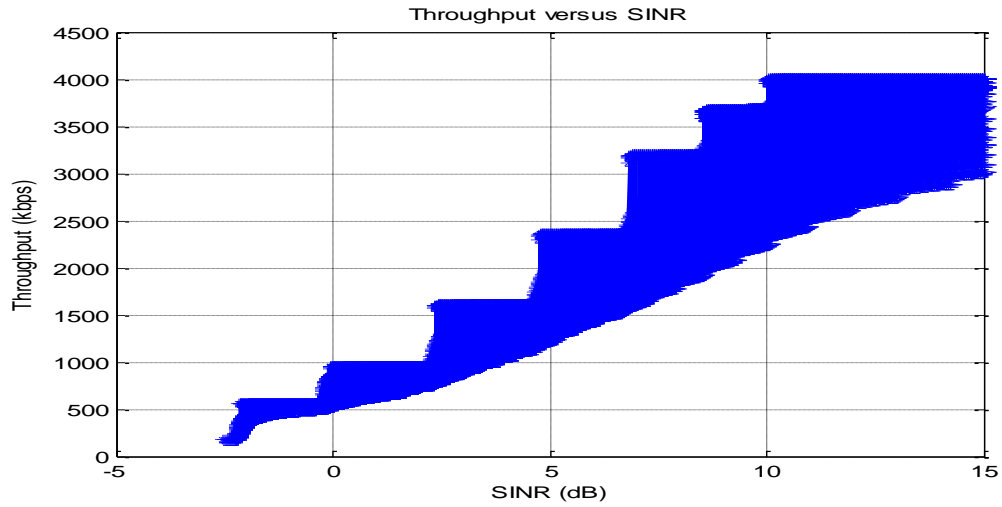


**Figure 3.2:** Throughput against SINR plot for R = 4 Mbps

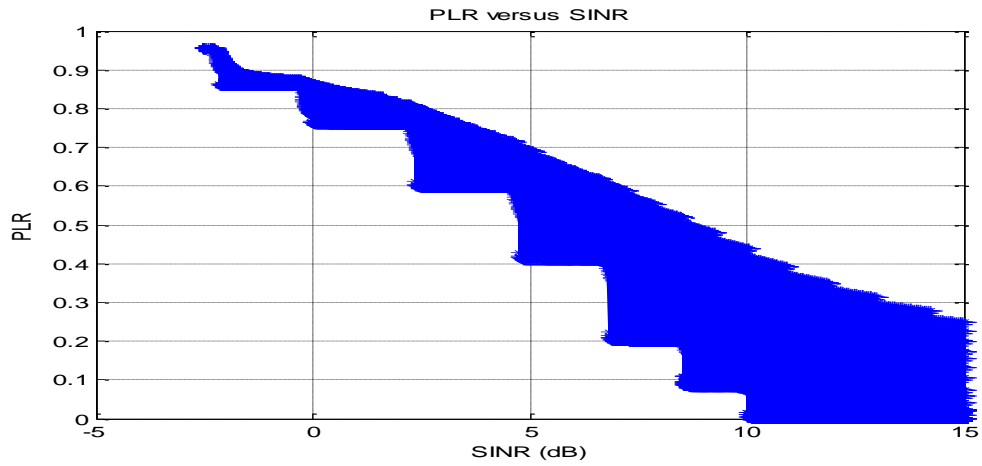


**Figure 3.3:** Packet Loss Ratio against SINR plot for R = 4 Mbps

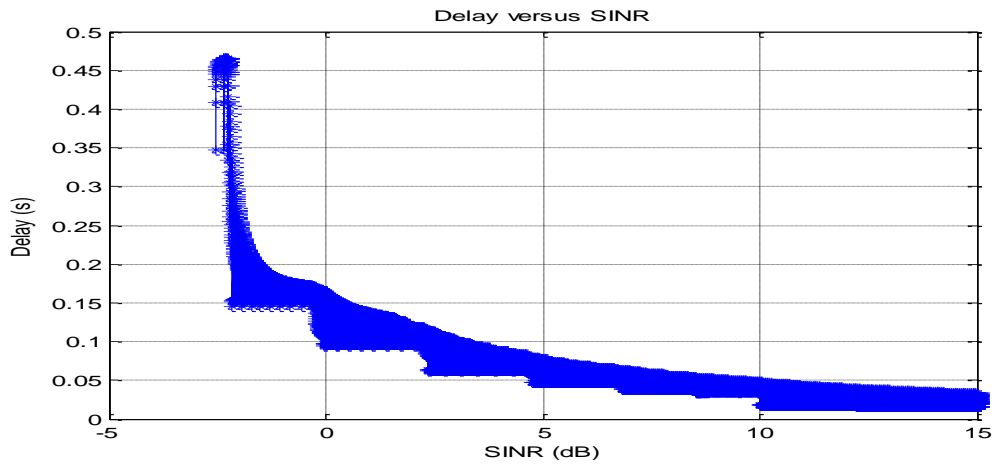


**Figure 3.4:** Average delay against SINR plot for R = 4 Mbps

### 3.5 Correlation between Output Performance Parameters and SINR

It is quite understandable that in every mobile data transmission, we would want to maximise the throughput and at the same time minimise the number of the packets lost and the end-to-end delay. The only issue is where and when those objectives can be achieved. In response to this statement, we propose an idea to find the correlation between the throughput, packet loss ratio and average end-to-end delay parameters against their SINRs with reference to the results obtained and illustrated in Figures 3.2, 3.3 and 3.4. We have previously observed also, that when the SINR is low, there will be no chance for the throughput to match its data rate and hence, the packet loss ratio and the delay will be high.

As we already know, throughput is a measure of the rate of data that has been successfully delivered to a receiver for a specific simulation time. It is therefore apparent that to maximise the throughput; we need to make the transmission data rate equal to the throughput itself, depending on the UE SINR. Therefore, in return, we can minimise the loss of packets and in doing so, reduce the delays of transmission which will ultimately prevent any bandwidth wastage/loss. Table 3.4 shows the correlation between the received throughput and the transmitted SINR with the recommended transmission data rate (R). The table will act as the platform for the design of the cross-layer optimiser (CLO) discussed in the next chapter.

**Table 3.4:** Correlation between Throughput and transmitted SINR with recommended data rate

<b>Throughput (Mbit/s)</b>	<b>SINR (dB)</b>	<b>Recommended Data Rate, R (Mbit/s)</b>
0.2	$< -2.19$	0.2
0.58	$-2.19 - -0.2$	0.58

<b>Throughput (Mbit/s)</b>	<b>SINR (dB)</b>	<b>Recommended Data Rate, R (Mbit/s)</b>
0.98	-0.2 – 2.29	0.98
1.65	2.29 – 4.63	1.65
2.40	4.63 – 6.77	2.40
3.23	6.77 – 8.33	3.23
3.70	8.33 – 10	3.70
4	> 10	4

### **3.6 Downlink Scenario of the Baseline Model**

Regarding the downlink transmission, the Remote Host is now configured as the transmitter while the UEs now become the receivers. The same set of parameters as specified in Table 3.2 and 3.3 are reused. However, two parameters need to be changed: the operating frequency from 1.93 GHz to 2.12 GHz and the eNodeB to the UE distance parameter which needs to be varied from 63.64 km to 197.99 km as shown in Table 3.5. The changes are required due to the FDD mode implementation and the much higher transmit power of the eNodeB as compared to the UEs which enable the eNodeB to transmit in a much broader coverage area, respectively.

In this situation, all four application services are initialised at the same Remote Host with four different ports, and the UEs acting as the receivers, are positioned initially 63.64 km away from the eNodeB. The same steps are adopted while implementing the uplink transmission simulation for the downlink transmission until the output performance parameters for the video streaming are measured. However, in this instance, the throughput, packet loss ratio, end-to-end delay calculations and eNodeB SINR are all measured at UE 4. It was anticipated that the varied

positions of the UEs due to their mobility, would lead towards the simulation to acquire a different Signal-to-Interference-plus-Noise Ratio (SINR). Hence, a different CQI is reported from the UEs and therefore the eNodeB would react by observing a different capacity available for the channel of the UEs through the Modulation and Coding Scheme (MCS) and transport block size assignment [84]. However, as the UEs continuously move closer to the eNodeB, the SINR obtained due to the distance is always better. Accordingly, the quality of the channel is likewise better and will be reported by the UEs every TTI. The assigned MCS will, therefore, tend to be more accommodating, increasing capacity for having fewer retransmissions while still maintaining the BLER below the 10 % target.

The same simulation setup is repeated with the eNodeB to UE distance incremented by 707.1 m for each simulation time until the UEs reach the distance of 197.99 km from the eNodeB. The fact that the basic channel model is used in the simulation (e.g. Friis Free Space Propagation Loss Model) depends primarily on the eNodeB transmit power while the other parameters are kept constant, thereby enabling the eNodeB to propagate its downlink signal much further away as compared to the uplink transmissions by the UEs. However, shorter coverage distances could be expected for the downlink transmission if instead, other detailed channel models were used. For example, the empirical COST231 Propagation Model which considers both the transmit and receive antennas' heights or the Two-Ray Ground Reflection Model which covers not only both transmit and receive antennas' heights, but also higher path-loss exponent. Notably, at this point, it needs to be stressed that all output performance parameters for each simulation time are recorded specifically for the video streaming service.

**Table 3.5:** Simulation parameters for a single eNodeB

<b>Parameter</b>	<b>Value</b>
Bandwidth	5 MHz
Operating Frequency	2.12 GHz
Duplex Mode	FDD
Transmission Scheme	SISO
Channel Model	Friis Propagation Loss Model
Scheduler	Proportional Fair (PF)
UE velocity	20 m/s = 72 km/h
eNodeB – UE Distance	63.64 – 197.99 km
Number of UEs	4
eNodeB Transmission Power	43 dBm
UE Transmission Power	21 dBm
Simulation Time	600 seconds

### **3.7 Analysis of the LTE Downlink Baseline Model Performance**

Since the transmit power of the eNodeB is twice (double) the transmit power of the UEs, we, therefore, can expect more simulation results to be obtained for the downlink transmission. A total of 117 sets of results were recorded for UE 4 which incorporates the video streaming application. Each set of results consisted of the following information:

- i) Throughput against time;
- ii) Packet Loss Ratio against time;
- iii) Average Delay against time; and
- iv) eNodeB SINR against time.

By using MATLAB, we can generate three graphs corresponding to the Throughput against SINR, Packet Loss Ratio against SINR and Average Delay against SINR for UE 4

travelling at 72 km/h to a specific waypoint following the random waypoint mobility model, towards the eNodeB. All three graphs presented in Figures 3.5, 3.6 and 3.7, display almost the same staircase-like pattern as shown in Figures 3.2, 3.3 and 3.4 respectively, with the PLR and Delay graphs displaying the downward pattern for higher SINRs. While the Throughput is the only graph showing the upward trend for higher SINRs. This observation confirms the findings found in Section 3.3 which identifies that for a certain range of SINR, the three output parameters will remain constant or stable regardless of how high the transmission data rate is increased. The striking difference between the DL and the UL transmissions is that even at a much lower SINR, which is -2 dB as in the case for DL transmission, the UE can still receive the video packets at approximately 1 Mbps as compared to 0 dB required for the UL transmission. This means that the capability of the UE to receive the video stream packets is dramatically enhanced by the higher transmission power of the eNodeB and which is also due to the higher MCS index supported by the downlink transmission as compared to that of the uplink transmission [32].

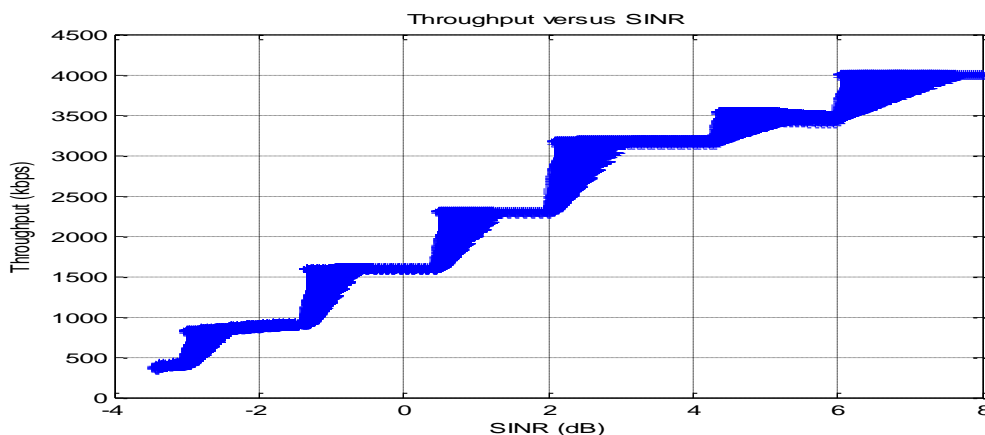


**Figure 3.5:** Throughput against SINR plot for R = 4 Mbps

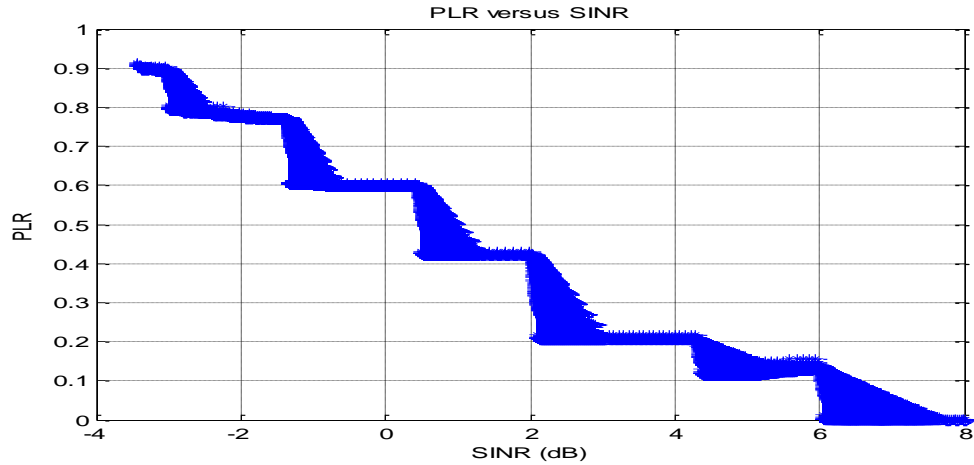


**Figure 3.6:** Packet Loss Ratio against SINR plot for R = 4 Mbps

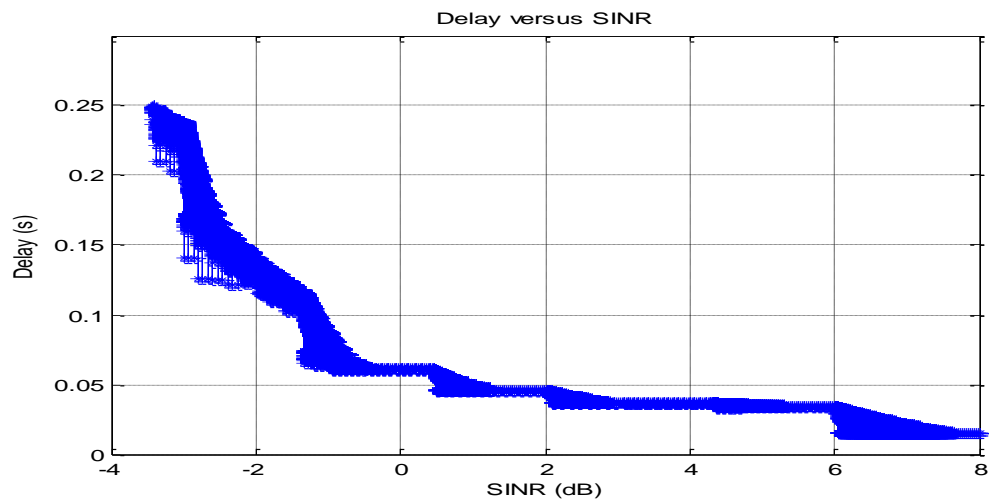


**Figure 3.7:** Average delay against SINR plot for R = 4 Mbps

### 3.8 Correlation between the Output Performance Parameters and SINR for the Downlink Transmission

In Section 3.5, we proposed an idea to find the correlation between output performance parameters and SINR. The same idea can also be carried out for the downlink transmission. We can avoid bandwidth wastage by minimising the loss of packets thereby reducing the transmission delays between the eNodeB and the particular UE. To perform this task, we

equalise the transmission data rate with the UE throughput based on the SINR measured at the particular UE. Table 3.6 shows the correlation between the received throughput and the measured SINR at the UE with the recommended transmission data rate (R) at the Remote Host.

**Table 3.6:** Correlation between Throughput and transmitted SINR with recommended data rate

<b>Throughput (Mbit/s)</b>	<b>SINR (dB)</b>	<b>Recommended Data Rate, R (Mbit/s)</b>
0.415	< -3.03	0.415
0.875	-3.03 – -2.0	0.875
0.92	-2.0 – -1.4	0.92
1.625	-1.4 – 0.41	1.625
2.33	0.41 – 2.0	2.33
3.21	2.0 – 4.26	3.21
3.5	4.26 – 6	3.5
4	> 6	4

### 3.9 Summary

This chapter describes the classical, baseline LTE simulation model which implements basic RRM before identifying the criteria or parameters that affect its output performance when UEs are located at the edge of the cell, moving towards the eNodeB. This situation is important as it is considered as one of the research challenges faced by many researchers and radio engineers in providing reliable and spectrally efficient communication links between the eNodeB and the UEs, especially for high data rate services such as video streaming applications. The

classical or the baseline communication model provides for an interesting observation when a high data rate application such as in the case of video streaming, is transmitted from a moving object in both the uplink and downlink transmission. This is evident as to what has been observed in the output performance parameters against the SINR. The staircase-like pattern for all three output performance parameters provides the basis for the proposed content-aware RRM model in the following chapter. Regarding the simulation exercise, the descriptions and comparisons of various system level simulation software are also presented at the beginning of the chapter and as explained later, the NS-3 software, complemented by the MATLAB software, are both used to perform the extensive simulations onwards.

## 4 CONTENT-AWARE RADIO RESOURCE MANAGEMENT MODEL

In the previous chapter, we identified the SINR as being the critical element affecting the output performance parameters of a conventional LTE network. Further, our observation revealed that the throughput of a particular UE is not linearly proportional to the measured SINR. The throughput of the UE does increase in a staircase-like pattern with respect to the measured SINR. Similarly, the packet loss ratio and the average delay graphs also follow the staircase-like pattern but in a downward direction as the measured SINR improves. This breakthrough has prompted us to develop a new technique in RRM where the packet loss and the average delay during transmission can be efficiently minimised while maintaining the throughput.

Accordingly, this chapter presents the proposed content-aware radio resource management model based on the baseline LTE communication model presented in Chapter 3 for both uplink and downlink transmissions. Furthermore, it also describes how the look-up tables are derived from the three output performance graphs obtained in the previous chapter. To substantiate the advantage of using the content-aware RRM model, comparison parameters are introduced to compare the performances of the baseline model and the proposed content-aware RRM model for three different UE velocities, shown as graphical representations. Next, analyses of both performances with regard to total packet loss and total delay are summarised in tabulated forms.

#### 4.1 Proposed Look-up Table for the Uplink Content-Aware RRM Model

In the previous chapter, the correlation between the throughput and UE SINR with its recommended data rate was introduced. Based on this observation, a new concept in radio resource management system is introduced which can dynamically adjust the transmitted data rate depending on the UE SINR performance to minimise packet loss. This concept, involving the cross-layer optimisation approach is called the Content-Aware RRM model, or sometimes called ‘joint source and channel coding’. To formulate this concept, Table 3.4 is reduced to Table 4.1 which becomes the proposed look-up table for the uplink content-aware RRM model.

**Table 4.1:** Proposed look-up table for the uplink Content-Aware RRM model

<b>Proposed Data Rate, R (Mbit/s)</b>	<b>SINR (dB)</b>
0.2	< -2.19
0.58	-2.19 – -0.2
0.98	-0.2 – 2.29
1.65	2.29 – 4.63
2.40	4.63 – 6.77
3.23	6.77 – 8.33
3.70	8.33 – 10
4	> 10

Table 4.1 proposes for the data rate of the UE to be adjusted accordingly. Accurate estimation of the current channel quality of the link between the UE and its associated serving eNodeB are estimated first. In a normal uplink transmission, the eNodeB has knowledge of the SINRs of the various subcarriers by measuring and evaluating both the SRS and PUSCH

signals transmitted by the respective UEs. Through acquiring estimates of the SINRs of all subcarriers allocated to a certain UE based on its unique RNTI or International Mobile Subscriber Identity (IMSI), the eNodeB can then determine the spectrally most efficient MCS for which a given target BLER is not exceeded. For that purpose, it may choose several different modulation schemes as well as using a variety of different channel coding rates [85]. After that, the selected MCS is signalled as part of the scheduling which is granted to the corresponding UE using the PDCCH.

However, in our design, the SINR values, apart from the scheduling grant, are fed back to the targeted UE using the same PDCCH, every 40 ms which is equivalent to the SRS signal periodicity. Accordingly, a newly designed cross-layer optimisation module will use the received SINR values from the UE's PHY layer together with the information on the current data rate of its video streaming packets from the APP layer. This will dynamically assign the suitable data rate for its video streaming packets in the APP layer based on the proposed look-up table in Table 4.1. The cross-layer optimiser concept designed at the UE is shown in Figure 4.1. It is worthy to note, that to make the CLO backward compatible with any prior system (e.g. 3G and 2G), this does not involve changing protocols of any sort, to any layers especially the PHY and MAC layers to enable the CLO to be easily attached to or detached from the UE.

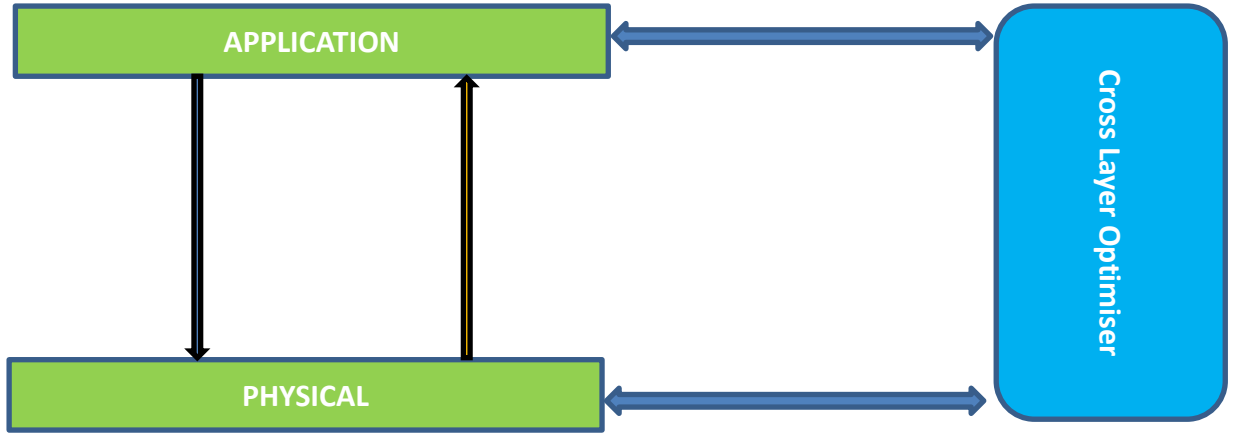


**Figure 4.1:** Cross-layer optimiser for Content-Aware RRM at UE side

## 4.2 Comparison Parameters

Before we can evaluate the performance of the proposed content-aware RRM model, we need to establish new parameters used to compare the performance of the proposed model and the baseline model. The new parameters are defined as shown below:

$$\varphi_T = \int_0^t \text{Throughput} dt \quad (1)$$

$$\varphi_P = \int_0^t \text{PLR} dt \quad (2)$$

$$\varphi_D = \int_0^t \text{Delay} dt \quad (3)$$

where

$\varphi_T$  = Total data received = Area under the curve for throughput.

$\varphi_P$  = Area under the curve for packet loss ratio.

$\varphi_D$  = Area under the curve for average end-to-end delay.

All three parameters above represent areas under the curves for all three output performance parameters: throughput, packet loss ratio, and the average delay calculated with respect to the total simulation time. Improvements can only take place if  $\varphi_T$  for one system is

higher, while  $\varphi_P$  and  $\varphi_D$  are lower than those of its counterparts.

Next, the new parameters will be implemented on both the content-aware RRM and baseline RRM models for comparative purposes. We anticipate that these parameters will exhibit better performance in the content-aware model as compared to those in the baseline model.

### **4.3 Results Analysis of the Uplink Transmission**

In this section, the performance of the proposed content-aware RRM model is compared to the baseline model. Using the same specifications as defined in Table 3.2 and Table 3.3; both models are simulated for 10 minutes with all UEs following the random waypoint mobility model from the edge of the cell towards the eNodeB at three different velocities corresponding to three different scenarios. The reason why the random waypoint mobility model is chosen is that in a typical driving or pedestrian scenario, most of the time, the UEs are travelling in a straight path which is the shortest distance between two waypoints. Only at certain waypoints, are the UEs required to make turns before reaching their final destination point.

The simulations are divided into three different performance parameters: throughput, packet loss ratio and average delay implemented for UE velocities of 72 km/h, 50 km/h and 5 km/h respectively. The three different velocities are chosen to correspond to a faster vehicular, normal vehicular and a pedestrian respectively. In each scenario, the UEs are positioned at 14142.14 m away from the eNodeB. Only UE 4 which transmits video streaming services at 4 Mbps for both models will be analysed. During the entire 10-minute simulation in each scenario, only UE 4 which is located initially at 10000 m East and 10000 m South from the eNodeB, starts to move after 2 seconds with its corresponding speeds and never changes direction. Tables 4.2, 4.3 and 4.4 summarise the performance of both models showing all three comparison

parameters.

### 4.3.1 Scenario 1

The first simulation was performed when the UE velocities were set at a constant velocity of 72 km/h for both models. When the simulation hit 2 seconds, the UE 4 velocity in the  $x$  and  $y$  directions were recorded as  $-12.701$  m/s and  $15.4494$  m/s, respectively. Figures 4.2, 4.3 and 4.4 show the comparison of output performance graphs for both the baseline model and the content-aware RRM model.

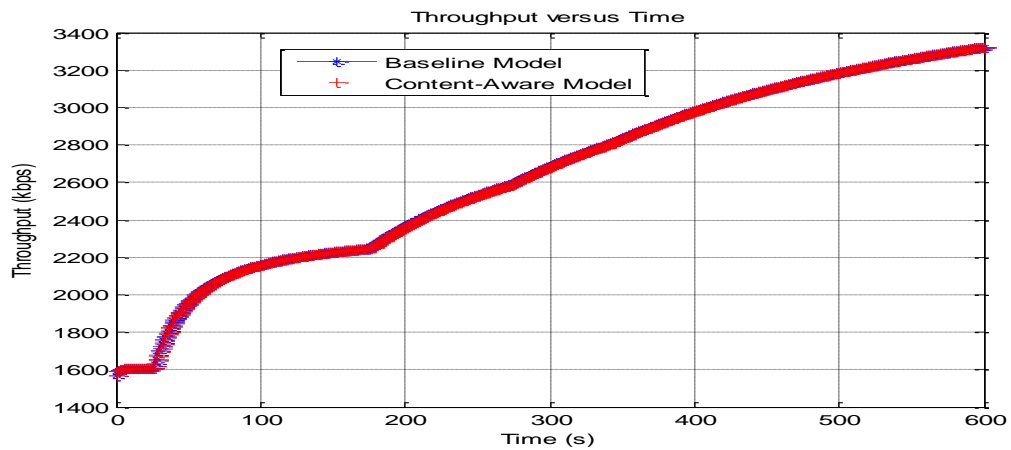


**Figure 4.2:** Throughput against time for uplink video delivery

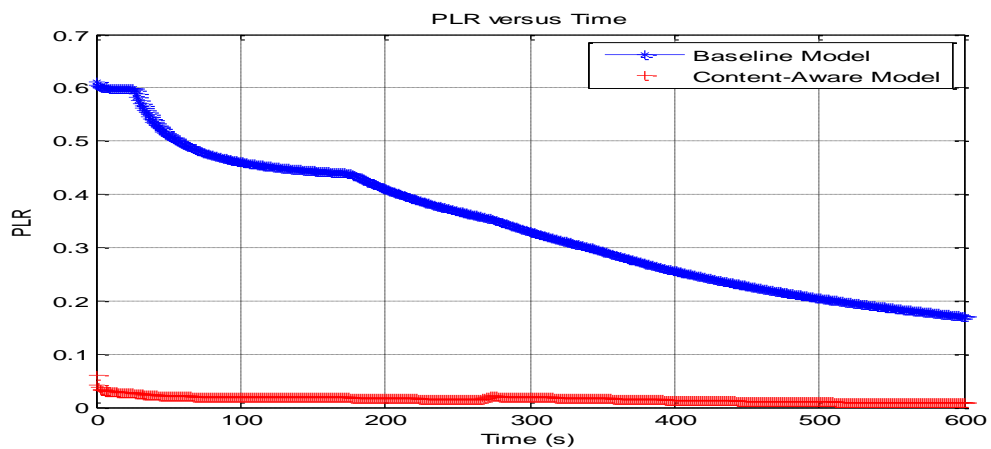


**Figure 4.3:** Packet loss ratio against time for uplink video delivery

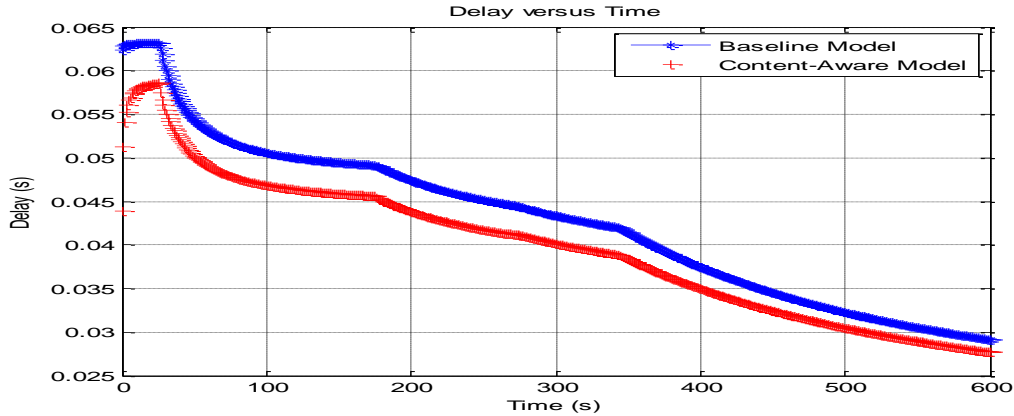


**Figure 4.4:** Average delay against time for uplink video delivery

In the previous figures, the throughput of UE 4 for the baseline model is levelled at 1 Mbps for the first 25 seconds. It then starts to increase in a decaying exponential pattern until reaching 175 seconds before it continues to increase almost linearly afterwards. The constant performance for the first 25 seconds is also shared by the packet loss ratio and the average delay graphs. The throughput only starts to improve when the packet loss ratio and the average delay begin displaying the improving downward pattern. This result is expected since the UE is initially located at the edge of the cell. Hence, the measured SINR is at its lowest point which, therefore, contributes to its lowest throughput. Even after 2 seconds when the UE starts to move at a constant velocity of 72 km/h towards the eNodeB, the measured SINR is still not acceptable for the UE to transmit higher than the 1 Mbps data rate. The situation only starts improving after 25 seconds when the distance between the eNodeB and the UE reaches the minimum threshold level and is deemed suitable to transmit at the higher data rate.

For the content-aware RRM model, an almost similar pattern is seen in the Throughput performance graph, and much better performance is achieved in both the packet loss ratio and average delay performances. After 10 minutes of the simulation, in which a total amount of  $\varphi_T$

= 1.5839 Mbit of data is transmitted by the UE 4, is there a staggering 95.23 % improvement in the packet loss ratio ( $\varphi_P = 9.7803$ ) and also a 7.14 % improvement ( $\varphi_D = 23.8658$ ) in the average delay as compared to those of the baseline model. The reason for this behaviour, is when the UE 4 PHY layer receives the feedback on its channel condition status, (i.e. measured SINR) from the eNodeB, the cross-layer optimiser in the UE 4 uses the SINR value to match with the suitable data rate in its look-up table, and then instructs the APP layer to change it to the present data rate, accordingly. If the current data rate is the same as the proposed data rate, then no further action is taken. Even though the total amount of data transmitted in the baseline model is slightly higher ( $\varphi_T = 1.5857$  Mbit) than that of the content-aware RRM model, the total number of packets lost during the transmission in the channel is enormous ( $\varphi_P = 204.8655$ ) therefore, resulting in bandwidth wastage. The content-aware RRM model also experiences a much less total delay as depicted in Table 4.2 which means that the QoS can be preserved for the video streaming application.

**Table 4.2:** Comparison of Baseline and Content-Aware RRM models at UE velocity = 72 km/h

<b>Baseline RRM Model</b>	<b>Content-Aware RRM Model</b>
$\varphi_T = 1.5857$ Megabit	$\varphi_T = 1.5839$ Megabit
$\varphi_P = 204.8655$	$\varphi_P = 9.7803$ (95.23 % improvement)
$\varphi_D = 25.7003$	$\varphi_D = 23.8658$ (7.14 % improvement)
Maximum delay = 0.0632 s	Maximum delay = 0.0586 s (7.28 % improvement)
Actual packet loss = 0.171784	Actual packet loss = 0.00841547 (95.10 % improvement)

### 4.3.2 Scenario 2

The next simulation is performed by changing the velocities of the UEs from 72 km/h to 50 km/h while the remaining specifications are fixed at their initial values. After the simulation hit 2 seconds, the UE 4 velocity in the  $x$  and  $y$  directions were recorded as -8.82085 m/s and 10.7296 m/s, respectively. For both models, the graph patterns are almost like those observed in Scenario 1 since the gap between the two velocities is not that large. The only difference observed between the current observations with those in Scenario 1 is the rate of change for all three output parameters in both models which are slightly lower in Scenario 2. This means that both models experience a longer time to reach the threshold SINR measurement before their performance starts to improve. However, even at the slower UE velocity, and a slightly less amount of data transmitted ( $\varphi_T = 1.4392$  Mbit) in Scenario 2 for the content-aware RRM model, the improvements with respect to the packet loss ratio and average delay, as compared to those of the baseline model, are still maintained around 95.32 % ( $\varphi_P = 11.2829$ ) and 7.27 % ( $\varphi_D = 26.4227$ ) respectively, as summarised in Table 4.3.

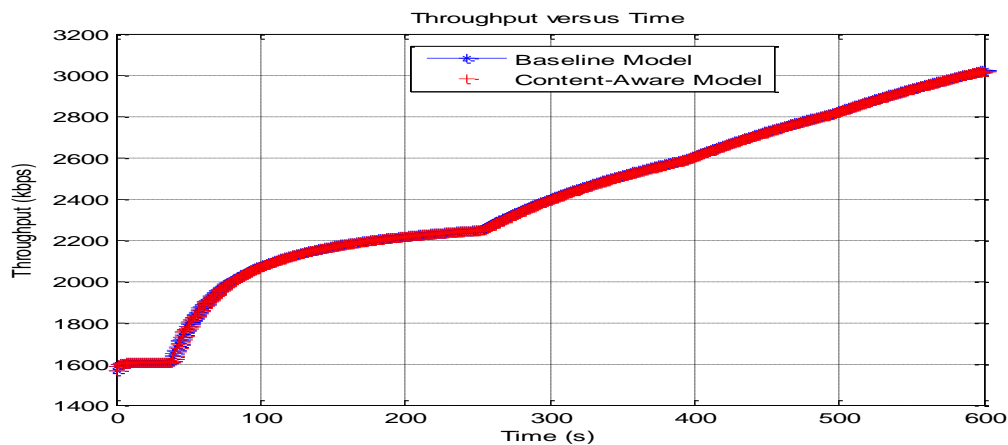


**Figure 4.5:** Throughput against time for uplink video delivery

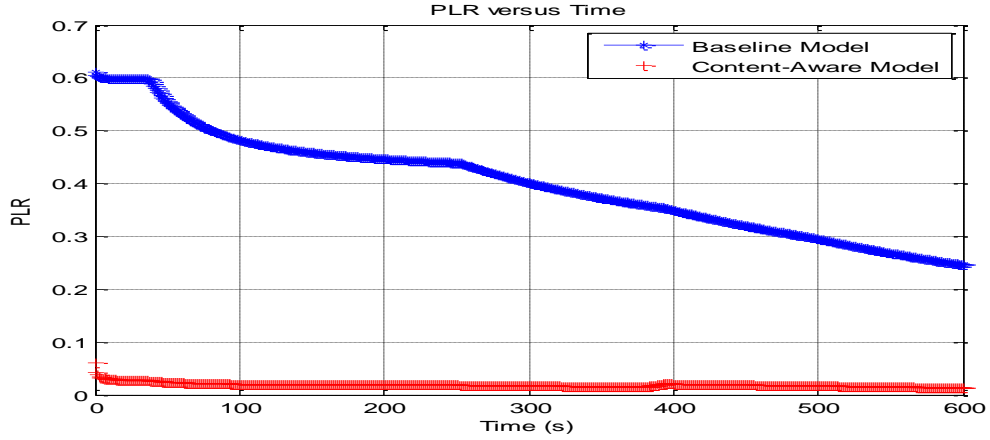


**Figure 4.6:** Packet loss ratio against time for uplink video delivery

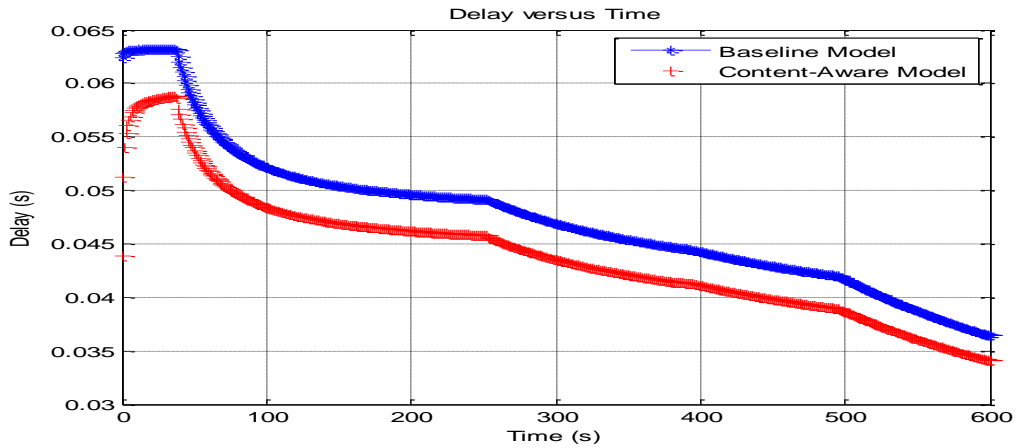


**Figure 4.7:** Average delay against time for uplink video delivery

**Table 4.3:** Comparison of Baseline and Content-Aware RRM models at UE velocity = 50 km/h

Baseline RRM Model	Content-Aware RRM Model
$\varphi_T = 1.4413$ Megabit	$\varphi_T = 1.4392$ Megabit
$\varphi_P = 240.8514$	$\varphi_P = 11.2829$ (95.32 % improvement)
$\varphi_D = 28.4931$	$\varphi_D = 26.4227$ (7.27 % improvement)
Maximum delay = 0.0632 s	Maximum delay = 0.0588s (6.96 % improvement)
Actual packet loss = 0.246918	Actual packet loss = 0.013297 (94.61 % improvement)

### 4.3.3 Scenario 3

The last part of the simulation is performed by setting all four UE velocities to the pedestrian speed of 5 km/h. As the simulation hit 2 seconds, the UE 4 velocity in the  $x$  and  $y$  directions were recorded as -0.88272 m/s and 1.07373 m/s, respectively. In Figures 4.8, 4.9 and 4.10, all three output parameters for both the baseline and the content-aware RRM models produce a flat performance initially until the 380<sup>th</sup> second, again due to much slower SINR values reaching the threshold before they start to improve. The throughput of the baseline model contributes  $\varphi_T$  of about 1.0023 Megabit, the packet loss ratio is heavily degraded with  $\varphi_P = 350.2561$ , and the average delay accumulates  $\varphi_D = 36.9541$ .

In contrast, the performance metrics for the content-aware model also displayed in the same figures, are strikingly much better than its counterpart. Despite producing  $\varphi_T$  of only 1.0005 Megabit of data, the total number of lost packets have been drastically reduced to 95.53 % ( $\varphi_P = 15.6412$ ), and the total average delay has improved by 6.85 % ( $\varphi_D = 34.4212$ ). The performance metrics comparison for both models is tabulated in Table 4.4. This similar observation as in Scenario 1 and 2 confirm that by having the same amount of data for both models, the content-aware RRM model can effectively improve the packet loss ratio and average delay performance for video streaming/conferencing applications as compared to the baseline model.

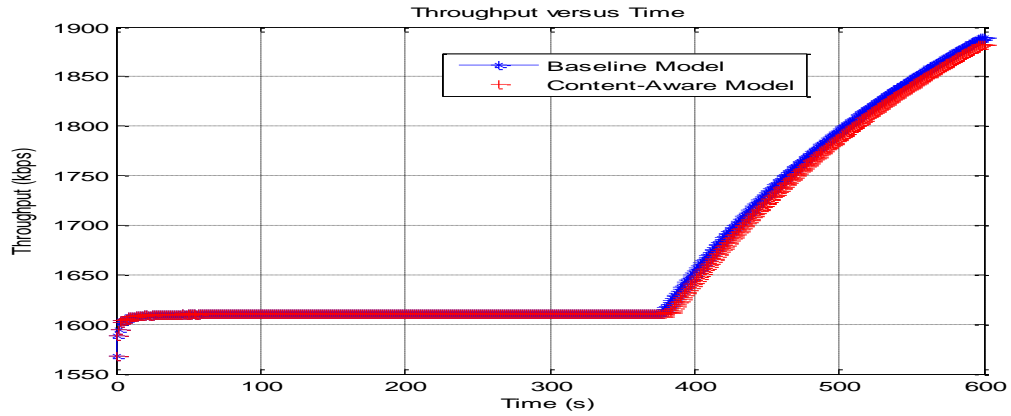


**Figure 4.8:** Throughput against time for uplink video delivery

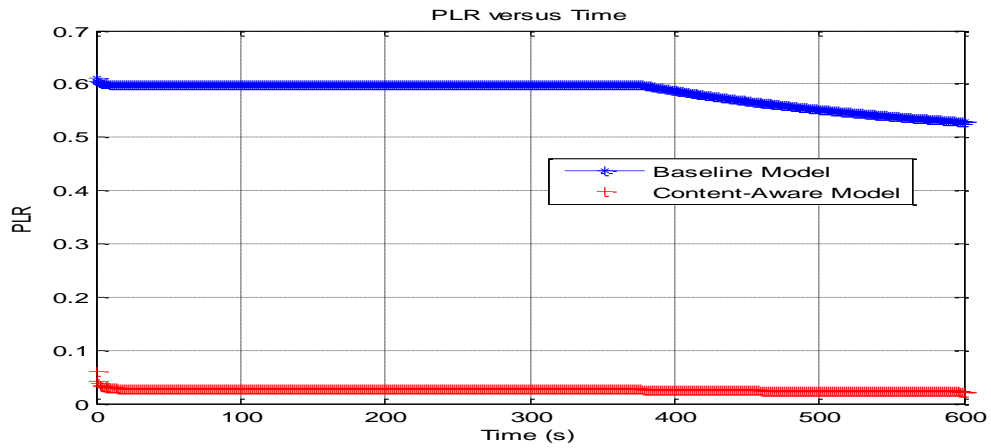


**Figure 4.9:** Packet loss ratio against time for uplink video delivery

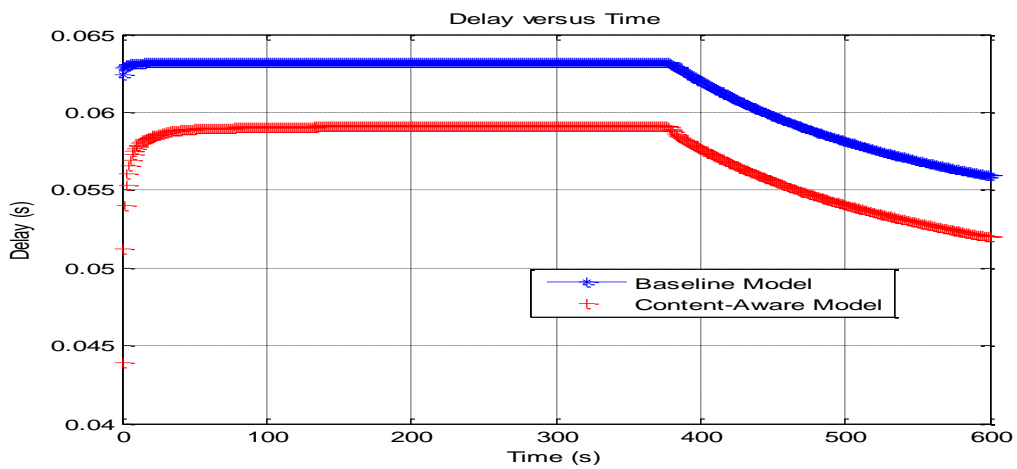


**Figure 4.10:** Average delay against time for uplink video delivery

**Table 4.4:** Comparison of Baseline and Content-Aware RRM models at UE velocity = 5 km/h

<b>Baseline RRM Model</b>	<b>Content-Aware RRM Model</b>
$\varphi_T = 1.0023$ Megabit	$\varphi_T = 1.0005$ Megabit
$\varphi_P = 350.2561$	$\varphi_P = 15.6412$ (95.53 % improvement)
$\varphi_D = 36.9541$	$\varphi_D = 34.4212$ (6.85 % improvement)
Maximum delay = 0.0632 s	Maximum delay = 0.0591s (6.49 % improvement)
Actual packet loss = 0.529259	Actual packet loss = 0.0224166 (95.76 % improvement)

#### 4.3.4 Mobility Analysis for the LTE Uplink Video Packet Transmission

In Sections 4.3.1, 4.3.2 and 4.3.3, we observed the output performance of both the baseline model and the proposed model for the uplink video packet transmission in three different UE velocities. In the following figures, UE mobility comparisons are made to all the three-performance metrics for both models in all three UE velocities, which are 5 km/h, 50 km/h and 72 km/h. As mentioned in Section 4.3, all UEs follow the same random waypoint mobility model in all three scenarios which correspond to three different UE velocities.

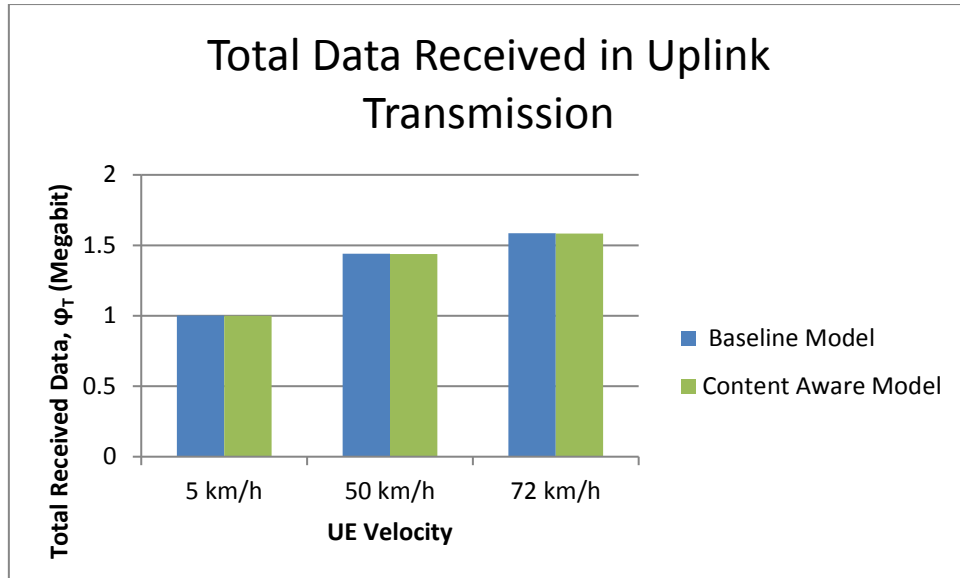


**Figure 4.11:** Total received data in uplink video packet transmission in three different UE velocities

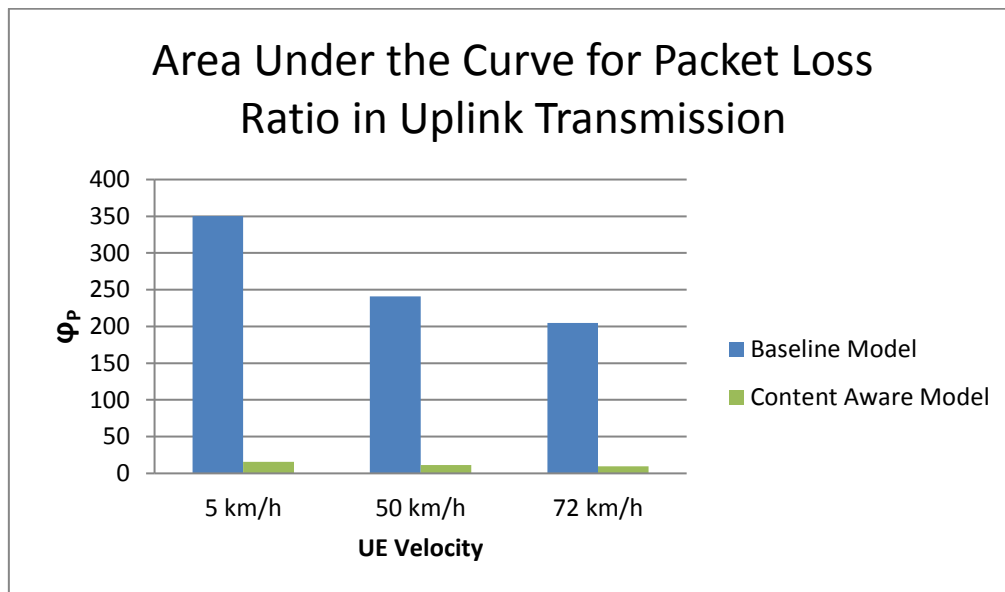


**Figure 4.12:** Area under the curve for packet loss ratio in uplink video transmission in three different UE velocities

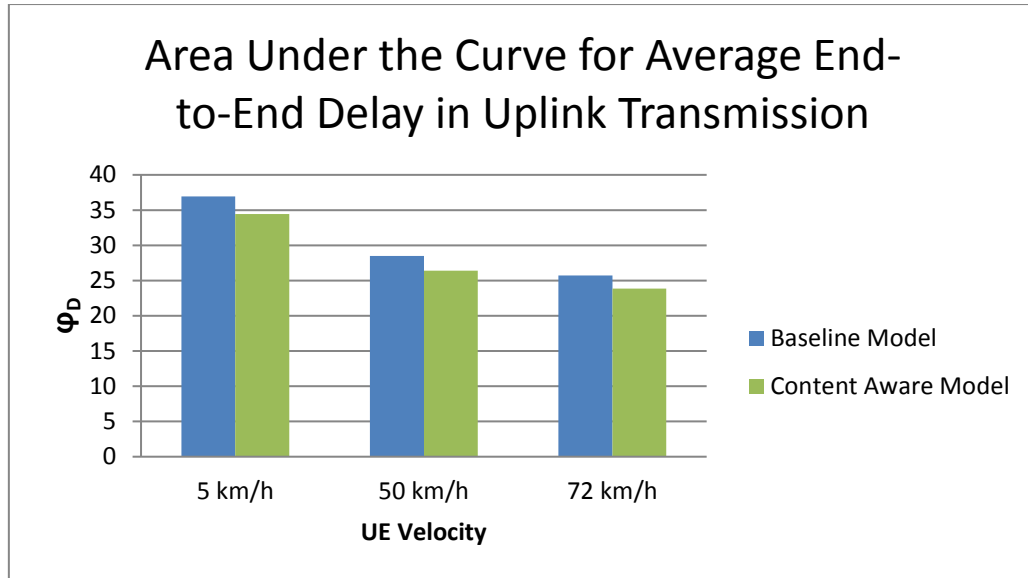


**Figure 4.13:** Area under the curve for average delay in uplink video transmission in three different UE velocities

In Figure 4.11, we observe that the total received data at the remote host increases for both models as the UE velocity is increased from 5 km/h to 50 km/h and then to 72 km/h. This is because the faster the UEs are moving towards the eNodeB, the faster the SINR values are in reaching the minimum threshold, resulting in higher throughput. The amount of data received by both models are almost similar because in the baseline model the wireless channel saturates the constant 4 Mbps data rate transmitted from the UE, causing some of the video packets to be lost in transmission. While in the content-aware RRM model, the transmitted data rate initially at 4 Mbps, is dynamically adjusted to suit the channel condition resulting in an insignificant number of lost packets.

In Figure 4.12, as the UE velocity increases from 5 km/h to 50 km/h and later to 72 km/h, the number of lost packets during the transmission in both models is reduced, accordingly. This is where the proposed model has made the most impressive gain with regard to the number of received packets with an increase of 27.86 % for 50 km/h and 37.47 % for 72 km/h when

compared with that of 5 km/h UE velocity.

The content-aware RRM model also achieves a significant improvement in terms of average end-to-end delay as shown in Figure 4.13. The delay in the video packet transmission is reduced to 23.24 % when the UE velocity is increased from 5 km/h to 50 km/h. A further 9.68 % improvement can be observed when the UE velocity is then increased to 72 km/h. This performance is vital because the video streaming/conferencing application is highly non-tolerant to delays, as specified in its QoS level.

All in all, we can conclude that UE mobility also plays a significant role in determining the overall performance of both the proposed model and the baseline model. Coupled with the higher UE velocity, the content-aware RRM model can significantly improve its overall performance as compared to the baseline model.

#### 4.4 Proposed Look-up Table for the Downlink Content-Aware RRM Model

In Section 4.1, we proposed a look-up table for the uplink content-aware model where the cross-layer optimiser will adjust the data rates in the UE APP layer based on the measured SINR fed back from the PHY layer of the eNodeB accordingly. Thus, the same process can be undertaken for the downlink content-aware RRM model as well by deriving a similar look-up table from Table 3.6 as shown in Table 4.5.

**Table 4.5:** Proposed look-up table for downlink content-aware RRM model

Proposed Data Rate, R (Mbit/s)	SINR (dB)
0.415	< -3.03
0.875	-3.03 – -2.0
0.92	-2.0 – -1.4

<b>Proposed Data Rate, R (Mbit/s)</b>	<b>SINR (dB)</b>
1.625	-1.4 – 0.41
2.33	0.41 – 2.0
3.21	2.0 – 4.26
3.5	4.26 – 6
4	> 6

For the downlink, the channel estimation is undertaken in the targeted UE by measuring the SINR based on the reference signal (RS) transmitted periodically by the eNodeB. This SINR information is then fed back to the eNodeB as input for the cross-layer optimiser before the exhaustive search is made to decide on the most suitable data rate for video transmission from the proposed look-up table. Once the matching data rate is found, then the CLO will instruct the remote host to change its current data rate to the new one.

**Table 4.6:** 4-bit CQI table [33]

<b>CQI index</b>	<b>Modulation</b>	<b>Code Rate x 1024</b>	<b>Efficiency</b>
0	Out of range		
1	QPSK	78	0.1523
2	QPSK	120	0.2344
3	QPSK	193	0.3770
4	QPSK	308	0.6016
5	QPSK	449	0.8770
6	QPSK	602	1.1758
7	16QAM	378	1.4766
8	16QAM	490	1.9141
9	16QAM	616	2.4063
10	64QAM	466	2.7305

<b>CQI index</b>	<b>Modulation</b>	<b>Code Rate x 1024</b>	<b>Efficiency</b>
11	64QAM	567	3.3223
12	64QAM	666	3.9023
13	64QAM	772	4.5234
14	64QAM	873	5.1152
15	64QAM	948	5.5547

In normal LTE downlink transmission, the eNodeB will, based on the channel quality, allocate the available RBs to different users and choose the proper modulation and code scheme (MCS) for multiple users. The channel quality is estimated by the UEs at the receiver side in terms of the SINR; however, instead of transmitting back the SINR values to the eNodeB using the PUCCH, the receiver feeds back the channel quality information to the eNodeB in terms of CQIs according to Table 4.6 [33]. In this table, each CQI value corresponds to one MCS, and the better the channel quality is, the better MCS that the channel can support, and thus the CQI value can reflect the channel quality [86].

For our design, apart from the CQI values, the SINR values are also fed back to the eNodeB using the same PUCCH which will be further used as input to our newly designed cross-layer optimiser at the transmitter side. The eNodeB can easily identify the SINR values for a certain UE by its unique RNTI or International Mobile Subscriber Identity (IMSI). The reasons for both the CQI and SINR values feedback are because CQI values are used for link adaptation while SINR values provide a more accurate estimation of the channel condition before the cross-layer optimiser can decide on adjusting the video data rates accordingly. For adapting to fast channel quality variations, periodic CQI and SINR reporting schemes are used with a reporting interval of 1 ms or 1 TTI. The PHY layer in the eNodeB provides the SINR information to the APP layer in the Remote Host. Since the APP layer of the Remote Host is not aware of radio

resource management on the frequency spectrum, the CQI values, which, consist of both wideband CQI (i.e., a single value of channel state representing all RBs in use) and inband CQIs (i.e., a set of values representing the channel state for each RB) are not useful for adaptations in the APP layer. The reason is that adaptations for every CQIs are not practical and impossible to implement in real-time systems. So, only SINR values are used for the data rate adaptation in the Remote Host. Our proposed cross-layer optimiser at the transmitter side is shown in Figure 4.14.

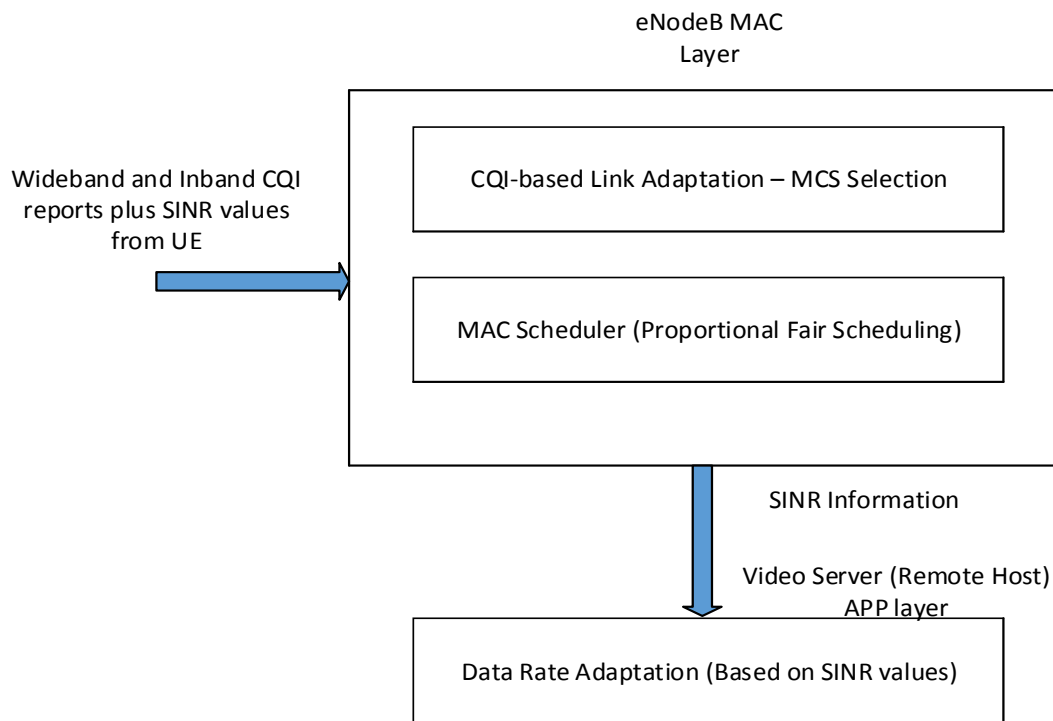


**Figure 4.14:** Cross-layer optimiser in the downlink transmission

#### 4.5 Results Analysis of the Downlink Model

The proposed look-up table in Section 4.4 is embedded in the CLO and coupled together with the baseline model which gives rise to the name content-aware RRM model. The CLO which is assumed to be positioned inside the EPS is the key enhancement made towards the baseline model. Eventually, we can evaluate both the content-aware and the baseline RRM

models for their performances. Repeating the same process carried out previously for the uplink video transmission, and using the specifications defined in Table 3.5 and Table 3.3, both models are simulated for 10 minutes with all UEs moving from the edges of the cell towards the eNodeB following the random waypoint mobility model at three different velocities, only after the simulation time hits 2 seconds. This 2-second gap is essential to allow any communication handshakes and signalling exchanges to occur before actual packet transmissions can be performed.

As usual, the three performance parameters that are of interest are the UE throughput, packet loss ratio and the average delay evaluated for three different scenarios based on the UE velocities. Notably, only UE 4 which receives the video streaming service from the remote host is considered based on its performances. Again, during the whole 10-minute simulation in each scenario, UE 4 which is located initially at 89500 m East and 89500 m South from the eNodeB, never changes direction after the 2 seconds until the end of the simulation. Tables 4.7, 4.8 and 4.9 summarise the performance of both models highlighting the three comparison parameters previously defined in Section 4.2.

#### **4.5.1 Scenario 1**

The first set of simulations were performed when the UE velocities were set at a constant velocity of 72 km/h for both models, and the UEs are positioned at the edge of the cell forming a square box at a distance of 126.57 km from the eNodeB. When the simulation hit 2 seconds, the UE 4 velocity in the  $x$  and  $y$  directions were recorded as -12.701 m/s and 15.4494 m/s, respectively. Figures 4.15, 4.16 and 4.17 display the output performance graphs for both the baseline and the content-aware RRM models.

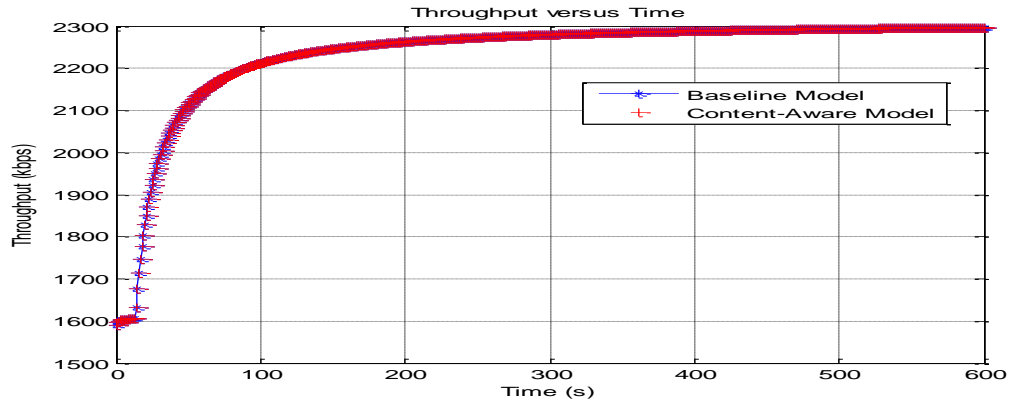


**Figure 4.15:** Throughput against time for downlink video delivery

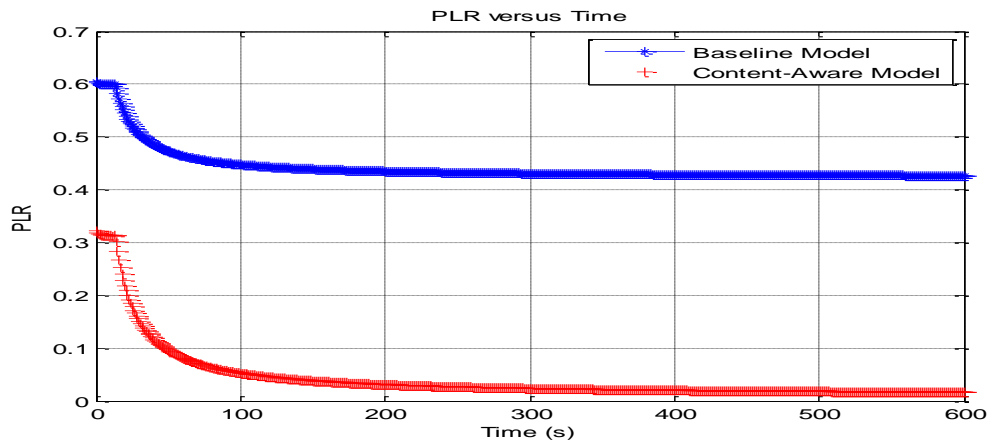


**Figure 4.16:** Packet loss ratio against time for downlink video delivery

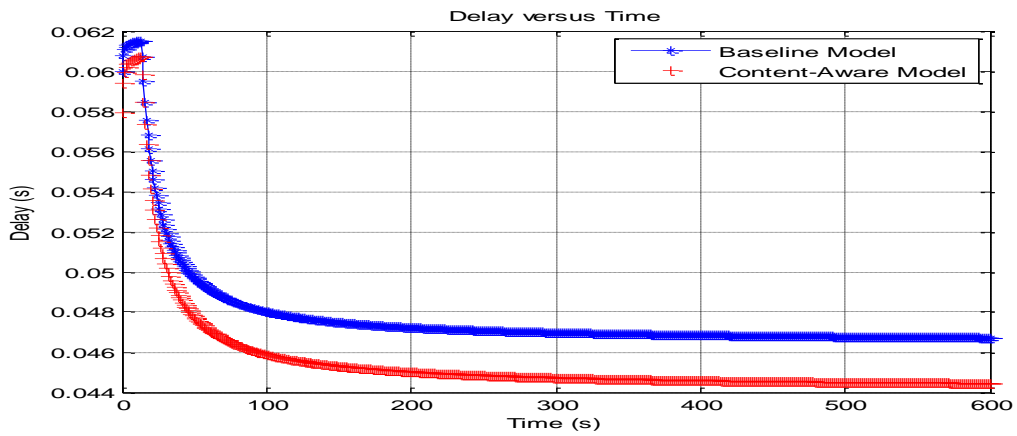


**Figure 4.17:** Average delay against time for downlink video delivery

In Figure 4.15, we observe that the UE 4 throughput for the baseline model is constant at 1.60 Mbps for the first 15 seconds before it starts to increase at a decaying exponential rate for the rest of the simulation time. This behaviour is supported by the other two graphs (Figures 4.16 and 4.17), that show the packet loss ratio, and the average delay levelled at 0.6 and 0.061 s for the first 15 seconds respectively followed by the decrease in the packet loss ratio and average delay as the SINR improves until the end of the simulation time. The entire situation makes sense because the UE was initially positioned at the edge of the cell that is the worst RF condition for any UE to be at and thus a very weak throughput is expected.

For the content-aware RRM model where the CLO is applied to the current baseline model, we observe that its throughput curve (Figure 4.15), mimics the same pattern as that of the baseline model. However, the much-sought improvement can be observed for the packet loss ratio in Figure 4.16, and the average delay graph also displays a significant improvement in Figure 4.17. Over the 10 minutes of simulation, the total amount of data received by both models is the same which is 1.34117 Megabit each. With this amount of data, the content-aware RRM model vastly outperforms its counterpart, the baseline model with a 90.1 % improvement in the packet loss ratio and a significant 4.54 % improvement in the average delay. This means by employing the content-aware RRM model; we can avoid a great deal of bandwidth wastage and preserving the QoS of the video streaming/conferencing application as opposed to the baseline model where the QoS could be effectively compromised.

**Table 4.7:** Comparison of Baseline and Content-Aware RRM models at UE velocity = 72 km/h

<b>Baseline RRM Model</b>	<b>Content-Aware RRM Model</b>
$\varphi_T = 1.3411$ Megabit	$\varphi_T = 1.3411$ Megabit

Baseline RRM Model	Content-Aware RRM Model
$\varphi_P = 265.8244$	$\varphi_P = 26.3114$ (90.1 % improvement)
$\varphi_D = 28.7001$	$\varphi_D = 27.3983$ (4.54 % improvement)
Maximum delay = 0.0615	Maximum delay = 0.0607 (1.3 % improvement)
Actual packet loss = 0.427426	Actual packet loss = 0.0170424 (96.01 % improvement)

#### 4.5.2 Scenario 2

The second set of simulations was performed by setting the UE velocities to 50 km/h and maintaining their original positions at 126.57 km from the eNodeB for both models. After the simulation hit 2 seconds, the UE 4 velocity in the  $x$  and  $y$  directions were recorded as -8.82085 m/s and 10.7296 m/s, respectively.

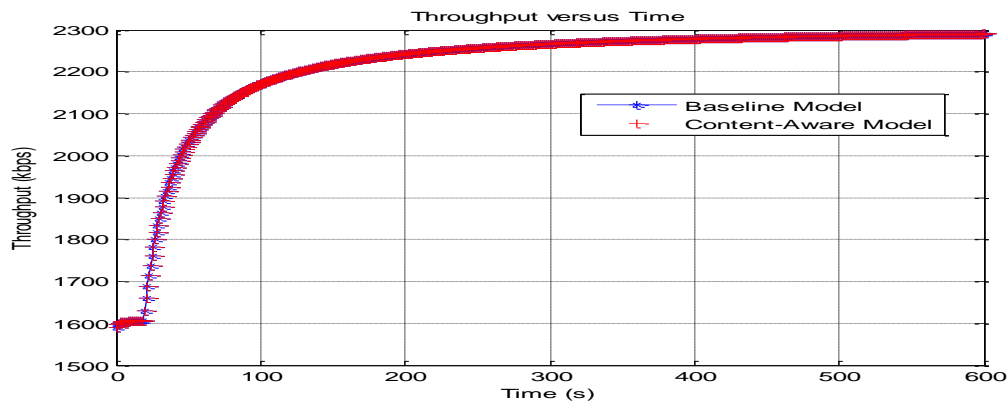


**Figure 4.18:** Throughput against time for downlink video delivery

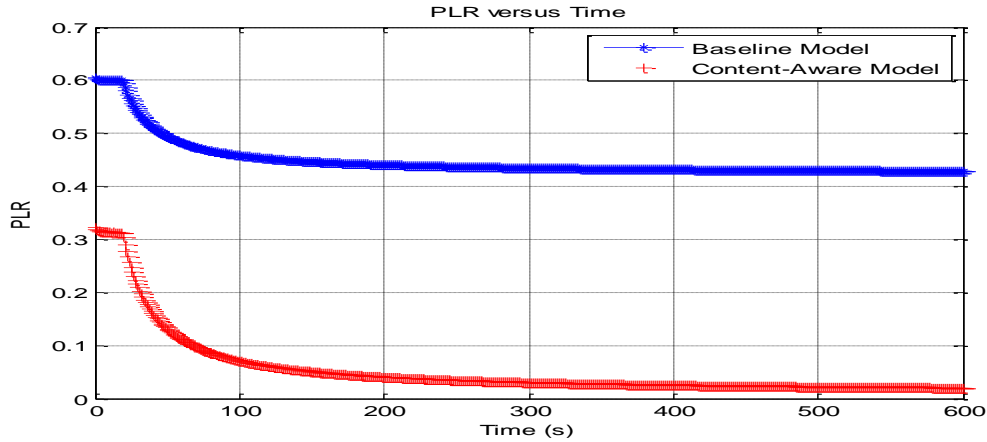


**Figure 4.19:** Packet loss ratio against time for downlink video delivery

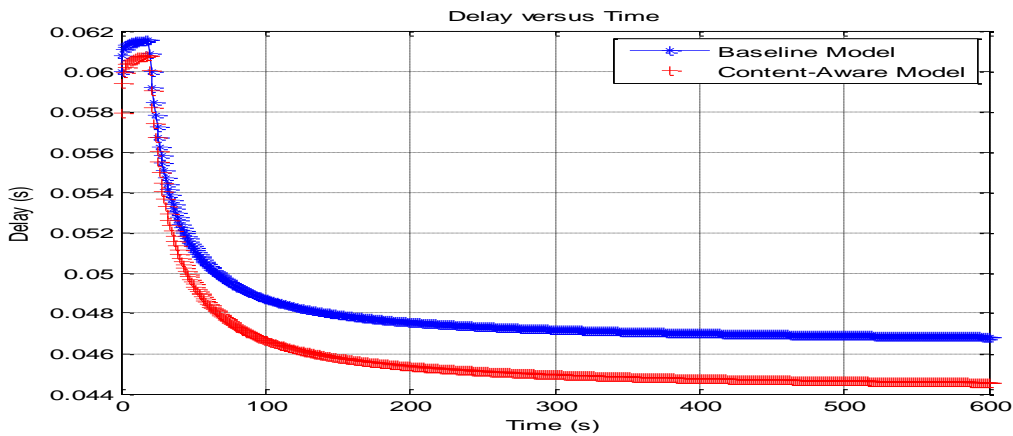


**Figure 4.20:** Average delay over time for downlink video delivery

As reflected in Figures 4.18, 4.19 and 4.20, all graphs for both models follow the same trend as those in Scenario 1 with the turning point starting a little later at 20 seconds. Due to the slower UE speed moving towards the eNodeB from the edge of the cell, the SINR takes a longer time to meet the threshold level before the UE can receive higher than 1.60 Mbps throughput. The same applies to the PLR and average delay graphs where their performances continually improve after the 20<sup>th</sup> second.

Even so, the content-aware RRM model still achieves greater enhancement with respect to the packet loss rate and average delay, in comparison with the baseline model. We observe

that for the same amount of data received by the UE ( $\varphi_T = 1.3263$  Megabit), almost 88 % improvement is gained for the arrival of video packets and about 4.4 % gain in the average delay as summarised in Table 4.8. This achievement emphasises the results which we have analysed in Scenario 1 where the implementation of content-aware RRM model can dramatically reduce unwanted packet losses while preserving the QoS of the data bearer.

**Table 4.8:** Comparison of Baseline and Content-Aware RRM models at UE velocity = 50 km/h

<b>Baseline RRM Model</b>	<b>Content-Aware RRM Model</b>
$\varphi_T = 1.3263$ Megabit	$\varphi_T = 1.3263$ Megabit
$\varphi_P = 269.5153$	$\varphi_P = 32.6476$ (87.89 % improvement)
$\varphi_D = 28.9694$	$\varphi_D = 27.6948$ (4.4 % improvement)
Maximum delay = 0.0615s	Maximum delay = 0.0608s (1.14 % improvement)
Actual packet loss = 0.429163	Actual packet loss = 0.0200236 (95.33 % improvement)

### 4.5.3 Scenario 3

The final part of the downlink simulation is carried out not only by placing all the UEs at 126.57 km from the eNodeB, but their velocities are also set to the pedestrian speed of 5 km/h. As the simulation hit 2 seconds, the UE 4 velocity in the  $x$  and  $y$  directions were recorded as -0.88272 m/s and 1.07373 m/s, respectively.

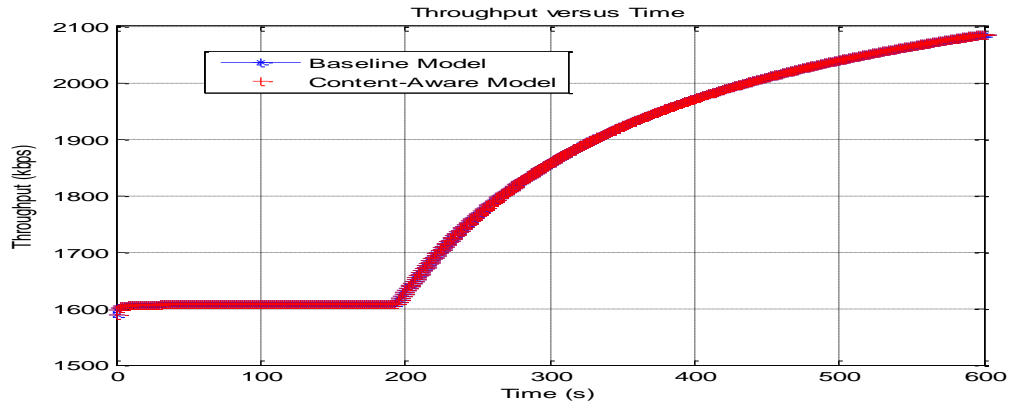


**Figure 4.21:** Throughput against time for downlink video delivery

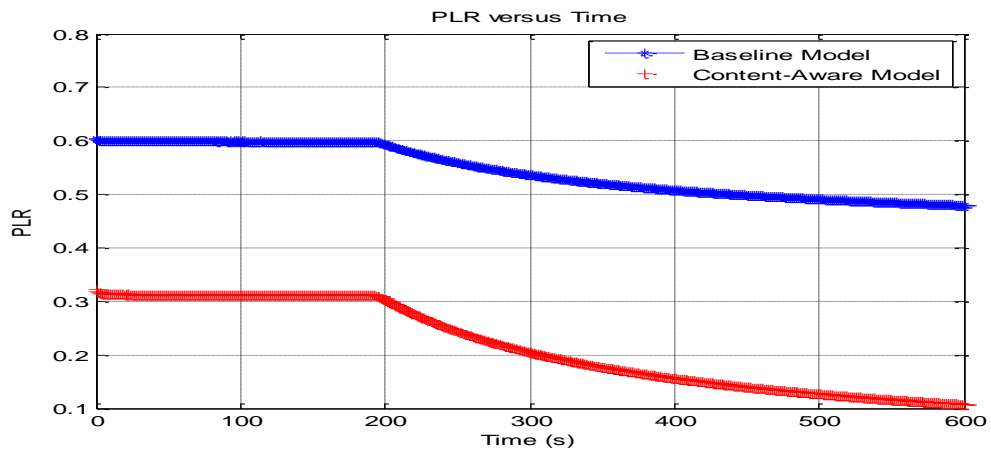


**Figure 4.22:** Packet loss ratio against time for downlink video delivery

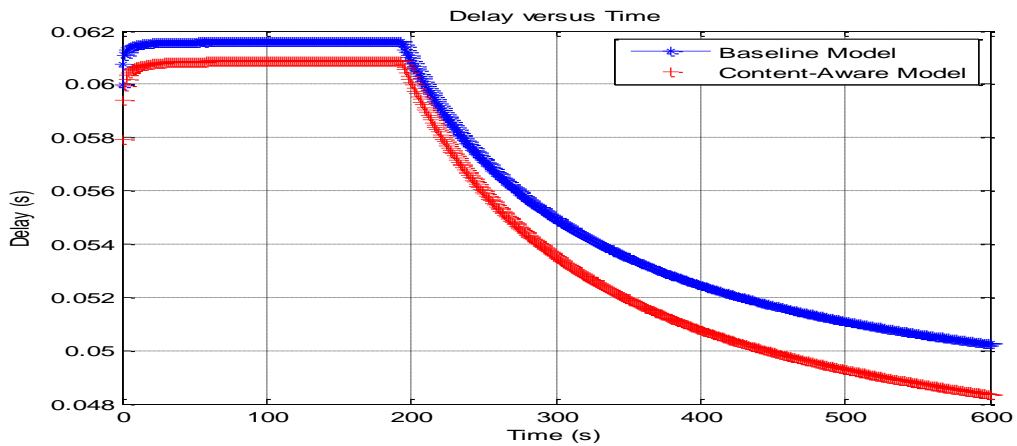


**Figure 4.23:** Average delay against time for downlink video delivery

After the 10-minute simulation, the results in Figures 4.21, 4.22 and 4.23 for the baseline model have been consistent until the 195<sup>th</sup> second before we can observe any improvements in the throughput as well as the packet loss ratio and average delay. Comparing the results from Scenario 1 and Scenario 2 together, we can therefore say, that performance of the video packet transmission is at its worst when the UE moves with the slowest velocity from the edge of the cell towards the eNodeB. This corresponds to the parameters that suffer the most which are the packet loss ratio followed by the average delay.

In contrast, a much better performance for the content-aware RRM model is shown in the same figures. It is demonstrated via the statistics shown in Table 4.9 where, with the amount of data received by UE 4 amounting to 1.0971 Megabit, the total number of received packets has increased to 59.99 %, and the total average delay has been reduced to 2.34 %. Even though the results obtained for the content-aware RRM model in this scenario are not as good as those in Scenario 1 and 2, the performance improvements achieved, as compared to those for the baseline model, prove that cross-layer optimisation, with the implementation of its proposed look-up table, can significantly increase performance of the LTE system regardless of the channel condition and the UE velocities.

**Table 4.9:** Comparison of Baseline and Content-Aware RRM models at UE velocity = 5 km/h

<b>Baseline RRM Model</b>	<b>Content-Aware RRM Model</b>
$\varphi_T = 1.0971$ Megabit	$\varphi_T = 1.0971$ Megabit
$\varphi_P = 326.6245$	$\varphi_P = 130.6888$ (59.99 % improvement)
$\varphi_D = 33.6441$	$\varphi_D = 32.8571$ (2.34 % improvement)
Maximum delay = 0.0616s	Maximum delay = 0.0609s (1.14 % improvement)

Baseline RRM Model	Content-Aware RRM Model
Actual packet loss = 0.480245	Actual packet loss = 0.107718 (77.57 % improvement)

#### 4.5.4 Mobility Analysis for the LTE Downlink Video Packet Transmission

Like Section 4.3.4, in this section, we analyse the UE mobility effect on the video packet transmission performance for both models in the downlink path. Again, three UE velocities; 5 km/h, 50 km/h and 72 km/h, are considered for comparison purposes. Section 4.5 explains in detail how the simulation is performed exclusively for the downlink transmission.

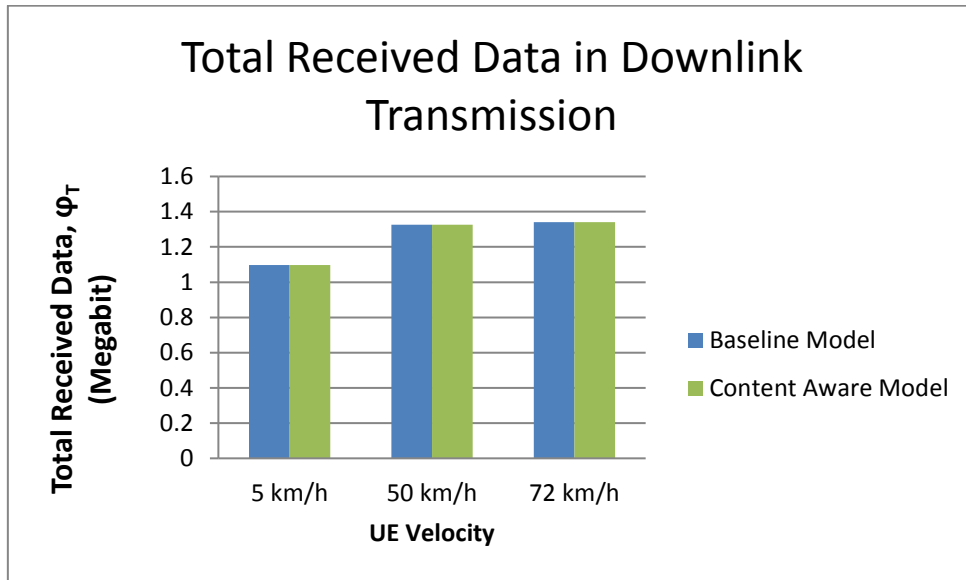


**Figure 4.24:** Total received data in downlink video packet transmission in three different UE velocities

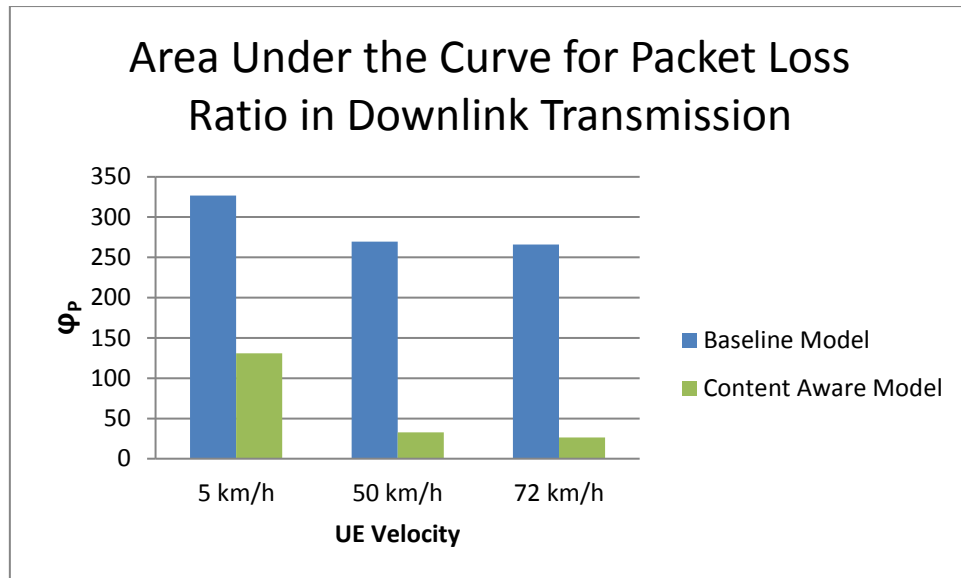


**Figure 4.25:** Area under the curve for packet loss ratio in downlink video transmission in three different UE velocities

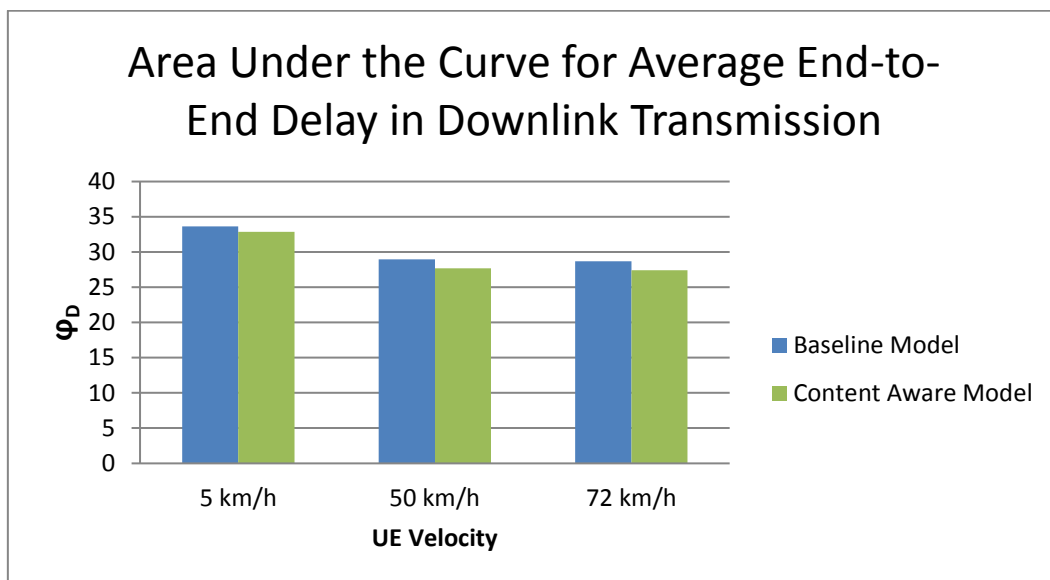


**Figure 4.26:** Area under the curve for average delay in downlink video transmission in three different UE velocities

In Figure 4.24, the UEs in both the baseline model and the proposed model appear to receive the same amount of data from the remote host as the UE velocity is increased from 5

km/h to 50 km/h followed by 72 km/h. Even so, both models are experiencing a different approach before the data arrives at the respective UEs. As shown in Figure 4.25, when the UE velocities are increased from 5 km/h to 50 km/h, the baseline model only manages to achieve a 17.48 % improvement with regard to the number of received packets whereas the content-aware RRM model successfully gains the number of received packets as high as 75.02 %. The insignificant improvement of 1.37 % with respect to the packet loss ratio posed by the baseline model is in stark contrast to the 19.41 % gain displayed by the proposed model, even as the UE velocities have small increases from 50 km/h to 72 km/h. This means that, for the same amount of data received by both UEs, the number of packets lost during the downlink transmission is far too vast for the UE in the baseline model as compared to that in the proposed model, although the UE velocities are increased at the same rate. The same reason mentioned in the uplink transmission applies here in the downlink transmission. In the baseline model, the constant 4 Mbps data rate transmitted from the remote host is saturated by the wireless channel, while in the proposed model, even though the UE data rate was set to 4 Mbps initially, the CLO implementation within the transmitter has consistently changed the transmitted data rate, based on the received SINR values, effectively reducing the number of lost packets.

In Figure 4.26, as the UE velocities are increased from 5 km/h to 72 km/h, the average delay of the video packets in the baseline model improves by nearly 14.7 % whereas, in the proposed model, a significant gain of 16.61 % is achievable for the same performance metric. The reason why the average end-to-end delay improvement for both models are not as significant as those of the packet loss ratio is that both models perform the hybrid-ARQ (HARQ) process at their UE MAC layers which cause further delay to the received video packets. Also, since the baseline model incurs much higher lost packets as compared to the proposed model, it is evident that the more video packets that are lost during the transmission are retransmitted

from the eNodeB to UE 4, thus, resulting in slightly higher average end-to-end delay.

Overall, the performance of the content-aware RRM model in the downlink video packet transmission can be further increased by incorporating the mobility aspect of the UE mainly by increasing the UE velocity towards the eNodeB.

#### **4.6 Summary**

In this chapter, the proposed look-up tables and the corresponding cross-layer optimiser designs for the video packet delivery in both the uplink and downlink transmissions are presented. The proposed look-up tables, derived from the throughput performance of the LTE baseline simulation model in relation to its SINR values in Chapter 3, are embedded in their respective cross-layer optimisers, giving rise to the name, content-aware RRM model.

The proposed content-aware RRM model is simulated and compared with the baseline model as the UE moves from the edge of the cell towards the eNodeB at three different UE velocities. The results obtained can be summarised that the Content-Aware RRM model produces much better performance than the Baseline Model in either the uplink or downlink video packet transmission. In fact, for the same amount of throughput, the Content-Aware RRM model in all simulations proves its superiority in fulfilling QoS requirements especially regarding a very low packet loss ratio and average end-to-end delay performance as compared to the Baseline Model.

Further analysis has also been carried out to justify the superiority of the proposed model over the baseline model with respect to different UE velocities approaching the eNodeB. Again, the results obtained from the comparison study show that the proposed model vastly outperformed the baseline model with regard to the low packet loss ratio and average delay for the same amount of throughput. These results conclude that UE mobility can further enhance

the performance of the proposed content-aware RRM model especially when the UE is closing in towards the eNodeB.

## 5 PRACTICAL MEASUREMENTS

### 5.1 Introduction

In Chapter 3, we presented the correlation graphs and tables between the throughput, packet loss ratio, average delay and the UE or eNodeB SINR for both the uplink and downlink video packet transmissions. In Chapter 4, we introduced two look-up tables to implement in the cross-layer optimiser, one for each transmission where the data rate of the sources at the APP layer is adjusted depending on either the UE or the eNodeB SINR from the PHY layer for maximising throughput, minimising the packet loss ratio and preventing bandwidth wastage.

In this chapter, we provide practical comparisons of the results obtained in Chapters 3 and 4 by performing some testbed measurements for video packet transmission at a UK-based company, Rinicom Ltd [87]. Rinicom Ltd is a privately owned global technology company specialising in providing state-of-the-art solutions for wireless broadband communications, intelligent surveillance and first responder applications [87]. While wireless broadband communication is one of the research and business areas of the company, it is important to note, that the testbed developed for the comparison purposes is not based on the LTE network. The reason is that the LTE frequency spectrum is a licensed frequency band [88]. Without the license to proceed with the LTE measurement, this would have been considered illegal as the frequency spectrum is the most precious resource in wireless communications, regulated by OFCOM in the UK [89]. Instead, we have used PodNodes, (one of the products by Rinicom Ltd) as the replacement to emulate the LTE transmission. In fact, two PodNodes were used as the transmitter and receiver whereby, one acts as an eNodeB and the other acts as an interface to a UE. Although the PodNode technology used in the practical investigation does not precisely represent the real LTE platform, several factors have been introduced to establish the link

between the PodNode and the LTE system, as follows:

- (i) OFDM-based air interface: Both systems use OFDM as their primary air interface in which the LTE uses OFDMA for its downlink and SC-FDMA for its uplink which is centred at 2 GHz frequency. Whereas, PodNode technology uses Coded-OFDM for both its downlink and uplink transmissions centred at 1.44 GHz frequency. This OFDM-based modulation scheme is critical in deciding the close link between the LTE and the PodNode. Even though their operating frequencies are different, there exist, multiple LTE frequency bands that are commercially available in the UK and Europe. One frequency band that has gained interest by telecommunication operators is the 800 MHz frequency band which is much lower than the standard 2 GHz band. Accordingly, the operating frequency is not a primary concern when developing the LTE testbed using the PodNode technology because there are many options available for LTE licensed frequency bands.
- (ii) PHY layer specifications and protocol: From the PHY layer perspective, many of the main specifications and protocols are similar. For example, both systems implement Link Adaptation for their subcarriers which make use of adaptive modulation techniques starting from QPSK up to 64-QAM, depending on the channel condition. Another similarity between the two systems is their bandwidth scalability where the system or the channel bandwidth can be as low as 1.4 MHz for LTE and 5 MHz for PodNode which can be further expanded up to 20 MHz for both. Furthermore, both systems do not involve the APP layer protocol.
- (iii) Point-to-Point (P2P) and Point-to-MultiPoint (P2MP) link architecture: Both systems can be configured to provide either P2P or P2MP link architecture for data transmission. In LTE, the eNodeB can provide access for a single user or multi-

user functionality whereas, in the PodNode technology, each PodNode can be interconnected with each other through wireless mesh topology to provide either P2P or P2MP.

- (iv) PodNode technology as a part of LTE infrastructure: PodNode forms as part of the LTE network infrastructure and is also used as a backhaul between the eNodeB and the Serving/Packet Data Gateway. If network performance measurements were carried out on the PodNode, it would also affect the performance of the LTE network. This means that the PodNode contribution in providing network support for the LTE platform is crucial and justifies the link between the LTE and the PodNode.

Based on the above points, the capability of PodNode technology to emulate the LTE network to compare with the theoretical simulation models can be considered acceptable. It is also important to note at this point, that the two systems can be realistically justified to be consistent as some of the PHY layer parameters such as the modulation and coding scheme, OFDM modulation and channel bandwidth can be correlated with each other. The purpose of comparing the measurement results and the theoretical simulation results is not to make exact one to one comparison between their output parameters but rather to compare the output performance pattern. To thoroughly understand the operation of the PodNode technology testbed emulating the LTE network, the following subchapter will provide details of the equipment used during the experiment setup.

## **5.2 System Description**

Before deploying the testbed, several assumptions are presented regarding limitations in the PodNode technology:

- (i) The LTE-EPC network model is replaced with the PodNodes technology whereby one PodNode is treated as an eNodeB coupled with SGW/PGW and the other PodNode acting as an interface to a UE.
- (ii) The wireless channel is replaced using a wired channel instead. Even using a wired channel, we can still emulate the variation of the SNR in the wireless channel using a variable attenuator, which means that the two PodNodes would be connected to each other via a variable attenuator.
- (iii) The variable attenuator could also cover the mobility aspect of the UE by decrementing the attenuation values to represent the UE approaching the eNodeB or vice versa.

The above assumptions are important because the entire testbed setup and measurements are located at Rinicom Ltd, under a fixed deployment scenario (i.e. on the third floor of Riverway House). The layout of the testbed and equipment are shown in Figure 5.1. The equipment (including software) essential in conducting the practical measurements are described as follows:

- a) PodNode [90]

Rinicom Ltd. has developed the PodNode as its latest technology innovation, which allows up to 12 portable mesh nodes to be easily connected into a self-forming, self-healing mesh network. By using coded orthogonal frequency division multiplexing (COFDM), the system offers a non-line-of-sight operation, making it mobile and dynamic. Hence, even in the most challenging and rapidly evolving environments, it can provide secure and robust communications.

Specifically, Rinicom's PodNode COFDM IP Ad-Hoc Mesh System consistently

monitors channel state information and reconfigures communication paths based on the predefined criteria which differ from conventional legacy wireless solutions. With the help of its smart routing algorithm, the system is intrinsically capable of self-healing, which allows the other nodes in the network to communicate with each other, either directly or through one or more intermediate nodes, even if one node is unable to operate or its communication link is not suitable for the chosen service (for instance, real-time video transmission). This makes the PodNode technology ideal for a rapid deployment scenario where each PodNode automatically routes data around the wireless network. Besides, it is also easily configured to operate without the need for user intervention.



**Figure 5.1:** Practical testbed for LTE uplink video delivery

A PodNode MESH network can support up to 50 Mbps data throughput and, thus, true

real-time 1080p HD video is possible to be transmitted. Also, the advantage of applying ad-hoc mesh topology is evident, as data communications in a point-to-point or point-to-multipoint modes can be preserved as the mesh nodes themselves can be used as repeaters for long-range communications.

Rinicom's PodNodes are flexible regarding fixed and mobile deployment. The mobile applications cater for vehicle-mounted convoy applications, body worn, mobile and advanced ground robot control whereas, the typical fixed scenario is deployed for first responder, rapidly deployable wireless networks, surveillance applications and long-range wireless IP networks.

The attractive feature of the PodNode technology is that each PodNode can be remotely controlled through Rinicom's web interface and thus, enabling the network operator to control every PodNode independently, or just to monitor the network status.

Several variants have been developed for the PodNode system, namely PodNode-I, PodNode-R, PodNode-M and PodNode-OEM. The full technical specifications of the first three PodNode variants are displayed in Table 5.1. Most of the technical specifications for the three PodNodes are the same apart from minor differences regarding weight and dimensions. The only striking difference between the three is that PodNode-I has to be connected with a direct power supply; it does not operate on batteries whereas PodNode-R and PodNode-M have built-in batteries. This means PodNode-R and PodNode-M are more suitable for mobile testbed deployment as compared to PodNode-I which is more preferable for stationary deployment. In our testbed setup, we have chosen PodNode-I to emulate the LTE transceiver rather than the other two PodNodes due to the assumptions made earlier where the wireless channel and the UE mobility can both be replaced with a transmission line via a variable attenuator.

As shown in Figure 5.2, PodNode-I is a robust PodNode module enclosed in aluminium

which is ideal for standalone stationary operation. Another variant of PodNode is PodNode-PoE which has the same capability for stationary operation with comparable performance [91] and is also chosen to be the partner for PodNode-I chosen earlier as reflected in Figure 5.1.

**Table 5.1:** Technical specifications of three PodNode variants<sup>1</sup> [92]

Technical Specification				
	PodNode-I	PodNode-M	PodNode-R	
<b>RF Interface</b>	Antenna 1	TDMA transmit and receive		
	RF frequency	UHF, L-Band, S-Band		
	Frequency tuning	1MHz		
	Modulation	COFDM		
	Subcarrier modulation	QPSK, 16 QAM, 64 QAM (adaptive)		
	Output power	+27dBm Max		
	Output power tuning	0.5dB steps		
	Bandwidth	5 to 20 MHz		
	Bandwidth tuning	1 MHz		
	MESH capacity	Up to 50 Mbps		
<b>Physical</b>	Dimensions	162 mm x 127 mm x 40 mm	120 mm x 34 mm x 168 mm	202 mm x 120 mm x 56 mm
	Weight (excl. battery)	480g	651g	1047g
	Weight (incl. battery)		891g	1618g
	Enclosure	IP rated	IP rated	IP rated
	Mount	Free standing/tripod mount	Free standing/tripod mount	Free standing/tripod mount
	Operating temperature	-10°C to +40°C	-10°C to +45°C	-10°C to +45°C
<b>Battery</b>	Operating humidity	0 to 90%	0 to 90%	0 to 90%
	Weight		240g	571g
	Voltage		14.8V	14.8V
	Capacity	N/A	2.6AH	6Ah
	Duration		3 hours	3.5 hours
<b>Power</b>	Fixing		Clip in	Clip in
	DC input		9-16VDC	
<b>Mesh</b>	Power consumed @ +27dBm	14W	14W	22W Max (PodNode-R/SD)
	Number of nodes		Up to 12	
	MESH configuration		Ad-hoc, P2MP, P2P	
	Routing		Smart routing	



b) IP Camera (Network Camera)

The purpose of having an IP camera or network camera connected at one end of the PodNodes is to transmit the live video stream to a portable laptop or a computer at the receiving

<sup>1</sup> Rinicom Ltd. product list specifications. <[https://github.com/TransparencyToolkit/dataspec-sii/blob/master/sii\\_data/docs/1324-rinicom-ltd-product-list-specifications.pdf](https://github.com/TransparencyToolkit/dataspec-sii/blob/master/sii_data/docs/1324-rinicom-ltd-product-list-specifications.pdf)> [Accessed 15 February 2017]. Permission to reproduce this table has been granted by Rinicom Ltd.

end. The model used for the IP camera was an AXIS P1357 Network Camera, (Axis Communications) as shown in Figure 5.3. The model is equipped with H.264 and Motion JPEG video coder which makes it capable of delivering multiple H.264 and Motion JPEG video streams in 5-megapixel resolution or full frame rate HDTV 1080p resolution.

Other features that accompany this model are its wide dynamic range and day and night functionality which provide excellent image quality in daylight and dark conditions. For optimal depth of field and image sharpness, P-Iris control provides the precise control of the iris position. Apart from supporting Power over Ethernet (PoE), the camera also has a remote back focus function which enables fine-tuning of the focus from a computer [93].



**Figure 5.2:** PodNode-I<sup>2</sup> [100]

c) Iperf/Jperf Software

The Iperf and Jperf software are used in the testbed in which all the results for the output performance parameters are measured and are installed on both laptops before deploying the

---

<sup>2</sup> Rinicom website. <<http://www.rinicom.com/products/communications/podnode-i>> [Accessed 15 February 2017]. Permission to reproduce this figure has been granted by Rinicom Ltd.

testbed.

Iperf is free, commonly used network testing software that can create TCP and UDP data streams and measures the performance of a network. It was initially developed at the National Center for Supercomputing Applications at the University of Illinois by the Distributed Applications Support Team (DAST) of the National Laboratory for Applied Network Research (NLANR) [94].

Iperf is additionally, a cross-platform software tool that can be executed over any network or operating system including Microsoft Windows, Unix and Linux and ultimately, produce standardised output performance parameters. Thus, it can be used for the comparison of both wired and wireless networking equipment and technologies.

As mentioned earlier, the objective of the open-source software tool is to measure the bandwidth between two nodes in a computer network and the quality of the network link. The idea is to run Iperf on both computers and measure the performance between both, where one computer is configured as the client and the other as the server [95]. On the first computer, Iperf runs in server mode, as it waits to receive traffic from the client whereas, on the other computer, which runs in client mode, it generates TCP or UDP traffic and measures related performance parameters. When used for testing TCP capacity, Iperf measures the throughput of the received payload. Similarly, when used for testing UDP capacity, Iperf produces results for the datagram throughput and the packet loss.

Typically, the output presentation using Iperf contains a time-stamped report displaying the amount of the data transferred and the throughput measured for TCP measurement whereas, for UDP measurement, the output format is extended to include packet loss and jitter.



**Figure 5.3:** Axis P1357 network camera<sup>3</sup> [96]

As an alternative, we can also use Jperf which is the GUI-based version of Iperf. Jperf is a graphical front-end for the network testing tool Iperf. It can be used to determine the maximum network throughput of a WAN or LAN connection. Furthermore, the tests results are automatically graphed and displayed in a presentable format. Similar to Iperf, Jperf can also be used to measure packet loss, throughput and jitter. Jperf offers many advantages over Iperf for its reliability and ease of use, whereas Iperf is a command line driven application. The first step before Jperf can be installed on Microsoft Windows, for example, is to install the pre-requisite software, which is Java version 1.5 or later. Only then, do we download the Jperf-2.0.2.zip file from the Jperf Google code webpage. Next, we extract the contents of the zip file into a folder located on the computer or laptop's hard-drive without using an installer. Finally, we run the executable jperf.bat file to launch the Jperf utility [97]. Owing to the advantage of having a user-

---

<sup>3</sup> Axis P1357 Network Camera Data Sheet. <  
[https://www.axis.com/files/datasheet/ds\\_p1357\\_1471705\\_en\\_1702.pdf](https://www.axis.com/files/datasheet/ds_p1357_1471705_en_1702.pdf)> [Accessed 15 February 2017].  
Permission to reproduce this figure has been granted by Axis Communications AB. *Courtesy of Axis Communications AB. All rights reserved.*

friendly GUI-based platform and concurrently having the graphs plotted instantly, a decision is made to use Jperf rather than Iperf for the real testbed implementation.

d) **VLC Media Player**

The VLC Media Player is required to be installed on the first (primary) laptop (which will be used to configure the IP address of PodNode-I) to receive the live video stream transmitted from the IP Camera. Like Iperf/Jperf software, VLC software is freely available as open source software which can function across all platform, having the ability to play most multimedia formats and files as well as DVDs, Audio CDs, and various streaming protocols [98].

### **5.3 System Development and Implementation**

Before the complete layout of the testbed can be implemented, several hardware and firmware configurations need to be performed, especially for the IP Camera and the PodNodes.

#### **5.3.1 IP Camera Configuration**

First, one laptop is connected to the IP camera via a splitter where the splitter obtains power via the laptop's USB port. One output port from the splitter is connected to the network port of the laptop while the other output port is connected to the network connector PoE of the IP camera. Once completed, the laptop's IP address is configured using a static IP address, as the dynamic IP address is no longer suitable for use in this experiment. Since the IP camera already has a static IP address (192.168.1.34), the laptop's IP address can be configured to be (192.168.1.30) with a subnet mask of (255.255.255.0). The laptop is checked to ensure that it can detect the IP camera or not, using the 'ping' command.

As mentioned previously, the IP camera can be operated and controlled remotely using a computer. If the laptop successfully detects the IP camera, then we navigate via the internet using a web browser and type in the IP address of the IP camera where the 'Live View' home page of the IP camera is displayed.

Next, we go to 'Setup' section of the Live View page, and after typing in the following information:

- User Name: [root]
- Password: [admin]

A basic setup page is displayed as shown in Figure 5.4. The Image Appearance Capture Mode (Figure 5.4) is already configured as HDTV 1080p type which is the highest resolution provided and supported by the vendor for this camera. This resolution will be used later in the overall experiment setup. The last part of the IP camera's configuration adjusts the focus which is under the 'Basic Setup', where we select the 'Advanced' option to automatically fine tune the image focus of the IP camera so that a sharp image from the video is obtained. The next step is to detach all connections between the laptop and the IP camera.

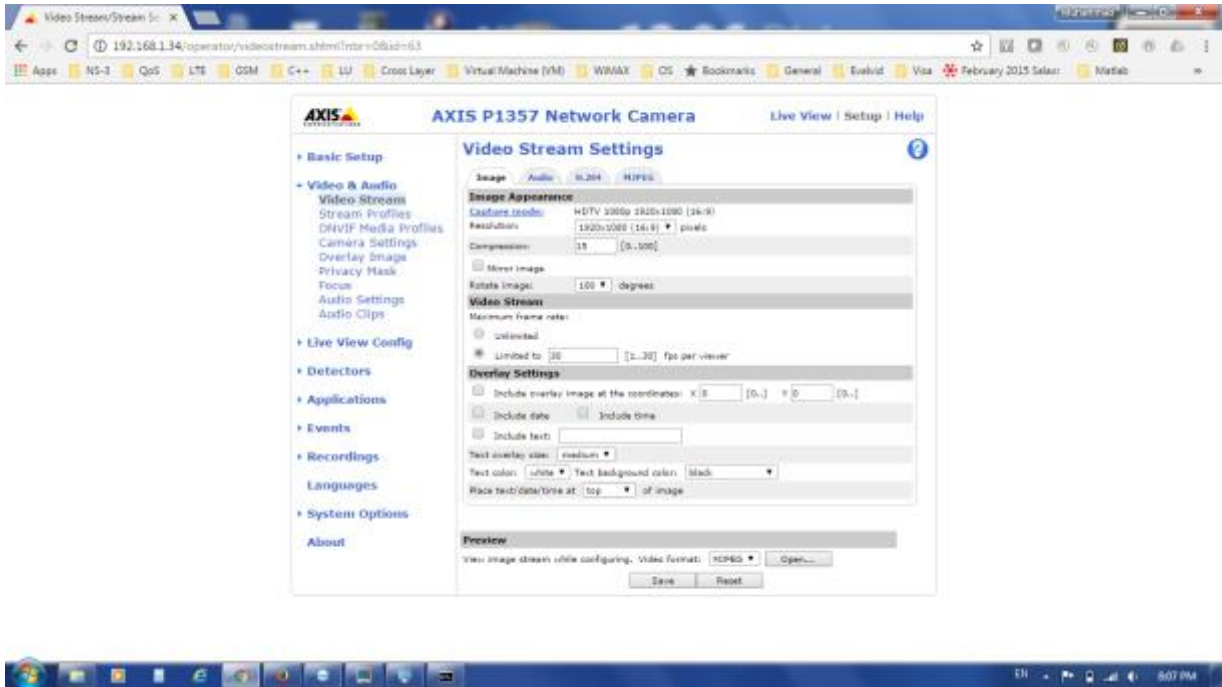


**Figure 5.4:** Basic setup of IP (network) camera

### 5.3.2 PodNodes Configuration

Both PodNodes, (PodNode-I and PodNode-PoE) are together connected via a variable attenuator using two coaxial cables for each side. Only PodNode-I is linked with the previous laptop through the Ethernet port. To power both PodNodes, an RS-232 serial cable is used for PodNode-I, whereas for PodNode-PoE, a PoE injector (e.g. PHIHONG Switching Power Supply, Single Port PoE IEEE802.3 at the PoE injector) is used, where, the output port of the injector is attached to the Ethernet port on the PodNode-PoE using the Ethernet cable to maintain an IP67 rating. Next, an alternate IP address is added to the laptop because the default IP address of the PodNode-I is set to (192.168.0.101). The alternate IP address is (192.168.0.165) and is configured along with the subnet mask of (255.255.255.0). The similar situation for setting up the IP camera is undertaken as previously performed by controlling and configuring PodNode-

I via the web browser. We locate the PodNode-I web server by typing in its default IP address (192.168.0.101) into the address field. The PodNode Login page is presented, as shown in Figure 5.5 and typing the word “*admin*” enters the Password. The user is then presented with the PodNode: Main Page as displayed in Figure 5.6.

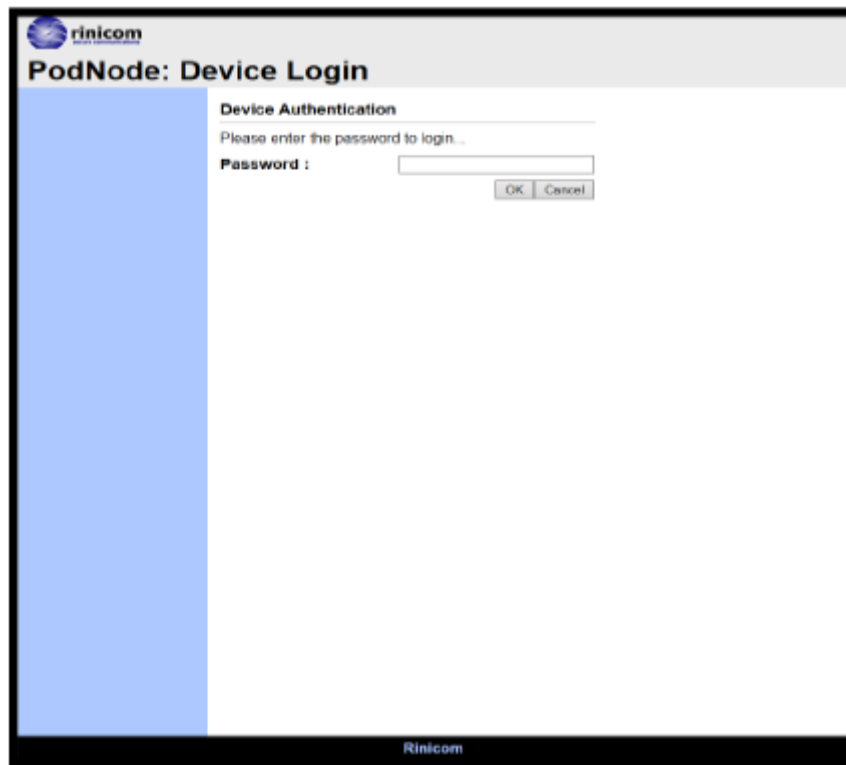


**Figure 5.5:** PodNode webpage: Device login

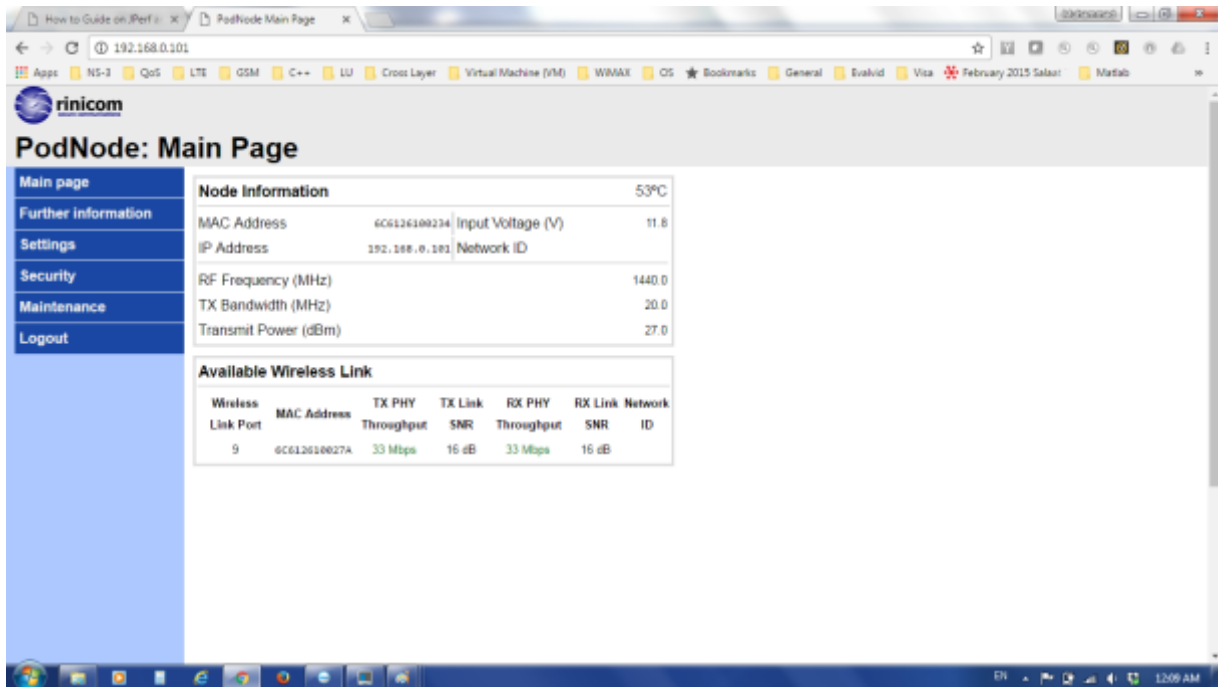


**Figure 5.6:** PodNode Webpage: Main page

As illustrated in Figure 5.6, the three principal features of PodNode include:

- (i) **RF Frequency:** The central frequency of the RF transmit signal in MHz where the frequency is centred at 1440 MHz;
- (ii) **Transmit Bandwidth:** The bandwidth of the RF transmit signal in MHz which is 20 MHz; and
- (iii) **Transmit Power:** The transmit power of the RF transmit signal in dBm with the value of 27 dBm.

Accordingly, the RF frequency is fixed for the testbed while the transmission bandwidth can be varied between 5 and 20 MHz and the transmit power can be changed to a maximum of 30 dBm. The reason why the RF frequency is already fixed at the current value is that the electronic devices in the PodNode are already tuned to that particular frequency and is recommended not to be changed during the entire process.

Another piece of information that is critical to our experiment is the TX Link SNR. This value is determined by how much attenuation is set by the variable attenuator. At the period in which the TX Link SNR value was recorded, the variable attenuator was tuned to 30 dB.

During this operation, the two PodNodes will communicate with each other with no meaningful data transmitted at this stage, as the communication between the two, is for signalling and synchronising purposes. Both PodNodes operate on Coded-OFDM modulation, followed by TDMA transmit and receive, and operate in time division duplex (TDD) mode instead of frequency division duplex (FDD) mode. This is the main reason why the TX PHY Throughput, RX PHY Throughput and RX Link SNR values can be observed. However, these values are not overly important to the experiment, except for the TX Link SNR values because the video packets will be transmitted using the UDP protocol instead of TCP protocol.

Even though the duplex mode for the testbed is entirely different from our LTE-FDD simulation model, the concept of ‘general communications’ which involves signalling protocols with time and frequency synchronisation remain the same as in the eNodeB and UE communications, especially when the UE is in idle mode. One similarity, though between our LTE-FDD simulation model and the PodNodes testbed, is that adaptive subcarrier modulation usage in the communication, which is interchangeable between QPSK, 16-QAM and 64-QAM, is reliant on the channel condition.

Each time the attenuation values were to be varied between 10 and 100 dB (one at a time), we needed to navigate to the ‘Maintenance’ submenu from the main page in the browser to select the ‘Hardware Reset’ option until the main page was refreshed with the new Available Wireless Link information. The last point worth mentioning is if the Tx Bandwidth and/or the Tx Power need(s) to be changed; we need to navigate back to the ‘Settings’ submenu and then change the required values. Similar to navigating via the Maintenance submenu followed by

Hardware Reset to reset the hardware to obtain new information related to the communication link. The same process is repeated once the variable attenuation and/or the PodNode settings are/is changed. This process was regularly practised in our final testbed setup, as discussed later in this section.

### **5.3.3 Overall Setup (with IP Camera)**

In Section 5.3.1 and Section 5.3.2, we configured the IP camera, the PodNodes and the main laptop with their respective IP addresses. In this section, the IP camera will be connected to the PodNodes, variable attenuator and the main laptop. The main laptop is placed at the left end of PodNode-I while the IP camera is positioned at the right end of PodNode-PoE.

The variable attenuation of 30 dB from the previous PodNode's configuration is maintained for this setup. The purpose of this experimental setup is to transmit video data captured by the IP camera to the main laptop, and recording it using the VLC Media Player software for approximately 12 minutes. The video streaming protocol via the VLC Media Player software found in the main laptop is configured by opening the 'Network Stream' by typing into the network URL space: `rtsp://192.168.1.34/axis-media/media.amp` or `rtsp://192.168.1.34/axis-media/media.amp?videocodec=h264&resolution=1920x1080&compression=30&fps'&`.

Either entry will produce the same H.264 compression format and video quality. Once the video image is stable, recording commenced for about 12 minutes. We need to be aware at this stage of the experiment that RTSP protocol uses the TCP protocol as its transport layer whereas our LTE-EPC simulation model uses the UDP protocol. To produce a fair comparison between the two, the video data is recorded first followed by re-transmitting the data in the next round of the testbed setup using the UDP protocol.

#### **5.3.4 Overall Setup (IP Camera replaced with the second laptop)**

Before proceeding to the final testbed setup, we configure the IP address of both laptops by connecting the laptops directly to each other via their network ports using an RJ 45 cable. A further IP address is added to the main laptop, (192.168.2.230) along with the subnet mask of (255.255.255.0). In the second laptop, we use the static IP address (192.168.2.224) with subnet mask (255.255.255.0). The default gateway of the second laptop is the same as the main laptop's IP address to ensure that the main laptop can identify and detect it. If required, the 'ping' command can be used to confirm whether the main laptop can detect the second laptop. Next, the RJ 45 cables are disconnected at both ends; only at this point, can we proceed to the last stage of the testbed setup.

Figure 5.7 illustrates the entire layout of the testbed setup. In this setup, the IP camera is replaced with the second laptop as observed on the right-hand side of the figure. The purpose of this final testbed setup is to transmit the video packets recorded earlier from the main laptop across to the second laptop and to measure output performance of the video data transmission using the Jperf software which is already installed in both laptops.



**Figure 5.7:** The overall setup where the IP camera on the right is replaced with the second laptop

The experiment in this section will emulate the wireless uplink LTE video packet transmission from the UE to the Remote Host via the eNodeB only. To observe the transmission, the following steps are performed:

- i) The variable attenuator is set at 100 dB attenuation initially before the attenuation value is decremented in 10 dB steps until reaching 10 dB attenuation while progressing the experiment.
- ii) The Transmit Bandwidth and the Transmit Power in the PodNode's main (home) page needs to be changed to 10 MHz and 21 dBm respectively.
- iii) By opening the Jperf software in both laptops, set the second laptop as the server, the listen port to 5001 and choose 1 for number of connections. In the 'Transport Layer' options, we select UDP and then set the UDP Buffer Size together with the

UDP Packet Size to 64 Kbytes (default value) and 1024 Bytes, respectively. For the main laptop, we set it as the client and enter the server address (which is the receiver address). The port number needs to be the same as that in the second laptop while ensuring the 'Parallel Streams' option (in connections) is selected as 1. Next, in the 'Application Layer' options, we choose the representative file from within the folder C:\Users\Syahrir\Videos\vlc-record-2017-02-02-17h58m07s-rtsp\_\_192.168.1.34\_554\_axis-media\_media.amp\_videocodec=h264&resolution=1920x1080&compression=30&fps\_&-mp4. Then, we allow the video file to be transmitted for 60 seconds and the output format in Kbits. In the 'Transport Layer' option, we choose 'UDP' instead of the 'TCP' protocol. UDP bandwidth represents the data rate of the video packets either in Mbytes/s or Kbytes/s. Since we have used the data rate of 4 Mbps for the LTE-EPC simulation model, we choose 4 Mbytes/s for the testbed implementation. For the UDP Buffer Size and UDP Packet Size, the values need to be the same with those on the server (second laptop) to avoid video packet fragmentation.

Once the above steps have been performed, only then, can we proceed with the video packet transmission. First, we perform a 'Hardware Reset' located on the PodNode's main (home) page until new Tx Link SNR information is displayed. Then, we allow the Jperf in server mode to run before executing Jperf in client mode. The server will listen to the client at port 5001 and prepare to receive the video packets transmitted from the client. After that, the experiment stops and all measured results at both the server and the client are recorded. The server will record the output performance parameters such as the throughput or bandwidth and

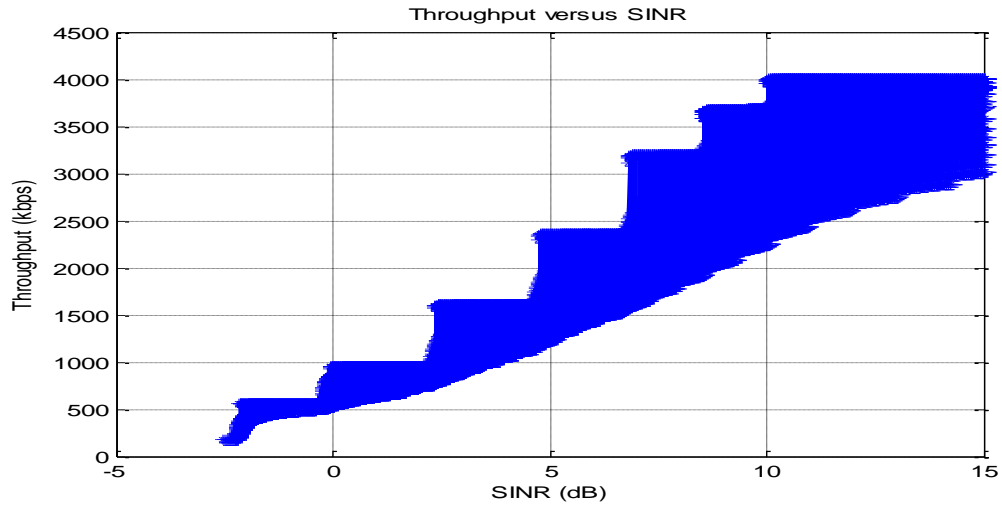
packet loss ratio whereas the client will record the transmitted data rate (or bandwidth) and the TX Link SNR. The same process is repeated for different values of channel attenuation (performed by the variable attenuator) and different values of UDP bandwidth (from 0.25 Mbytes/s to 16 Mbytes/s including the 4 Mbytes/s used initially).

## **5.4 Experimental Results and Discussion**

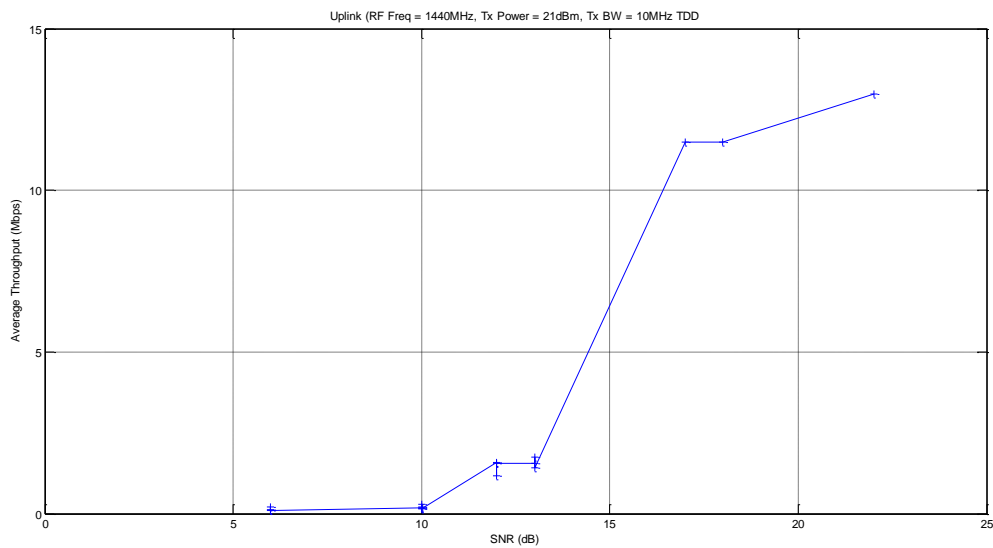
### **5.4.1 Results for the Emulated Uplink LTE Baseline Model**

Based on the experiments undertaken in Section 5.3.4, we combined all the results obtained when the attenuation was varied from 10 dB to 100 dB for all data rates ranging from 0.25 Mbytes/s to 16 Mbytes/s including the 4 Mbytes/s data rate. During the experiment, if the 4 Mbytes/s data rate was to be scrutinised for its performance, without varying it for other data rates, the results would have been inconclusive. The reason is that the attenuation values determined by the variable attenuator will not produce a significant TX Link SNR range of values. Moreover, we would also expect that no conclusions could be made from that situation. This is why the decision was made earlier in Section 5.3.4 to vary the data rates from 0.25 Mbytes/s to 16 Mbytes/s, and more importantly, to observe the impact of lower TX Link SNR values on the higher data rates.

Therefore, in consideration of the above, every time the video packets were transmitted from the client to the server, the server would capture the output performance parameters mentioned previously, such as the throughput or the bandwidth and the packet loss ratio. Whereas, the client would measure the transmitted data rate as well as the TX Link SNR. After that, we attempted to find the correlation between the throughput achieved for all data rates at the receiver and their corresponding TX Link SNR values. Based on this data, the average throughput against SNR was obtained, as illustrated in Figure 5.8 (b).



(a)



(b)

**Figure 5.8:** Average throughput versus SINR/SNR for uplink video delivery. (a) Simulated LTE baseline model. (b) Emulated LTE baseline model

From the graph in Figure 5.8 (b), the average throughputs of the received video packets are shown to increase with higher SNR, but the increase is not in direct proportion to each other. This is due to the link adaptation performed by the PodNodes where the specific modulation

type and coding rate are applied for a specific range of SNR values. Furthermore, the average throughput against the SNR performance pattern of this practical testbed is almost similar with the average throughput against the SINR performance pattern of the baseline simulation model obtained much earlier, as indicated in Figure 5.8 (a). Obviously, both graphs are not the same because of the following:

- i) Different network platforms, (PodNodes testbed for practical measurements as compared to the LTE-EPC platform for the simulation model); and
- ii) Different technical settings, (different regarding the RF frequency and duplex mode leading toward differences in the transmit bandwidth – 1440 MHz, TDD and 10 MHz for practical measurements as compared to 2100 MHz, FDD and 5 MHz for the simulation model).

We would also expect the graph to be shifted further to the right as shown in Figure 5.8 (b) since the operating frequency is much lower than that of the LTE-EPC simulation model. This means that even if the transmit power for both situations were the same, with lower operating frequency and the further the distance a signal could travel, would therefore also mean that higher data rates are more likely to survive. Furthermore, as mentioned previously, the TX Link SNR values obtained from the measurements were inadequate to cover all significant points on the graph due to the limitations of the PodNodes testbed. All these reasons have resulted in both the graphs in Figure 5.8 to be somewhat different with regard to their results, but their average throughput against SINR performance patterns are almost the same. Eventually, however, the practical measurement results obtained for the baseline model would justify the simulation results obtained earlier for the baseline simulation model. This observation is significant because even with a few parameters that are similar between the PodNode and the

LTE as described in Section 5.1, the practical measurement results for the average throughput and SNR would still display a similar staircase-like pattern as those of the theoretical simulation model. Moreover, as long as the crucial parameters such as the OFDM modulation and adaptive modulation and coding schemes remained intact. This further confirms the suitability of the PodNode technology to emulate the LTE platform. We can conclude this by saying; if we were to use the same LTE-EPC network platform for the practical testbed as those used in the simulation, we would have obtained similar results and thus, a similar pattern for both situations.

#### 5.4.2 Results for the Emulated Uplink LTE Content-Aware RRM Model

From the graph shown in Figure 5.8 (b), we next propose a look-up table which will display the correlation between the video data rate, R and SNR. The same concept as applied previously in Chapter 4.1 is used again for the practical testbed measurements. The proposed look-up table can also be used as a part of the content-aware RRM model for the practical PodNode testbed. To maximise the throughput and minimise the packet loss ratio, it is desirable to select the maximum data rate, R at a certain SNR value while maintaining the packet loss ratio at an acceptable level. The proposed look-up table is shown in Table 5.2.

**Table 5.2:** Proposed look-up table for uplink practical PodNode testbed

<b>Proposed Data Rate, R (Mbps)</b>	<b>SNR (dB)</b>
0.1	6
0.2	10
1.45	12 – 13
11	17 – 18

Based on the look-up table, we rerun the experiments conducted in Section 5.3.4 using the above-proposed data rates for the video streaming application corresponding to its dedicated SNR. The purpose is to confirm whether, by implementing the content-aware RRM method, we can maximise the throughput while keeping its packet loss ratio at its minimal level.

However, this time we tune the variable attenuator first to obtain the required SNR before setting the related data rate. Again, since the UDP Bandwidth unit at the client side is defined in either Kbytes/s or Mbytes/s, the proposed data rate in the look-up table needs to be translated from Mbps to Mbytes/s. For example, if the proposed data rate of 0.1 Mbps is to be used, then it needs to be defined as 0.1 Mbytes/s on the client side. As usual, all results obtained from both the client and the server are recorded and tabulated as shown in Table 5.3.

**Table 5.3:** Performance of content-aware RRM model for emulated uplink video delivery

<b>Proposed Data Rate, R [Mbps]</b>	<b>SNR [dB]</b>	<b>Average Throughput [Mbps]</b>	<b>Packet Loss [%]</b>
0.100	6	0.0988	6/ 734 = 0.82 %
0.200	10	0.198	10/ 1466 = 0.68 %
1.45	12	1.45	1/10623 = 0.0094 %
1.45	13	1.45	1/10623 = 0.0094 %
11	17	10.935	13/80625 = 0.016 %
11	18	11.008	9/80625 = 0.011 %

We observe that in all cases, the average throughput is almost similar to the transmitted data rates and the packet loss is well below 1 %. As the SNR improves from 6 dB to 18 dB which is symbolising the UE movement approaching the eNodeB in LTE, packet loss performance also improves acquiring a lower percentage. This demonstrates that by applying the concept of the content-aware RRM model, we have achieved the maximum average throughput and successfully maintained the packet loss below 1 %. Again, this observation is almost in agreement with the packet loss ratio against the time performance of the content-aware RRM simulation model for three different UE velocities as shown in Tables 4.7, 4.8 and 4.9 and is summarised in Table 5.4. The faster the UE velocity travelling towards the eNodeB, the higher the SNR, and the lower the packet loss ratio. Thus, the practical testbed results that we have measured for the content-aware RRM model in Table 5.3 justifies and confirms the simulation results obtained earlier for the content-aware RRM simulation model as shown in Table 5.4.

**Table 5.4:** Performance of content-aware RRM model for simulated uplink video delivery

UE Velocity [km/h]	Actual Packet Loss [%]
5	2.24
50	1.33
72	0.84

## 5.5 Summary

In this chapter, we developed a practical video streaming testbed using PodNodes to emulate the uplink LTE-EPC network in the simulation model. The practical testbed and the simulation model are different from each other in several ways especially with regard to the RF frequency, duplex mode and transmit bandwidth. Therefore, some underlying assumptions need to be made to compensate for limitations in the hardware environment. Furthermore, the LTE

spectrum band is a licensed band [88] and therefore making it even more difficult to conduct the LTE testbed experiment. Even so, we managed to obtain a similar ‘staircase-like’ pattern for the average throughput with respect to its SNR for both the practical and baseline simulation model.

For the content-aware RRM in both the simulation model and the practical element, the results obtained are in cohesion where the video streaming data rates have achieved maximum throughput, and at the same time, the packet loss ratio is minimised. Ultimately, we have successfully made practical comparisons for both the results obtained for the LTE-EPC baseline simulation model as well as the results for the content-aware RRM model using the practical testbed developed on PodNodes. Furthermore, these results confirm the viability of the proposed content-aware RRM model to be used in the current LTE/LTE-Advanced systems.

The practical measurement exercise described above is not alleged to be complete, and further tests could still be performed. For example, exploring the throughput of the downlink channel, changing system bandwidth and transmit power could provide additional information. However, due to the project’s timescale and equipment availability constraints, it was decided that these additional measurements be conducted within the frame of future research.

## 6 CONCLUSION AND FUTURE WORKS

### 6.1 Conclusion

Various methods of radio resource management for LTE/LTE-Advanced traffic have been studied regarding QoS handling of video packet transmission. Even so, some of the previous methods highlighted in this thesis, lack consideration on the compatibility with legacy systems and standards, lack of a UE mobility study and the limited number of studies regarding performance metrics for a particular user and period.

As a result, the author has proposed a content-aware RRM model by employing a cross-layer optimisation approach between the PHY and the APP layer for both uplink and downlink video packet transmissions in a single LTE cell. The uniqueness of the CLO implementation is represented by the presence of two look-up tables corresponding to uplink and downlink video delivery, proposed as the primary decision-makers for matching the suitable video data rate with the channel SINR.

The proposed content-aware RRM model is derived following the completion of the simulation study on the output performance of the LTE baseline model for a single video data bearer in both the uplink and downlink transmission. The simulation results showed that the throughput increased in a “staircase-like” pattern, as the corresponding SINR measured values increased. Based on the findings, two look-up tables were prepared where a new video data rate is matched to its corresponding SINR value. Both look-up tables are embedded in two newly developed cross-layer optimisers; one for the uplink and the other for the downlink. The proposed CLO can dynamically adjust the video data rates in the APP layer depending on the measured SINR in the uplink and downlink transmissions. The two most important aspects when considering this concept is to minimise the packet loss ratio, as well as, the average end-to-end

delay as much as possible while achieving maximum throughput. Furthermore, the proposed CLO only accepts information from the PHY and APP layers and changes the data rate in the APP layer, without changing the MAC layer, therefore, making it compatible with legacy systems and standards. Another advantage of this CLO is the ease of use in which the CLO can be easily attached to and detached from, the UE or the eNodeB and EPS without manipulating the PHY and MAC layers.

To test and evaluate the performance of the proposed content-aware RRM model, a simulation tool is required, and NS-3 with LTE module was selected for this task. An LTE baseline model is also developed alongside the proposed model to serve as the benchmark performance. Extensive simulations are carried out for both models in three different UE velocities in both the uplink and downlink transmissions. The results have shown that while the video data throughput is comparable between the two models, the proposed content-aware RRM model performs better in average end-to-end delay and much better in packet loss ratio, as compared to the baseline model. More significant gains have been achieved for the proposed model as the UEs are simulated through higher velocities toward the eNodeB. These results support and recommend the potential use of the proposed content-aware RRM model even in a high mobility environment.

Finally, a practical testbed to emulate the single cell LTE network has also been developed to compare with the theoretical simulations undertaken in the earlier chapters. Due to the spectrum licensing issue, the practical testbed is developed on the PodNode platform at Rinicom Ltd. The video packet file is obtained from the Axis P1357 Network Camera, and the overall performance analysis is conducted using the Jperf software. The first emulation activity justifies the uplink throughput performance with respect to the measured SINR observed for the baseline model. The second test which involved the implementation of the look-up table

proposed in the uplink is also carried out, and the results reaffirm the suitability of the proposed content-aware RRM model to be used in the current LTE or LTE-Advanced systems for better performance in packet loss ratio and average packet delay.

## **6.2 Future Works**

Despite the excellent achievement shown by the proposed content-aware RRM model as reflected in its output performance metrics, there remain other factors to consider for future research. For instance, the practical measurements on the PodNode testbed explained in the previous chapter could be further investigated to examine the throughput effects by changing the system bandwidth and the transmit power in the downlink transmission. Apart from that, the current work could also be extended as follows:

### **6.2.1 Multi-user Content-Aware RRM**

In this thesis, even though the performance simulation for the content-aware RRM model is conducted with four UEs, corresponding to four application services, the performance metrics are tailored for only one UE that transmits or receives the video packets. Thus, the proposed model is only valid if one video application user exists in a single LTE cell. The research could naturally be extended to consider more than one video application user. The optimisation process by the relevant cross-layer optimiser will be more complicated as it will need to consider the available bandwidth before resource sharing can occur. In fact, it would be interesting to study the impact of the multi-user content-aware RRM model implementation in a multi-cell LTE system.

### **6.2.2 MIMO-OFDMA**

So far, the current work only assumes the single-input-single-output (SISO)

implementation. Since one of the IMT-Advanced specifications is the use of multiple-input-multiple-output (MIMO), especially when diversity is the primary objective, the content-aware RRM model could complement the MIMO implementation in the future by lowering its SINR threshold to match the same data rate.

### **6.2.3 Context-Aware RRM**

This thesis focuses mainly on PHY and APP cross-layer optimisation. From the PHY layer, SINR values are used to match the proper data rate at the APP layer. For future research, the input to the cross-layer optimiser will not necessarily be the SINR values and the present data rate, but it could make further requests on accessing a UE's context information which is typically located in the APP layer. The UE's context information could be related to the state of the application window or the type of application (i.e., interactive or non-interactive applications) itself. The optimisation process of this context-aware RRM model will be more complicated as more information will need to be considered before deciding on the necessary parameter re-calibrations. However, it is worthy of further investigation.

### **6.2.4 Internet-of-Things**

Internet-of-Things (IoT) is a new research area which has gained enormous interest by academicians and industry players alike in recent years. The capability of physical devices embedded with electronics, sensors etc. could integrate into existing network infrastructure, thereby creating opportunities for future integration into the 5G system which will evolve from the current LTE/LTE-Advanced system. For example, the Wireless Sensor Network (WSN), which is one of the IoT applications, is currently being investigated for its potential integration into the future IMT-2020 system. However, there are two key issues concerning WSN implementation that should be highlighted. The first issue is its low battery lifespan and the

second issue is related to the security of its data transmission. The currently proposed model could be implemented to overcome the first issue by reducing the rate of change of the WSN data rate which would lead to reduced processing time and thus, prolongs the battery life of the WSN nodes.

Since the current content-aware RRM model is highly dedicated for throughput maximisation in an LTE network, it may appear that the proposed model is not suitable for implementation in the reduced throughput WSN. In fact, for the low bit-rate WSN, only slight changes are needed to be carried out to the proposed model by considering both the delay requirement of the packet transmission and the channel condition instead of solely depending on the channel condition for throughput maximisation in the LTE network. This means the proposed look-up table for the cross-layer optimiser will make use of the input information on the current delay and the channel condition to change its current data rate dynamically.

## 7 REFERENCES

- [1] S. Pietrzyk, "OFDMA for Broadband Wireless Access", ARTECH House, 2006, p. 270.
- [2] J. Lim, "Adaptive Radio Resource Management for Uplink Wireless Networks," PhD Thesis, 2006.
- [3] IEEE Standard for Local and Metropolitan Area Networks Part 16: Air Interface for Fixed Broadband Wireless Access Systems.
- [4] IEEE 802.16m-2009 "IEEE Standard for Local and metropolitan area networks Part 16: Air Interface for Broadband Wireless Access Systems" Amendment: Advanced Air Interface.
- [5] S. Kumar, N. Marchetti, "IMT-Advanced: Technological Requirements and Solution Components", Second International Workshop on Cognitive Radio and Advanced Spectrum Management 2009 (CogART 2009), 2009, pp. 1 – 5.
- [6] S. Parkvall, D. Astely, "The Evolution of LTE towards IMT-Advanced", Journal of Communications Vol. 4, No. 3, 2009, pp. 146 – 154.
- [7] W. Kumwilaisak, Y. Thomas Hou, Q. Zhang, W. Zhu, C.-C. Jay Kuo, and Y. Zhang, "A Cross-Layer Quality-of-Service Mapping Architecture for Video Delivery in Wireless Networks", IEEE Journal on Selected Areas in Communications, Vol. 21, No. 10, December 2003, pp. 1685 – 1698.
- [8] Q. Zhang, W. Zhu, and Y. Zhang, "End-to-End QoS for Video Delivery Over Wireless Internet", in Proceedings of the IEEE, Vol. 93, No. 1, January 2005, pp. 123-134.
- [9] G. Markarian, L. Mihaylova, D. V. Tsitserov and A. Zvikhachevskaya, "Video Distribution Techniques Over WiMAX Networks for m-Health Applications", IEEE Transactions on Information Technology in Biomedicine, Vol. 16, No. 1, January 2012, pp. 24-30.
- [10] Juwita Mohd Sultan and Muhammad Syahrir Johal, "Cross Layer Scheduling in WiMAX QoS for Disaster Management", Journal of Telecommunication, Electronic and Computer Engineering (JTEC), Vol. 7, Issue 2, 2015, pp. 145-151.
- [11] D1.1 Initial Report on Advanced Radio Resource Management (A. Saul, 2009). Available. [http://projects.celtic-initiative.org/winner+/WINNER+%20Deliverables/D1.1\\_v1.0.1.pdf](http://projects.celtic-initiative.org/winner+/WINNER+%20Deliverables/D1.1_v1.0.1.pdf)
- [12] 3GPP RP-091440, "Work Item Description: Carrier Aggregation for LTE," December 2009.
- [13] Mohd Khairy Ismail, Muhammad Syahrir Johal and Azmi Awang Md Isa, "Current Developments in LTE-ADVANCED: Radio Resource Management Review", in proceedings of IEEE Student Conference on Research and Development (SCORED 2014), 16-17 Dec. 2014.
- [14] 3GPP TR 36.913. "Technical Report, 3<sup>rd</sup> Generation Partnership Project; Technical Specification Group Radio Access Network; Requirements for Further Advancements for E-UTRA (LTE-Advanced)", V0.0.4:2008-05.
- [15] Recommendations ITU-R M.1645. "Framework and Overall Objectives of the Future Deployment of IMT-2000 and Systems beyond IMT-2000:2003".
- [16] M. K. Ismail, A. A. M. Isa and M. S. Johal, "Review of Radio Resource Management For IMT-Advanced System", Jurnal Teknologi, Vol. 72, No. 4, 2015, pp. 113-119.

- [17] D. Martin-Sacristan, J. F. Monserrat, J. Cabrejas-Penuelas, D. Calabuig, S. Garrigas, and N. Cardona, "On the Way towards Fourth-Generation Mobile: 3GPP LTE and LTE-Advanced", *EURASIP Journal on Wireless Communications and Networking*, Article ID 354089, 2009.
- [18] E. Dahlman et al., "3G Evolution: HSPA and LTE for Mobile Broadband," 2nd ed., Academic Press, 2008.
- [19] S. Parkvall, A. Furuskar, and E. Dahlman, "Evolution of LTE toward IMT-Advanced," *IEEE Communications Magazine*, February 2011, pp. 84–91.
- [20] D. Astely, E. Dahlman, A. Furuskar, Y. Jading, M. Lindstrom, and S. Parkvall, "LTE: The Evolution of Mobile Broadband", *IEEE Communications Magazine*, April 2009, pp. 44–51.
- [21] 3GPP RAN Workshop on IMT-Advanced, Shenzhen, China, 07–08 April 2008, available at [ftp://ftp.3gpp.org/workshop/2008-04-07\\_RAN\\_IMT\\_Advanced/Docs/](ftp://ftp.3gpp.org/workshop/2008-04-07_RAN_IMT_Advanced/Docs/).
- [22] ISBN WINNER II: 978-1-905824-08-3, "Advanced Radio Technologies for Future Wireless Systems", June 2008.
- [23] I. Akyildiz, D. M. Gutierrez-Estevez, and E. C. Reyes, "The evolution to 4G cellular systems: LTE-Advanced", *Physical Communication* 3, Vol. 4, No. 3, 2010, pp. 217-244.
- [24] Peng Li, Yilin Chang, Nina Feng, and Fuzheng Yang, "A Cross-Layer Algorithm of Packet Scheduling and Resource Allocation for Multi-User Wireless Video Transmission", *IEEE Transactions on Consumer Electronics*, Vol. 57, No. 3, August 2011, pp. 1128 – 1134.
- [25] A. Abdel Khalek, C. Caramanis and R. W. Heath, "A Cross-Layer Design for Perceptual Optimization of H.264/SVC with Unequal Error Protection", *IEEE Journal on Selected Areas in Communications*, Vol. 30, No. 7, August 2012, pp. 1157 – 1171.
- [26] X. Cheng, and P. Mohapatra, "Quality-optimized Downlink Scheduling for Video Streaming Applications in LTE Networks," *IEEE Proceedings GLOBECOM-Communications Software, Services and Multimedia Symposium*, 2012, pp. 4834–4839.
- [27] S. Cicalo, M. Mazzotti, S. Moretti, V. Tralli and M. Chiani, "Cross-layer Optimization for m-Health SVC Multiple Video Transmission over LTE Uplink", *IEEE 15<sup>th</sup> International Conference on e-Health Networking, Applications and Services (Healthcom 2013)*, 2013, pp. 212 – 217.
- [28] N. Shabbir, H. Kashif, "Radio Resource Management in WiMAX", Master of Science in Electrical Engineering Blekinge Institute of Technology, 2009.
- [29] Yaser Barayan and Ivica Kostanic, "Performance Evaluation of Proportional Fairness Scheduling in LTE", in *Proceedings of the World Congress on Engineering and Computer Science 2013 Vol II WCECS 2013*, 23-25 October 2013.
- [30] K. I. Pedersen, T. E. Kolding, F. Frederiksen, I. Z. Kovacs, D. Laselva, and P. E. Mogensen, "An Overview of Downlink Radio Resource Management for UTRAN Long-Term Evolution", *IEEE Communications Magazine*, July 2009, pp. 86–93.
- [31] 3GPP 36.300, "Technical Specification Group Radio Access Network; Evolved Universal Terrestrial Radio Access (E-UTRA) and Evolved Universal Terrestrial Radio Access Network (E-UTRAN); Overall description; Stage 2 (Release 8)," Mar. 2008.
- [32] 3GPP 36.211, "Technical Specification Group Radio Access Network; Physical Channels and Modulation (Release 8)," Mar. 2008.
- [33] 3GPP 36.213, "Technical Specification Group Radio Access Network; Evolved Universal Terrestrial Radio Access (E-UTRA); Physical Layer Procedures (Release 8)," Mar. 2008.

- [34] 3GPP 23.401, "Technical Specification Group Services and System Aspects; GPRS Enhancements for E-UTRAN Access (Release 8)," Mar. 2008.
- [35] D. Niyato and E. Hossain, "Connection Admission Control Algorithms for OFDM Wireless Networks," IEEE Proceedings GLOBECOM, Sept. 2005, pp. 2455–59.
- [36] G. Song and Y. Li, "Utility-Based Resource Allocation and Scheduling in OFDM-Based Wireless Broadband Networks," IEEE Communications Magazine, Dec. 2005, pp. 127–34.
- [37] D. Niyato and E. Hossain, "Adaptive fair subcarrier/rate allocation in multirate OFDMA networks: Radio link level queuing performance analysis," IEEE Transactions on Vehicular Technology, 55(6), November 2006.
- [38] Arijit Ukil and Jaydip Sen, "QoS Aware Cross-Layer Optimized Resource Allocation in WiMAX Systems", 1st International Conference on Wireless Communication, Vehicular Technology, Information Theory and Aerospace & Electronic Systems Technology (Wireless VITAE 2009), 2009, pp. 818 – 822.
- [39] Mohd Khairy Ismail, Azmi Awang Md Isa, Muhammad Syahrir Johal and Mohd Riduan Ahmad, "Design and Development of Modified Proportional Fair Scheduler for LTE/LTE-Advanced", ARPN Journal of Engineering and Applied Sciences, Vol. 11, No. 5, March 2016, pp. 3280-3285.
- [40] A. K. Parekh and R. G. Gallager, "A generalized processor sharing approach to flow control in integrated services networks: The singlenode case", IEEE/ACM Transactions on Networking, Vol. 1, no. 3, June 1993, pp. 344-357.
- [41] MK Ismail, A Awang Md Isa, MS Johal and MSI M Zain, "Current Development in LTE/LTE-Advanced: Adaptive-Proportional Fair Scheduling in LTE", Journal of Telecommunication, Electronic and Computer Engineering (JTEC), Vol. 7, Issue 1, 2015, pp. 103-108.
- [42] Rehana Kausar, Yue Chen, Kok Keong Chai, Laurie Cuthbert and John Schormans, "QoS Aware Mixed Traffic Packet Scheduling in OFDMA-based LTE-Advanced Networks", The Fourth International Conference on Mobile Ubiquitous Computing, Systems, Services and Technologies: UBICOMM 2010, 2010, pp. 53 – 58.
- [43] R. Pabst, B.H. Walke, D.C. Schultz, P. Herhold, H. Yanikomeroglu, S. Mukherjee, H. Viswanathan, M. Lott, W. Zirwas, M. Dohler, H. Aghvami, D.D. Falconer, G.P. Fettweis, "Relay-based deployment concepts for wireless and mobile broadband radio," IEEE Communications Magazine 42 (5), 2005, pp. 80–89.
- [44] O. Mubarek, H. Yanikomeroglu, S. Periyalwar, "Dynamic frequency hopping in cellular fixed relay networks," in Proceedings of Vehicular Technology Conference, Spring May 2005.
- [45] L. Xiao, T. E. Fuja and D. J. Costello, "Mobile Relaying: Coverage Extension and Throughput Enhancement", IEEE Transactions on Communications, Vol. 58, 2010, pp. 2709-2717.
- [46] Won-Hyoung Park, Saewoong Bahk, "Resource management policies for fixed relays in cellular networks", Computer Communications, vol. 32, 2009, pp. 703–711.
- [47] Furaih Alshaalan, Saleh Alshebeili, and Abdulkareem Adinoyi, "Interference-aware Radio Resource Allocation Techniques for OFDMA-based Wireless Networks", International Conference on Wireless Communications, Networking and Information Security (WCNIS), 2010, pp. 546 – 550.
- [48] M. A. Abd Elgawad, M. M. Tatawy, and M. S. El-Mahallawy, "New Cross-layer QoS-based Scheduling Algorithm in LTE System", in Recent Researches in Communications

- and IT (CITCOM-32), 2010, pp. 190 – 194.
- [49] M. M. Tantawy, A. S. T. Eldein, and R. M. Zaki, “A Novel Cross-Layer Scheduling Algorithm for Long Term-Evolution (LTE) Wireless System”, Canadian Journal on Multimedia and Wireless Networks, Vol. 2, No. 4, December 2011.
  - [50] D. Wu, S. Ci, H. Luo, W. Zhang and J. Zhang, “Cross-Layer Rate Adaptation for Video Communications over LTE Networks,” IEEE Proceedings GLOBECOM-Wireless Communications Symposium, 2012, pp. 4834–4839.
  - [51] R. Radhakrishnan, B. Tirouvengadam, and A. Nayak, “Cross Layer Design for Efficient Video Streaming over LTE Using Scalable Video Coding”, Network Protocols and Algorithm, Vol. 4, No. 4, 2012.
  - [52] H. Luo, S. Ci, D. Wu, J. Wu and H. Tang, “Quality-Driven Cross-Layer Optimized Video Delivery over LTE”, IEEE Communications Magazine, February 2010, pp. 102–109.
  - [53] S. Karachontzitis, T. Dagiuklas and L. Dounis, “Novel Cross-Layer Scheme for Video Transmission over LTE-Based Wireless Systems”, IEEE International Conference on Multimedia and Expo (ICME 2011), 2011.
  - [54] D. Wang, V. S. Somayazulu and J. R. Foerster, “Efficient Cross-layer Resource Allocation for H.264/SVC Video Transmission over Downlink of an LTE System”, IEEE International Symposium on a World of Wireless, Mobile and Multimedia Networks (WoWWMoM), 2012.
  - [55] T. Issariyakul and E. Hossain, “Introduction to Network Simulator NS2”, Springer, 2012, p. 11.
  - [56] A. Varga and R. Hornig, “An Overview of the OMNET++ Simulation Environment”, in Proceedings of SIMU Tools, March 2008.
  - [57] H. N. Pham, D. Pediaditakis, and A. Boulis. From simulation to real deployments in wsn and back. Proceedings of the 2007IEEE International Symposium on a World of Wireless, Mobile and Multimedia Networks (WoWWMoM 2007), June 2007, pp. 1–6.
  - [58] E. Weingartner, H. v. Lehn and K. Wehrle, “A performance comparison of recent network simulators”, IEEE International Conference on Communications (ICC 2009), 2009.
  - [59] SimuLTE - LTE System Level Simulation Model and Simulator for INET & OMNeT++. Available: <https://github.com/inet-framework/simulte>
  - [60] Z. Lu and H. Yang, “Unlocking the Power of OPNET Modeler”, Cambridge University Press, 2012, p. 5.
  - [61] K. Fall, “Network emulation in the VINT/ns simulator,” in Fourth IEEE Symposium on Computers and Communications (ISCC'99), 1999, pp. 59-67.
  - [62] D. Estrin, M. Handley, J. Heidemann, S. McCanne, Y. Xu, and H. Yu, “Network visualization with the VINT Network Animator Nam,” Technical Report 99-703b, USC Computer Science Department, 1999.
  - [63] G. F. Lucio, M. Paredes-Farrera, E. Jammeh, M. Fleury and M. J. Reed, “OPNET Modeler and NS-2: Comparing the Accuracy of Network Simulators for Packet-Level Analysis using a Network Testbed”, WSEAS Transactions on Computers, January 2003.
  - [64] E. Altman and T. Jimenez, “NS Simulator for Beginners”, Lecture Notes. Available [Online]: [http://nsgam.sourceforge.net/wiki/index.php/Getting\\_Started\\_with\\_NS-2](http://nsgam.sourceforge.net/wiki/index.php/Getting_Started_with_NS-2) or <http://www-sop.inria.fr/members/Eitan.Altman/COURS-NS/n3.pdf>
  - [65] GNU General Public License, version 2. <http://www.gnu.org/licenses/gpl-2.0.html>.

- [66] T. R. Henderson, S. Roy, S. Floyd and G. F. Riley, “ns-3 Project Goals,” Available at: [www.nsnam.org/docs/meetings/wNS-2/wNS-2-NS-3.pdf](http://www.nsnam.org/docs/meetings/wNS-2/wNS-2-NS-3.pdf), October 10,2006.
- [67] T. R. Henderson, M. Lacage, and G. F. Riley, “Network Simulations with the ns-3 Simulator,” Demo paper at ACM SIGCOMM’08, August 2008.
- [68] 3GPP. Technical Specifications. Group Radio Access Network; Conveying MCS and TB size via PDCCH, 3GPP TSG-RAN WG1 R1-081483.
- [69] G. Piro, N. Baldo, and M. Miozzo, “An LTE module for the ns-3 network simulator”, WNS-3, 2011, pp. 415 – 422.
- [70] H. Moore, “MATLAB for Engineers”, Pearson Education Limited, Fourth Edition, 2015.
- [71] M. Gerasimenko, S. Andreev, Y. Koucheryavy, A. Trushanin, V. Shumilov, M. Shashanov and S. Sosnin, “Performance Comparison of System Level Simulators for 3GPP LTE Uplink”, Book Chapter 3 in NEW2AN/ruSMART 2012, LNCS 7469, 2012, pp. 186-197.
- [72] F. Kelly, “Charging and Rate Control for Elastic Traffic”, European Transactions on Telecommunications, February 1997, pp. 33-37.
- [73] P. Viswanath, D. N. C. Tse and R. Laroia, “Opportunistic beamforming using dumb antennas”, IEEE Transactions on Information Theory, vol. 48, no. 6, June 2002, pp. 1277-1294.
- [74] G. Caire, R. Muller and R. Knopp, “Hard Fairness Versus Proportional Fairness in Wireless Communications: The Single-Cell Case”, IEEE Transactions on Information Theory, vol. 53, no. 4, April 2007, pp. 1366-1385.
- [75] B. Dusza, C. Ide, P. B. Bok, and C. Wietfeld, “Optimized Cross-Layer Protocol Choices for LTE in High-Speed Vehicular Environments”, 9<sup>th</sup> International Wireless Communications and Mobile Computing Conference (IWCMC), July 2013, pp. 1046 – 1051.
- [76] OMNET++ webpage. <https://omnetpp.org/intro/what-is-omnet>
- [77] Riverbed webpage. <https://www.riverbed.com/my/products/steelcentral/opnet.html>
- [78] LTE module. Available: <https://github.com/rimonece/lte-model>
- [79] L. Diez, R. Aguero, J. Penhoat, E. St’ephan, and F. Heliot, “Exploiting the DASH framework to promote a dynamic transport selection for video streaming over LTE networks”, IEEE International Conference on Computer and Information Technology; Ubiquitous Computing and Communications; Dependable, Autonomic and Secure Computing; Pervasive Intelligence and Computing 2015, pp. 37 – 43.
- [80] F. Metzger, C. Steindl and T. Hoßfeld, “A Simulation Framework for Evaluating the QoS and QoE of TCP-based Streaming in an LTE Network”, 27th International Teletraffic Congress, 2015, pp. 168 – 176.
- [81] Adi. Syukri. Md. Yusof, Wee. Kuok. Kwee, A. Ee. Mae and Mohd. Fikri. Azli. Abdullah, “Performance Study of Channel-QoS Aware Scheduler in LTE Downlink Using NS3”, in Proceeding of The Seventh International Conference on Emerging Networks and Systems Intelligence (EMERGING 2015), 2015, pp. 44-49.
- [82] D. Munaretto, M. Zanforlin, and M. Zorzi, “Performance evaluation in ns-3 of a video delivery framework for next generation cellular networks,” in Proceedings of IEEE International Conference on Communications 2013: Workshop on Immersive & Interactive Multimedia Communications over the Future Internet, 2013, pp. 642-646.
- [83] G. Aiyetoro and F. Takawira, “A New User Scheduling Scheme in LTE/LTE-A

- Networks Using Cross-layer Design Approach,” in Proceedings of IEEE Military Communications Conference (MILCOM 2015), Oct. 2015, pp. 689 – 694.
- [84] E. Atxutegi, F. Liberal, K. J. Grinnemo, A. Brunstrom, A. Arvidsson and R. Robert, “TCP behaviour in LTE: impact of flow start-up and mobility,” 9th IFIP Wireless and Mobile Networking Conference (WMNC), 2016.
- [85] Andreas Müller and Philipp Frank, “Cooperative Interference Prediction for Enhanced Link Adaptation in the 3GPP LTE Uplink”, IEEE 71<sup>st</sup> Vehicular Technology Conference (VTC 2010-Spring), May 2010.
- [86] G. Wang, “Downlink Shared Channel Evaluation of LTE System,” Master of Science Thesis in Communication Engineering, Chalmers University of Technology, Gothenburg, Sweden, 2013.
- [87] Rinicom website. <http://www.rinicom.com>
- [88] OFCOM website. <https://www.ofcom.org.uk/spectrum/radio-spectrum-and-the-law>
- [89] OFCOM website. <https://www.ofcom.org.uk/about-ofcom>
- [90] Rinicom website. <http://www.rinicom.com/products/cofdm-ip-mesh-radios/podnode-cofdm-ip-mesh-technology/> [Accessed 15 February 2017].
- [91] PodNode-PoE Hardware Manual.
- [92] Rinicom Ltd. product list specifications. [https://github.com/TransparencyToolkit/dataspec-sii/blob/master/sii\\_data/docs/1324-rinicom-ltd-product-list-specifications.pdf](https://github.com/TransparencyToolkit/dataspec-sii/blob/master/sii_data/docs/1324-rinicom-ltd-product-list-specifications.pdf)
- [93] Axis P1357 Network Camera Data Sheet. Available [Online] <https://www.axis.com/za/en/products/axis-p1357/support-and-documentation>.
- [94] Wikipedia website. <https://en.wikipedia.org/wiki/lperf>
- [95] Umeh O. A., Akpado K.A., Okechukwu G. N., and Ejiofor H. C., “Throughput and Delay Analysis in a Real Time Network”, International Journal of Engineering and Applied Sciences (IJEAS), ISSN: 2394-3661, Volume-2, Issue-12, December 2015, pp. 27 – 34.
- [96] Axis P1357 Network Camera Data Sheet. Available [Online]. [https://www.axis.com/files/datasheet/ds\\_p1357\\_1471705\\_en\\_1702.pdf](https://www.axis.com/files/datasheet/ds_p1357_1471705_en_1702.pdf)
- [97] Jperf software download. Available <http://www.softpedia.com/get/Network-Tools/Network-Testing/JPerf.shtml#download>
- [98] VLC Media Player website. <http://www.videolan.org/vlc/index.en-GB.html>
- [99] 3GPP TR 136.931 V9.0.0 (2011-05), “LTE; Evolved Universal Terrestrial Radio Access (E-UTRA); Radio Frequency (RF) requirements for LTE Pico Node B (3GPP TR 36.931 version 9.0.0 Release 9)”, May 2011.
- [100] Rinicom website. <http://www.rinicom.com/products/communications/podnode-i>, [Accessed 15 February 2017].